ABSTRACT

Title of Dissertation: INVESTIGATIONS OF SOLVENT POLARITY AT LIQUID/LIQUID INTERFACES BY SHG SPECTROSCOPY USING MOLECULAR RULERS

William Hobbs Steel, Doctor of Philosophy, 2004

Dissertation directed by: Professor Robert A. Walker
Department of Chemistry and Biochemistry

Homologous series of solvatochromic surfactants have been synthesized to study polarity at liquid/liquid interfaces. Each surfactant series consists of hydrophobic, *para*-nitroanisole-based chromophores attached to ionic headgroups by *n*-alkyl spacers. By incorporating these components these molecules have the capability of functioning as molecular rulers: probes of molecular-scale variation in solvation forces across liquid/liquid interfaces. Changing the chromophore-headgroup separation should enable different members of a homologous series to span different interfacial widths, thus exposing the chromophore to different chemical environments. This idea is explored by using surface-specific, non-linear optical spectroscopy. Resonance-enhanced second harmonic generation spectra of molecular rulers have been collected at weakly and strongly associating liquid/liquid interfaces.

At weakly associating interfaces between water and four alkanes (cyclohexane, methylcyclohexane, octane, and hexadecane), data suggest that all four water/alkane interfaces are molecularly sharp (< 9 Å), but that differences in the solvent molecular structure alter the transition from aqueous to organic solvation across the interface. Polarity across two interfaces (cyclohexane and hexadecane) changes gradually over the distance spanned by ruler surfactants. In contrast, the transitions at the interfaces between water and both methylcyclohexane and octane appear much more abrupt. These findings appear to correlate with each organic solvent's ability to pack and associated free volume. More free volume in the organic phase leads to a more abrupt water/alkane interface.

At strongly associating interfaces between water and four alcohols (1-octanol, 1-decanol, 3-octanol, and 2,6-dimethyl-4-heptanol), data suggest that all four water/alcohol interfaces contain a region of reduced polarity between the polar water phase and the bulk alcohol. We attribute this region to the alignment of the alkyl chains of the interfacial alcohol molecules. Polarity across the two interfaces with linear alcohols changes gradually over the distances spanned by ruler surfactants. In contrast, transitions at the interfaces between water and the two branched alcohols appear much more abrupt. These differences appear to correlate well with the solute accessible free volume within the alcohols. The width of the interfaces between water and the linear alcohols appears to be directly related to the length of the alkyl chain on the alcohol.

INVESTIGATIONS OF SOLVENT POLARITY AT LIQUID/LIQUID INTERFACES BY SHG SPECTROSCOPY USING MOLECULAR RULERS

By

William Hobbs Steel

Dissertation submitted to the Faculty of the Graduate School of the
University of Maryland, College Park in partial fulfillment
of the requirements for the degree of
Doctor of Philosophy
2004

Advisory Committee:

Professor Robert A. Walker, Chair
Professor Millard H. Alexander
Professor Janice E. Reutt-Robey
Professor John D. Weeks
Professor Mikhail A. Anisimov, Dean's Representative

DEDICATION

To my family: past, present, and future

ACKNOWLEDGEMENTS

The four years I have spent in graduate school have left me indebted to the many people that have guided, helped, and encouraged me in countless ways. I can offer here only a small amount of the thanks each is truly due. I am thankful, firstly, to Dr. Robert Walker, my advisor, who has demonstrated immeasurable patience and guidance throughout my tenure at the University of Maryland. Were it not for our meeting when I was a perspective graduate student this dissertation may very well not have been possible. Through broken limbs, unsettled career choices, and life-altering personal developments he has listened and offered advice and support in a manner unexpected from a research advisor. Academically he has been a powerful motivator, talented teacher, and supportive mentor. These are all qualities I admire greatly and hope to possess one day. I feel honored to call him my friend and comforted to know that he will continue to be.

The members of the Walker Research Group, past and present, have been my co-workers and friends, and I am thankful for them in both regards. The current graduate students, Okan Esenturk, Carmen Beildeck, Michael Pomfret, Wendy Heiserman, and Suleyman Can have been the source of numerous discussions, both scientific and social. I am especially thankful for the feedback they provided about my research presentations during my recent job search. Their wealth of ideas and suggestions will be missed. I must thank Dr. Xiaoyi Zhang, a former member of the group, who taught me the instrumental details of our lab setup, and was always available to answer my questions about it when I struggled. In addition to these, there are several undergraduate students that I have had the pleasure of working with in our lab. Thank you to Ryan Nolan,

Radika Rupasinghe, Yuen Lau, and Dan Burden – all are talented, dedicated young scientists that have bright futures ahead of them.

I would like to thank Jason Lagona and Patrick Brown; two graduates students in the department that have shared many conversations with me. They have offered advice on synthetic and analytical techniques that might aid my work, as well as been outstanding friends. I will miss them and wish them the success that they both so richly deserve.

My family has always been a source of support in my life, and particularly the past four years. Thank you, especially, to my father, who encouraged me to return to graduate school and stay the course. No matter what path I have chosen to follow, you have offered your advice and guidance, allowing me to choose the life that I want, but always hoping I chose correctly. Your love and support have meant the world to me. I would like to thank my brothers, Adam and Chuck, for countless things, in particular advice on anything from my career to my love life.

Finally, I wish to thank my new wife. While our paths have been joined for only a short time, your love and support has been the final push I needed to complete my graduate work. Your unceasing compassion and caring have made me a better person, and will make me a better teacher. I look forward to drawing from that same well for years to come, and providing you with everything you so greatly deserve.

TABLE OF CONTENTS

LIST OF TABLES

LIST OF FIGURES

Chapter I. Introduction

Of the many simple, yet eye-catching sights we come across in our everyday lives, few are more intriguing than seeing two liquids fail to mix. The separation of oil from water in a glass jar has long captured the gaze and curiosity of people in kitchens and chemistry labs, alike. Aside from the novelty of watching the two phases separate no matter how hard or long one shakes the jar, the oil and water system has significant consequences in our lives, not just on our salads. Oil/water and other liquid/liquid interfaces are used in a number of prominent chemistry applications,[1-4] biological studies,[5-7] as well as in engineering[8,9] and other fields.[10] For over 40 years the pharmaceutical industry has used partitioning across the water/octanol interface to measure the efficiency with which drugs will reach the intended target receptors in our bodies.[11] Biologists and environmental scientists have used liquid/liquid interfaces to study and imitate photosynthesis in an effort to design artificial systems for the use of solar energy.[12] Liquid/liquid interfaces are also instrumental in studies of molecular recognition of DNA[13] and environmental remediation of water supplies.[14,15] This dissertation describes efforts designed to determine the width of various liquid/liquid interfaces between water and organic solvents. In order to do so, I have probed changes in solvent polarity across liquid/liquid interfaces using a family of surfactant molecules synthesized specifically for this task. These surfactants are named molecular rulers.

In addition to the applications mentioned above, there are numerous other studies that endeavor to uncover the fundamental properties of liquid/liquid interfaces. Although small when compared to the body of work relating to other interfacial systems, including air/liquid and solid/liquid interfaces, the study of liquid/liquid interfaces is developing

rapidly. New techniques have been developed in recent years that have allowed scientists to probe these previously inaccessible, buried interfaces. Now, in fact, we have reached the point where *how* we study the interface is as important as the results of the study itself. Indeed, different methods of probing liquid/liquid interfaces produce different interpretations as they each investigate a unique quantity or property of the region. Techniques include fluorescence measurements,[16-19] X-ray reflectivity,[20] neutron scattering,[21,22] and non-linear optical spectroscopy.[23,24] Each technique probes the interface in a different way, observing or measuring a different property associated with the boundary. One important aspect common to all these studies is that they probe the equilibrium distribution of the solvent (and solute, if present) at the liquid/liquid interface. They provide information about the properties of the interface, but do not address the issue of interfacial width. The work presented in this dissertation focuses specifically on this topic.

As mentioned above, each technique that has been used to study interfaces probes a different interfacial property. Neutron and X-ray scattering experiments probe structural properties of the interface, while optical methods probe intermolecular interactions between the solvent and the probe molecules. Of the many solvent sensitive observables to choose from (including density, dielectric constant, refractive index, etc.), the work in this dissertation focuses on solvent polarity at liquid/liquid interfaces. The polarity of a solvent is related to the magnitude of the electric field inside the cavity surrounding a solute molecule in solution, which in turn depends upon the sizes of the solute and solvent dipoles and the solvent polarizability.[25] Changing the ability of the solvent to pack around the solute molecule will alter the magnitude of the electric field,

and thus the polarity of the solvent. When a solute molecule is placed at or near an interface, a change in solvent packing occurs which alters the electric field inside the solute cavity; therefore a solvent polarity different from that in bulk solution is observed.

By measuring the solvent polarity at interfacial regions we can gain insights into the solvation a probe molecule experiences at the interface. Solvation refers to the non-covalent interactions between the solvent and solute molecules. One way to measure solute-solvent interactions involves recording excitation spectra of the solute in solutions of different solvents. The solvatochromic effect describes the change in the excitation wavelength of the solute as the polarity of the solvent changes.[25,26] In solution the excited and ground state dipoles of a solute molecule are generally lowered compared to their gas phase values. If the excited state dipole is larger than the ground state dipole (as is usually the case), it will be preferentially lowered. The result is that the transition energy of the solute is decreased upon dissolving it in solution. An excitation spectrum of the solute in solution will produce a longer excitation wavelength than in the gas phase, which is termed a red shift in the excitation energy. As the solvent polarity increases the red shift becomes more pronounced due to the continued lowering of the excited state dipole. This property of the solute is called solvatochromism, and it serves as the heart of the investigations of solvent polarity at liquid/liquid interfaces presented in this work.

As an example of this phenomenon, Figure I.1 shows a plot of the excitation wavelengths of *para*-nitroanisole (PNAS) versus solvent polarity. Here solvent polarity has been characterized by the Onsager polarity function, f(D),[27]

$$f(D) = \frac{2(D-1)}{2D+1} \qquad \text{(I.1)}$$

where D is the solvent static dielectric constant. The Onsager polarity function is related to non-specific interactions between the solute and solvent molecules, and for this work is preferred to the numerous other empirical scales of solvent polarity, including the $E_T(30)$ and π^* scales.[17,28,29] In Figure I.1, as solvent polarity increases from the apolar solvents, such as cyclohexane, to the more polar solvents like acetonitrile and water, a shift of more than 20 nm in the excitation wavelength of PNAS is observed. This monotonic red shift is an indicator that the solute (PNAS) is sensitive to long-range solvation forces, such as dipole-dipole interactions and dispersion forces.[27] By recording an excitation spectrum of a solvatochromic probe molecule such as PNAS at a liquid/liquid interface we can infer the solvation environment surrounding the probe. In order to accomplish such a task, we must utilize a surface specific technique that only observes the excitation of solute molecules at the interface.

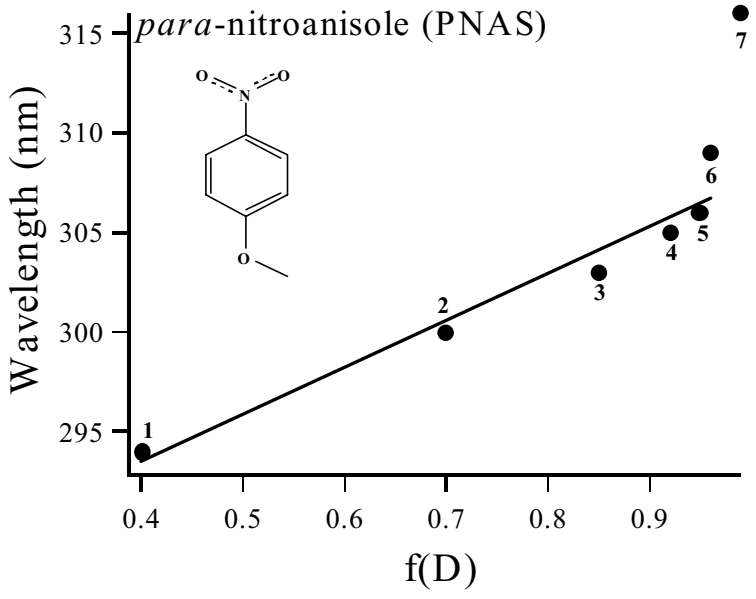

Figure I.1 Solvatochromic behavior of PNAS as a function of solvent polarity. Data correspond to bulk excitation maxima of PNAS in (1) cyclohexane, (2) diethyl ether, (3) 1-octanol, (4) ethanol, (5) methanol, (6) acetonitrile, and (7) water.

In the 1990's the technique of attenuated total internal reflectance spectroscopy (ATR) was used by Grieser and co-workers to probe the electronic absorption spectrum of 2,6-diphenyl-4-(2,4,6-triphenyl-1-pyridino) phenoxide, or $E_T(30)$ (see Figure I.2), at the interfaces between water and *n*-heptane, *n*-decane, and cyclohexane.[17] The absorption peaks of $E_T(30)$ at these interfaces led to the determination of the local solvent polarity experienced by the chromophore. In each case the maximum absorbance wavelength at the interfaces was different from values in bulk solutions of the different solvents, implying that the interfacial properties are distinct from those of either phase. In addition, Teramae and co-workers used total internal reflection fluorescence (TIRF) to observe the behavior of 8-anilo-1-naphthalenesulfonate (ANS) (see Figure I.2) at the water/heptane interface.[16] Like Greiser, Teramae determined the interfacial polarity was comprised of contributions from the aqueous and organic phases. The implementation of these techniques at liquid/liquid surfaces was a marked advancement in interfacial characterization and showed how interfacial polarity could be inferred based on the optical behavior of the probe molecule. However, results from these studies are specific to the equilibrium distribution the solute probe molecules adopt at each liquid/liquid interface, and thus no information about how polarity changes with respect to position relative to the interface is available from them. Further, while these total internal reflection (TIR) techniques are considered surface specific, meaning they sample probe behavior at the interface as opposed to in bulk solution, they are known to sample chromophore absorbance up to tens of nanometers into the solvent phase with the lower refractive index. Thus, if interfacial effects die off over shorter distances, TIR data necessarily sampled contributions from species at the surface and in bulk solution. The

ability to distinguish surface behavior from bulk solution properties is a key factor in the work presented in this dissertation.

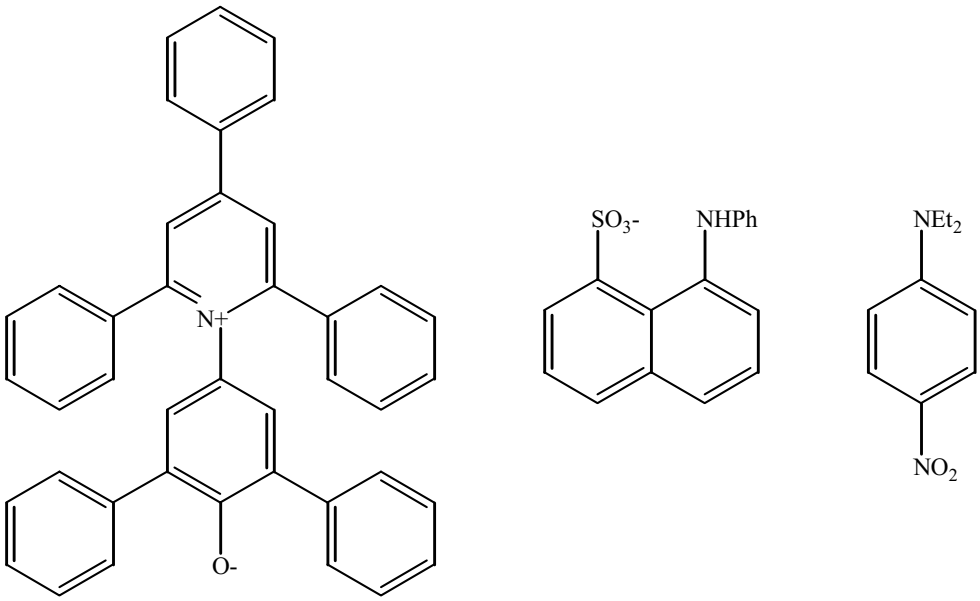

Figure I.2 Chemical structures of 2,6-diphenyl-4-(2,4,6-triphenyl-1-pyridino) phenoxide ($E_T(30)$), 8-anilo-1-naphthalenesulfonate (ANS), and N,N-diethyl-*para*-nitoaniline (DEPNA).

Another powerful technique used in the study of liquid/liquid interfaces is X-ray reflectivity. These experiments profile changes in electron density normal to the interface.[20,30] A coherent beam of X-rays penetrates one of the solvent phases and grazes the liquid/liquid interface at a shallow angle. The scattering due to each solvent is observed, which allows for the determination of the composition of the sampled region. This technique is surface specific, more so than TIRF measurements, yet it probes only solvent structure not solvent interaction with any solute species present at the liquid/liquid interface. Similarly, in neutron scattering experiments, the specular

reflectivity of neutrons off of liquid/liquid interfaces is observed.[22,31,32] As in X-ray scattering, these experiments develop a density profile across the interfacial region, only now the experiments are sensitive to proton position. Here again, the technique is surface specific, but only provides information about the solvent structure at the interface, not how the solvents interact with any solute species present.

The final technique discussed herein is the one used to conduct the work presented in the remainder of this thesis, non-linear optical second harmonic generation (SHG).[23,24] In this process, two photons of frequency ω are converted to a single photon of frequency 2ω via a nonlinear interaction with molecules. This conversion is only allowed when, within the dipole approximation, the system lacks inversion symmetry, such as at an interface between two phases or in a non-centrosymmetric crystal. The first observation of SHG was in 1961 by Franken from a crystalline quartz sample,[33] and eight years later Brown and Matsuoka reported their observations on SHG intensity as a function of adsorbed contaminants on silver surfaces, marking the first use of the technique as a probe of surface chemistry.[34] SHG has subsequently been applied to study other surfaces, including air/solid, air/liquid, solid/liquid, and liquid/liquid interfaces.[35-41] The technique is powerful not only for it ability to probe adsorption at buried surfaces, but also because it allows for the determination of the average orientation of the molecules adsorbed to interfaces.[42,43]

SHG has proven to be a valuable method for probing solvent polarity at interfaces. Recent SHG studies of solvent polarity at solid/liquid and liquid/liquid interfaces are in some cases the immediate predecessors of the work presented in this thesis, and in others they represent the foundations that this body of work is built upon.

Xiaoyi Zhang completed a number of SHG studies of solid/liquid interfaces, in the process characterizing solvent polarity in these regions as a function of solvent structure,[44] substrate functionality,[45,46] and chromophore separation from the interface.[47] Other work done at liquid/liquid interfaces includes that of Eisenthal and co-workers. Their SHG studies of aqueous/organic liquid/liquid interfaces led to the development of a model of interfacial polarity that serves as the starting point of my investigations. Using the chromophoric probe N,N-diethyl-*para*-nitoaniline (DEPNA) (see Figure I.2), Eisenthal determined that interfacial polarity could be represented by averaged contributions from the two adjacent solvent phases.[48]

Work presented in this dissertation shows that the previous models of interfacial solvation have considerable limitations. While several results indicate that interfacial polarity is dependent upon the properties of the adjacent solvent layers, including the work of Grieser, Teramae, and Eisenthal, they provide no insight as to how interfacial polarity converges to that of bulk solution limits. A series of experiments performed by Kitamura and co-workers examined the dynamic fluorescence anisotropy of sulforhodamine 101 (SR101) at the water/1,2-dichloroethane and water/carbon tetrachloride interfaces.[49] Their results indicated that the anisotropy was sensitive to the width of the interface and the location of the probe. Molecular dynamic simulations performed by Benjamin and co-workers have also predicted that the polarity should be sensitive to the solute's equilibrium distribution at the interface.[50] Much of the work presented in this dissertation addresses the issues raised in these studies, including observing polarity at different solute distributions relative to the interface and determining interfacial widths.

The remainder of this thesis is organized as follows: Chapter II briefly examines the molecular dynamics simulations that motivated the need for the development of molecular rulers. To test the predictions that interfacial polarity is sensitive to the equilibrium distribution of the solute at the liquid/liquid interface, three solutes, *para*-nitroanisole, *para*-nitrophenol, and 2,6-dimethyl-*para*-nitrophenol, were examined at the water/cyclohexane interface. Chapter III addresses the motivations for new tools for probing interfacial polarity and the methods used to produce them. It describes the synthetic procedure developed to generate molecular ruler probes, a family of ionic surfactant that has been used successfully to probe interfacial polarity at a variety of water/organic liquid/liquid interfaces. Chapter III also includes a description of the characterization of the molecular rulers, including their optical behavior, and surface activity. Finally, it reports the first use of molecular rulers as probe of interfacial solvation in SHG experiments.

Chapter IV presents a thorough investigation of solvation at weakly associating interfaces between water and alkane solvents. The four solvents used for interfacial studies include cyclohexane, methylcyclohexane, octane, and hexadecane. Results are analyzed in terms of the structural differences between the solvents, with considerations of solvent molecular volume playing a large role in the observed interfacial polarities. Chapter V repeats the same investigation found in Chapter IV, but for four strongly associating interfaces between water and 1-octanol, 1-decanol, 3-octanol, and 2,6-dimethyl-4-heptanol. As in Chapter IV, solvent structure and molecular volume are considered in the analysis of results from these strongly associating interfaces. Chapter V also includes concluding remarks and future directions that this project might lead.

Chapters III, IV, and V are all modified versions of manuscripts that either appeared in press or have been submitted for review, and as such, there is some redundancy in these chapters. The results presented in Chapter II have also appeared in press in two separate journal submissions, and will also include some redundant material.

References

(1) Freiser, H. *Chem. Rev.* **1988**, *88*, 611-616.

(2) Dorsey, J. G.; Dill, K. A. *Chem. Rev.* **1989**, *89*, 331-346.

(3) Piron, A.; Brevet, P. F.; Girault, H. H. *J. Electroanal. Chem.* **2000**, *483*, 29-36.

(4) Knock, M. M.; Bain, C. D. In *223rd ACS National Meeting*; American Chemical Society, Washington, D.C.: Orlando, FL, 2002.

(5) Leo, A.; Hansch, C.; Elkins, D. *Chem. Rev.* **1971**, *71*, 525.

(6) Watarai, H.; Freiser, H. *J. Am. Chem. Soc.* **1983**, *105*, 191-194.

(7) Shioya, T.; Nishizawa, S.; Teramae, N. *Langmuir* **199**, *15*, 2575-2579.

(8) Ueno, K.; Kitagawa, F.; Kitamura, N. *Lab on a Chip* **2002**, *2*, 231-234.

(9) Kile, D. E.; Chiou, C. T. *Environ. Sci. Technol.* **1989**, *23*, 832-838.

(10) Chhabra, V.; Free, M. L.; Kang, P. K.; Truesdail, S. E.; Shah, D. O. *Tenside, Surfactants, Detergents* **1997**, *34*, 156-168.

(11) Sangster, J. *Octanol-Water Partition Coefficients*; John Wiley and Sons: New York, 1997; Vol. 2.

(12) LeBlanc, R.; Konka, V. In *Liquid Interfaces in Chemical, Biological and Pharmaceutical Applications*; Volkov, A. G., Ed.; Marcel Dekker, Inc.: New York, 2001; Vol. 95, pp 641-648.

(13) Nakano, K. In *Liquid Interfaces in Chemical, Biological and Pharmaceutical Applications*; Volkov, A. G., Ed.; Marcel Dekker, Inc.: New York, 2001; Vol. 95, pp 515-532.

(14) Koester, C. J.; Simonich, S. L.; Esser, B. K. *Anal. Chem.* **2003**, *75*, 2813-2829.

(15) Richarson, S. D. *Anal. Chem.* **2003**, *75*, 2831-2857.

(16) Bessho, K.; Uchida, T.; Yamauchi, A.; Shioya, T.; Teramae, N. *Chem. Phys. Lett.* **1997**, *264*, 381-386.

(17) Perera, J. M.; Stevens, G. W.; Grieser, F. *Coll. & Surf. A* **1995**, *95*, 185-192.

(18) Ishizaka, S.; Kim, H.; Kitamura, N. *Anal. Chem.* **2001**, *73*, 2421-2428.

(19) Kovaleski, J. M.; Wirth, M. J. *J. Phys. Chem.* **1995**, *99*, 4091-4095.

(20) Tikhonov, A. M.; Mitrinovic, D. M.; Li, M.; Huang, Z.; Schlossman, M. L. *J. Phys. Chem. B* **2000**, *104*, 6336-6339.

(21) Penfold, J.; Richardson, R. M.; Zarbakhsh, A.; Webster, J. R. P. *J. Chem. Soc. Faraday Trans.* **1997**, *93*, 3899-3917.

(22) Cubitt, R.; Fragneto, G.; Ghosh, R. E.; Rennie, A. R. *Langmuir* **2003**, *19*, 7685-7687.

(23) Corn, R. M.; Higgins, D. A. *Chem. Rev.* **1994**, *94*, 107-125.

(24) Eisenthal, K. B. *Chem. Rev.* **1996**, *96*, 1343-1360.

(25) Suppan, P.; Ghoneim, N. *Solvatochromism*; The Royal Society of Chemistry: Cambridge, UK, 1997.

(26) Suppan, P. *J. Photochem. Photobiol. A* **1990**, *50*, 293.

(27) Onsager, L. *J. Am. Chem. Soc.* **1936**, *58*, 1486-1493.

(28) McRae, E. G. *J. Phys. Chem.* **1957**, *61*, 562.

(29) Laurence, C.; Nicolet, P.; Dalati, M. T. *J. Phys. Chem.* **1994**, *98*, 5807-5816.

(30) Daillant, J. *Current Science* **2000**, *78*, 1496-1506.

(31) Staples, E.; Penfold, J.; Tucker, I. *J. Phys. Chem. B* **2000**, *104*, 606-614.

(32) Thomas, R. K. In *General Review Characterization Methods of Surfactant Systems*; Marcel Dekker, Inc.: New York, 1999; Vol. 83, pp 417-479.

(33) Franken, P. A.; Hill, A. E.; Peters, C. W.; Weinreich, G. *Phys. Rev. Lett.* **1961**, *7*, 118-120.

(34) Brown, F.; Matsuoka, M. *Phys. Rev.* **1969**, *185*, 985-987.

(35) Lagugne-Labarthet, F.; Yu, T.; Barger, W. R.; Shenoy, D. K.; Dalcanale, E.; Shen, Y. R. *Chem. Phys. Lett.* **2003**, *381*, 322-328.

(36) Higgins, D. A.; Abrams, M. B.; Byerly, S. K.; Corn, R. M. *Langmuir* **1992**, *8*, 1992-2000.

(37) Yamaguchi, A.; Kato, R.; Nishizawa, S.; Teramae, N. *Chem. Lett.* **2003**, *32*, 798-799.

(38) Uchida, T.; Yamaguchi, A.; Ina, T.; Teramae, N. *J. Phys. Chem. B* **2000**, *104*, 12091-12094.

(39) Perrenoud-Rinuy, J.; Brevet, P. F.; Girault, H. H. *Phys. Chem. Chem. Phys.* **2002**, *4*, 4774-4781.

(40) Antoine, R.; Bianchi, F.; Brevet, P. F.; Girault, H. H. *J. Chem. Soc. Faraday Trans.* **1997**, *93*, 3833-3838.

(41) Naujok, R.; Higgins, D. A.; Hanken, D. G.; Corn, R. M. *J. Chem. Soc. Faraday Trans.* **1995**, *91*, 1411-1420.

(42) Makov, G.; Nitzan, A. *J. Phys. Chem.* **1994**, *98*, 3459-3466.

(43) Schweighofer, K.; Benjamin, I. *J. Phys. Chem. A* **1999**, *103*, 10274-10279.

(44) Zhang, X.; Cunningham, M. M.; Walker, R. A. *J. Phys. Chem. B* **2003**, *107*, 3183-3195.

(45) Zhang, X.; Esenturk, O.; Walker, R. A. *J. Am. Chem. Soc.* **2001**, *123*, 10768-10769.

(46) Zhang, X.; Walker, R. A. *Langmuir* **2001**, *17*, 4486-4489.

(47) Zhang, X.; Steel, W. H.; Walker, R. A. *J. Phys. Chem. B* **2003**, *107*, 3829-3836.

(48) Wang, H.; Borguet, E.; Eisenthal, K. B. *J. Phys. Chem. B* **1998**, *102*, 4927-4932.

(49) Ishizaka, S.; Satoshi, H.; Kim, H.; Kitamura, N. *Anal. Chem.* **1999**, *71*, 3382-3389.

(50) Michael, D.; Benjamin, I. *J. Phys. Chem. B* **1998**, *102*, 5145-5151.

Chapter II. Solvent Polarity at Liquid/Liquid Interfaces – Effects of Solute Identity

1. Introduction

Aqueous/alkane interfaces figure prominently in a host of phenomena ranging from solvent extraction to membrane modeling to emulsification.[1] As a result, there is considerable interest in characterizing the properties of these boundaries. Over the past 25 years developments in surface-specific, experimental techniques have prompted numerous studies investigating these important regions.[2-6] Various theoretical models have provided additional insight about these interfaces. Molecular dynamics simulations have developed detailed pictures of how interfaces alter solvent properties, such as density, relaxation dynamics, and long range order.[7-10] However, many predictions from these studies have not been verified due to experimental difficulties associated with accessing buried interfaces noninvasively. In this chapter, we show that different solutes sample markedly different environments *at the same interface*. While this result may seem intuitive, it does represent the first direct evidence that interfacial properties depend on more than simply the bulk properties of two adjacent phases. The materials presented in this chapter form the basis of a published communication[11] in *The Journal of the American Chemical Society* (volume 125, issue 5, pages, 1132-1133).

One property of liquid/liquid interfaces that can be probed is solvent polarity.[12,13] Solvent polarity is a measure of the electric field induced inside a solute cavity and depends on the size of the solute and solvent dipoles, as well as solvent polarizability.[14] While there is no well-defined measure of solvent polarity, as there is for other solvent

properties, such as viscosity, there are several scales used to report it.[15,16] In our work we characterize polarity using the Onsager polarity function,[16] f(D), as described in Chapter 1. The importance of solvent polarity cannot be underestimated in solution-phase chemistry. For example, Reichardt reported that the rates of S_N2 reactions depend dramatically on polarity, changing by up to seven orders of magnitude with shifting solvent polarities.[14] Given the importance of solvent polarity in solution-phase chemistry, this property should play a leading role in controlling interfacial solute concentration, conformation, and reactivity.

Several years ago, Eisenthal and co-workers used resonance enhanced second harmonic generation (SHG) to measure effective excitation spectra of known solvatochromic chromophores adsorbed to different liquid/liquid interfaces as well as the air/water interface.[12] Data revealed that the interfacial polarity could be described by averaged contributions from the two adjacent phases. A series of molecular dynamics simulations by Michael and Benjamin showed this result to be consistent with an interface that was molecularly sharp but thermally roughened.[17] These simulations also suggested that results should be very sensitive to solute distribution across the interface. Michael and Benjamin found that moving the probe molecule closer to the less polar phase (1,2-dichloroethane) caused the excitation spectrum to blue-shift compared to the excitation spectrum of the probe at the interfacial dividing surface.

In contrast to these models, Kitamura used total internal reflection fluorometry (TIRF) to study liquid/liquid interfaces and found that the average-polarity model breaks down as the polarity of the organic phase increases.[18] While interfacial polarity may well depend on solvent identity, the TIRF technique is not surface specific, and results could

represent a convolution of surface and bulk behavior of solutes. Another limitation of both SHG and fluorescence studies is the size of the probe molecules used. Typically, probe molecules have been significantly larger than solvent species, meaning that results necessarily reflect averages over several molecular diameters. The smallest probe used was N,N'-diethyl-*para*-nitroaniline (DEPNA, see Figure I.2). This molecule was employed in the SHG experiments performed by Eisenthal and co-workers, and served as the probe in simulations performed by Benjamin and co-workers. Due to its smaller size, DEPNA offers the best spatial "resolution", to date, of the experiments investigating solvent polarity at liquid/liquid interfaces. However, as simulations have predicted, interfacial polarity should shift as the position of the probe is changed relative to the interfacial plane. With the ability to adopt only one equilibrium distribution at an interface, DEPNA alone can not provide a complete analysis of interfacial polarity. To address this, a series of interfacial probes of similar structures can be observed at the same interface.

2. Experimental considerations

We have chosen to examine the interfacial polarity of the aqueous/cyclohexane interface using small, solvatochromic probes that differ subtly in their functionality. Each of the probes contains only one aromatic ring and is similar to the probes modeled by Benjamin and co-workers. The three probes are shown in Figure II.1, and include *para*-nitrophenol (PNP), *para*-nitroanisole (PNAS), and 2,6-dimethyl-*para*-nitrophenol (dmPNP). Of these three, PNAS is considerably less polar than PNP and its hydrophobic analog dmPNP. While these three compounds share similarities in their structures, they

display different partitioning behavior across liquid/liquid interfaces. Particularly, at the water/cyclohexane interface, PNP partitions to the water phase by a ratio of over 100:1, while PNAS partitions to the cyclohexane layer by approximately 20:1, and dmPNP partitions almost equally between water and cyclohexane in a 1:1 ratio. By taking advantage of these varied solubilities in an aqueous phase, we hope to slightly alter the equilibrium distribution of chromophores across the aqueous/cyclohexane interface. In doing so we can begin to test predictions about how the properties of an aqueous phase converge to those of an organic phase across an interfacial region.

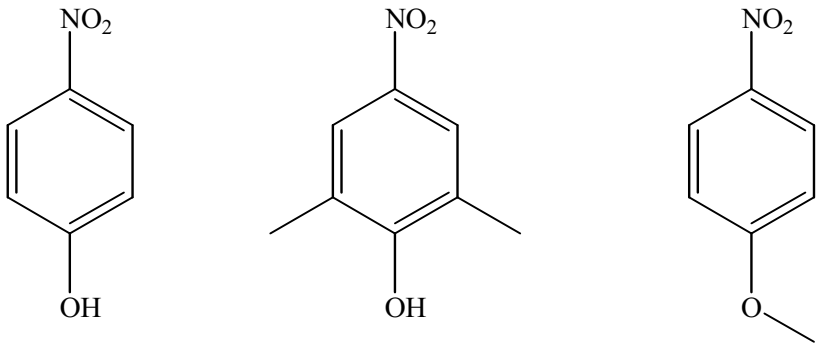

PNP dmPNP PNAS

Figure II.1 Chemical structures of *para*-nitrophenol (PNP), 2,6-dimethyl-*para*-nitrophenol (dmPNP), and *para*-nitroanisole (PNAS).

All three of these solutes show negative solvatochromism, meaning that first excited-state excitation energies red-shift with increasing solvent polarity.[19] The origin of this red shift is due to preferential solvation of each solute's more polar excited state relative to their respective ground states. Figure II.2 shows the solvatochromic behavior of both PNP and dmPNP plotted as excitation wavelength versus solvent polarity. As in

the plot of the solvatochromic response of PNAS in Figure I.1, solvent polarity has been characterized by the Onsager polarity function, f(D):

$$f(D) = \frac{2(D-1)}{2D+1} \qquad \text{(II.1)}$$

where D is the solvent static dielectric constant.

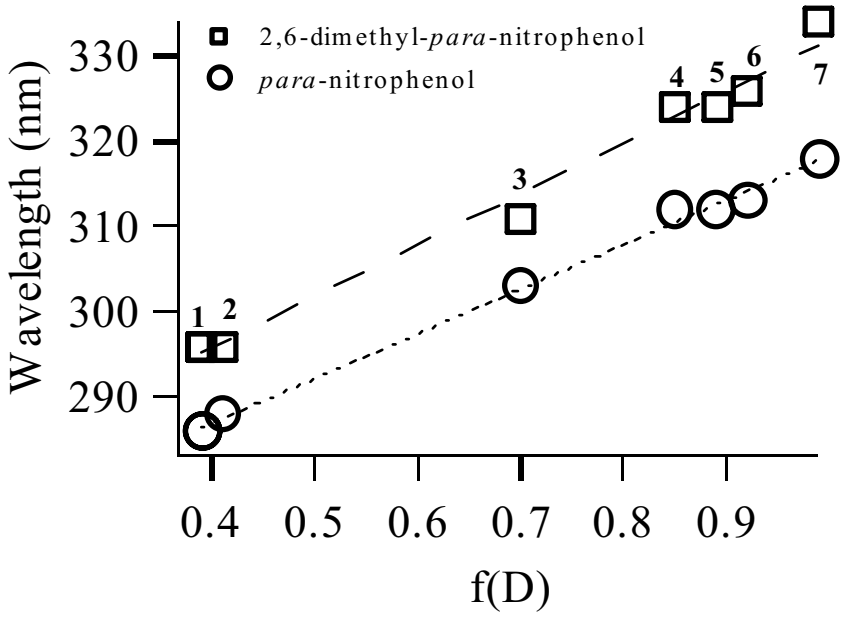

Figure II.2. Solvatochromic behavior of dmPNP (squares) and PNP (circles) in bulk solvents: (1) octane, (2) cyclohexane, (3) diethyl ether, (4) octanol, (5) hexanol, (6) ethanol, and (7) water.

The monotonic solvatochromic behavior of both PNP and dmPNP (and PNAS as shown in Figure I.1) as a function of solvent polarity indicates that these solutes are sensitive primarily to long-range, nonspecific dipolar forces such as those used in dielectric continuum models.[19,20] The entire excitation window of dmPNP is red-shifted slightly from that of PNP due to the electron donating properties of the two methyl

substituents. The larger window of excitation maxima for dmPNP relative to PNP and PNAS (38 nm vs. 30 nm and 24 nm, respectively) suggests that the dmPNP undergoes a larger change in dipole upon excitation from the ground to the first excited electronic state.

To probe the solvatochromic behavior of these solutes at the water/cyclohexane interface, we have used SHG to measure effective excitation spectra of adsorbed species. Briefly, this surface specific technique is sensitive to the energetics and orientation of electronic transition moments.[5,21,22] The intensity of the detected SH signal (at 2ω) scales quadratically with the second-order susceptibility, $\chi^{(2)}$:

$$I(2\omega) \alpha | \chi^{(2)} |^2 \; I(\omega)^2 \qquad \text{(II.2)}$$

where I(ω) is the intensity of the incident field and $\chi^{(2)}$ is a third rank tensor that under the dipole approximation is zero in isotropic environments. The $\chi^{(2)}$ tensor is responsible for the technique's inherent surface specificity and contains both resonant and nonresonant contributions. The resonant contribution to $\chi^{(2)}$ is typically much larger than the nonresonant piece and can be related to the molecular hyperpolarizability:

$$\chi_R^{(2)} = \sum_{k,e} \frac{\left\langle \mu_{gk} \mu_{ke} \mu_{eg} \right\rangle}{(\omega_{gk} - \omega - i\Gamma)(\omega_{eg} - 2\omega + i\Gamma)} \qquad \text{(II.3)}$$

where μ_{ij} is the transition matrix element between states i and j. (Here, g refers to the ground state, k to an intermediate, virtual state, and e to contributing excited states.) Brackets denote an orientational average over all contributing states. When 2ω is resonant with ω_{eg}, $\chi^{(2)}_R$ becomes large, leading to a strong enhancement in the observed intensity at 2ω. Thus, measuring the scaled intensity [$I(2\omega)/I^2(\omega)$] as a function of 2ω records *effective* excitation spectra of solutes adsorbed to liquid/liquid interfaces.

Previous SHG experiments of solid/liquid interfaces have shown that interfacial solvent polarity depends sensitively on the intermolecular forces between the two phases.[23]

3. Results and discussion

Figure II.3 shows SH spectra of PNP, PNAS, and dmPNP adsorbed to water/cyclohexane interfaces. Overlaid on each spectrum are dotted and dashed lines denoting the excitation maxima of each species in bulk cyclohexane and water, respectively. Interfacial polarity models based on averaged contributions from adjacent

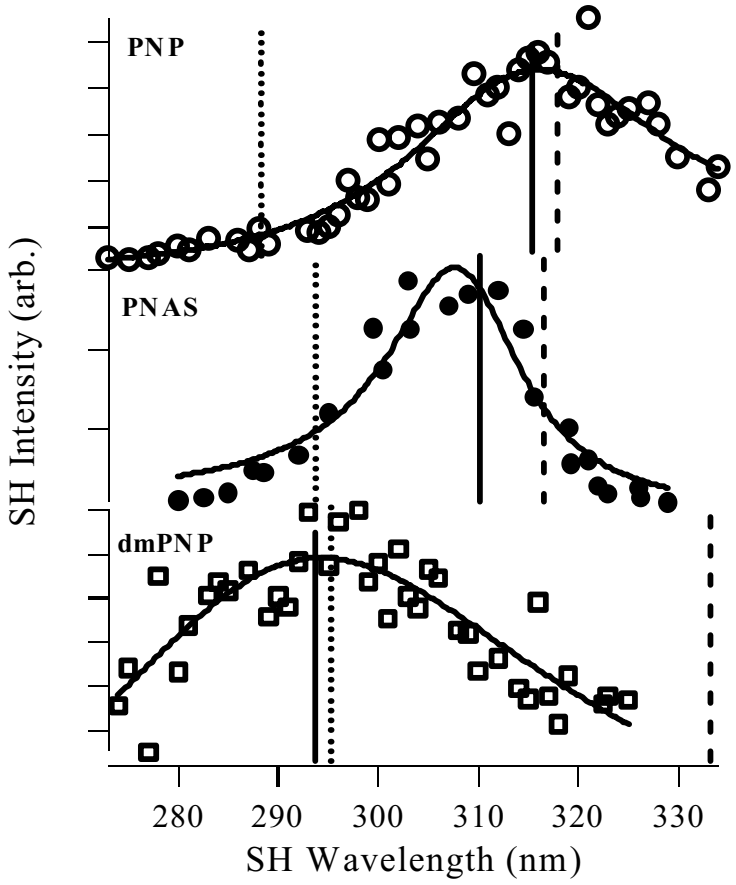

Figure II.3. SH spectra of PNP (open circles), PNAS (filled circles), and dmPNP (open squares) at the water/cyclohexane interface. Dotted and dashed lines denote excitation maxima of each species in cyclohexane and water, respectively. (Note that the nonresonant contribution to $\chi^{(2)}$ can shift the excitation maximum from the apparent spectral maximum.)

phases predict that the SH spectra should show maxima at approximately 303 nm for PNP, 305 nm for PNAS, and 315 nm for dmPNP. The spectra in Figure II.3 clearly contradict these predictions, and indicate that each solute samples a unique solvation environment at the same interface. While all solutes are studied at comparable surface concentrations at identical interfaces, the PNP samples a polar environment as evidenced by the SHG maximum of 315 nm. This is very close to the bulk excitation maximum of PNP in water (318 nm). PNAS is surrounded by an environment that reflects contributions from both the aqueous and organic phases. In contrast, the interfacial polarity probed by dmPNP is the same as that in bulk cyclohexane (λ_{max} = 296 nm).

The dramatic differences in solvent polarity observed by PNP and dmPNP appeal to intuition. The partitioning data described above indicate that PNP favors being solvated in the water phase more than 100 times over the non-polar cyclohexane phase. The presence of the two methyl groups on the dmPNP, compared to its hydrophilic analog PNP, increases the hydrophobicity of the molecule, causing the dmPNP to be preferentially solvated in the organic phase at water/cyclohexane interface. The spectra in Figure II.3 represent the first experimental observation that interfacial polarity is indeed sensitive to solute distribution at the liquid/liquid interface, as predicted by the simulations of Benjamin and co-workers.

Quantitative measurements of polarization-dependent, SH intensities support this picture of dmPNP being "pulled" upwards into the cyclohexane phase. Different polarization combinations (of ω and 2ω) sample different elements of the $\chi^{(2)}$ tensor.[24,25] Provided that the (ground and excited state) electronic structure of the probe is well

characterized, these experiments enable average molecular orientations to be calculated.[22,24,25] The average orientation of the PNP adsorbed to the water/cyclohexane interface has the pseudo-C_2 symmetry axis 55° away from the surface normal, whereas the dmPNP solutes are oriented only 43° from the surface normal. While the difference in orientations is small, it is significant and reproducible. These orientations are consistent with a picture that has both functional groups of PNP interacting with the aqueous phase and the two methyl groups of dmPNP "pulling" the solute into the organic phase. The cartoon in Figure II.4 depicts a schematic representation of this effect.

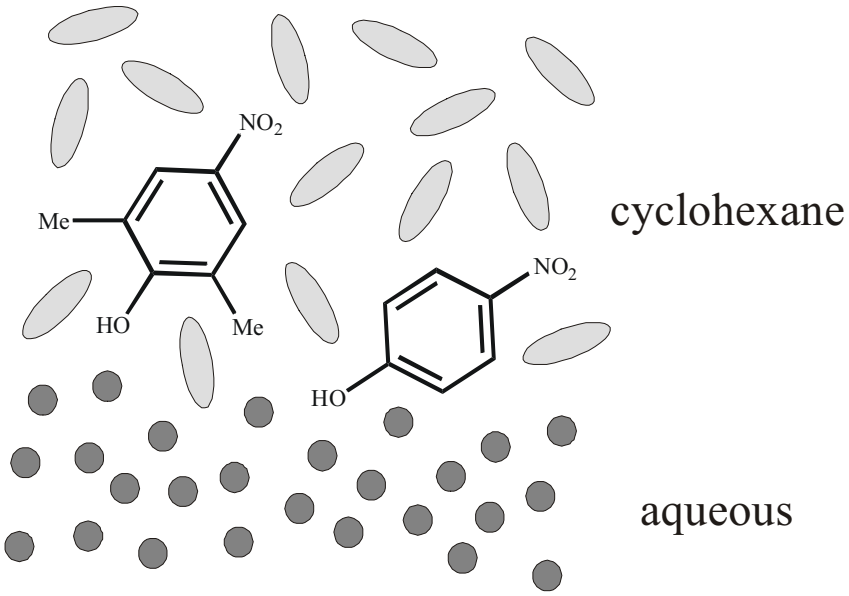

Figure II.4. A schematic representation of dmPNP and PNP orientations at the water/cyclohexane interface.

While the partitioning data and orientation measurements provide a reasonable explanation for the behavior displayed by PNP and dmPNP, they fail to explain the interfacial polarity sampled by PNAS. The hydrophilic PNAS partitions more than 20:1 into the cyclohexane phase, and we might expect it to sample an interfacial polarity indicative of a bulk alkane at the water/cyclohexane interface. However, the spectra in Figure II.3 indicate that PNAS is surrounded by an environment reflecting contributions from both the aqueous and organic phases. PNAS differs from PNP and dmPNP in that it lacks the ability to donate a hydrogen bond to the polar water phase. Studies of PNAS at solid/liquid interfaces[21] determined that it was capable of adopting two orientations, a "nitro up" and a "nitro down". In each orientation the probe sampled a different polarity, one polar and one non-polar. In SH spectra of PNAS at these interfaces there were two peaks, one for each orientation. The spectrum of PNAS adsorbed to the water/cyclohexane interface in Figure II.3 contains only one peak, and therefore we conclude that the interfacial PNAS molecules adopt the same orientation. Unsuccessful attempts were made to record orientation measurements of PNAS at the water/cyclohexane interface, and we are therefore unable to state the orientation of these probe molecules relative to surface normal. Regardless, the collection of spectra in Figure II.3 indicates that each solute samples a unique environment and that details are very sensitive to solute structure.

4. Conclusion

To summarize, the data collected at the water/cyclohexane interface show that subtle alterations of solute structure can alter significantly the solute's local solvation

environment at *the same* liquid/liquid interface. This finding implies that the interfacial chemical environment is determined as much by the identity of the solute as by gradients in the solvent properties across the interfacial boundary and supports predictions that dramatic changes in solvation should accompany small changes in solute position relative to a sharp boundary. As a consequence, emerging models of solution phase surface chemistry must consider solute location within the anisotropic, interfacial region.[26-28] Despite these findings, there is no information about how interfacial solvent polarity converges to bulk solution limits. These results strongly motivate the need for accurate, experimental profiles of how solvent properties change across different liquid/liquid interfaces.

References

(1) Safran, S. A. *Statistical Thermodynamics of Surfaces, Interfaces, and Membranes*; Addison-Wesley: Reading, MA, 1994.

(2) Wirth, M. J.; Burbage, J. D. *J. Phys. Chem.* **1992**, *96*, 9022-9025.

(3) Mitrinovic, D. M.; Zhang, Z.; Williams, S. M.; Huang, Z.; Schlossman, M. L. *J. Phys. Chem. B* **1999**, *103*, 1779-1782.

(4) Penfold, J.; Richardson, R. M.; Zarbakhsh, A.; Webster, J. R. P. *J. Chem. Soc. Faraday Trans.* **1997**, *93*, 3899-3917.

(5) Eisenthal, K. B. *J. Phys. Chem.* **1996**, *100*, 12997-13006.

(6) Scatena, L. F.; Richmond, G. L. *J. Phys. Chem. B* **2001**, *105*, 11240-11250.

(7) Benjamin, I. *Chem. Rev.* **1996**, *96*, 1449-1475.

(8) Chipot, C.; Wilson, M. A.; Pohorille, A. *J. Phys. Chem. B* **1997**, *101*, 782-791.

(9) Dang, L. X. *J. Phys. Chem. B* **2001**, *105*, 804-809.

(10) Senapti, S.; Berkowitz, M. L. *Phys. Rev. Lett.* **2001**, *87*, 176101.

(11) Steel, W. H.; Walker, R. A. *J. Am. Chem. Soc.* **2003**, *125*, 1132-1133.

(12) Wang, H.; Borguet, E.; Eisenthal, K. B. *J. Phys. Chem. B* **1998**, *102*, 4927-4932.

(13) Ishizaka, S.; Satoshi, H.; Kim, H.; Kitamura, N. *Anal. Chem.* **1999**, *71*, 3382-3389.

(14) Rieichardt, C. *Solvents and Solvent Effect in Organic Chemistry*; 3rd ed.; Wiley-VCH: Weiheim, Germany, 2003.

(15) Matyushov, D. V.; Schmid, R.; Ladanyi, B. M. *J. Phys. Chem. B* **1997**, *101*, 1035-1050.

(16) Onsager, L. *J. Am. Chem. Soc.* **1936**, *58*, 1486-1493.

(17) Michael, D.; Benjamin, I. *J. Phys. Chem. B* **1998**, *102*, 5145-5151.

(18) Ishizaka, S.; Kim, H.; Kitamura, N. *Anal. Chem.* **2001**, *73*, 2421-2428.

(19) Suppan, P.; Ghoneim, N. *Solvatochromism*; The Royal Society of Chemistry: Cambridge, UK, 1997.

(20) Wong, M. W.; Frisch, M. J.; Wiberg, K. B. *J. Am. Chem. Soc.* **1991**, *113*, 4776-4782.

(21) Zhang, X.; Cunningham, M. M.; Walker, R. A. *J. Phys. Chem. B* **2003**, *107*, 3183-3195.

(22) Zhuang, X.; Miranda, P. B.; Kim, D.; Shen, Y. R. *Phys. Rev. B* **1999**, *59*, 12632-12640.

(23) Zhang, X.; Esenturk, O.; Walker, R. A. *J. Am. Chem. Soc.* **2001**, *123*, 10768-10769.

(24) Dick, B.; Gierulski, A.; Marowsky, G. *Appl. Phys. B* **1985**, *38*, 107-116.

(25) Simpson, G. J.; Rowlen, K. L. *Acc. Chem. Res.* **2000**, *33*, 781-789.

(26) Stefanovich, E. V.; Troung, T. N. *J. Chem. Phys.* **1997**, *106*, 7700-7705.

(27) Schweighofer, K.; Benjamin, I. *J. Phys. Chem. A* **1999**, *103*, 10274-10279.

(28) Senapti, S.; Chandra, A. *Chem. Phys.* **1999**, *242*, 353-366.

Chapter III. Molecular Rulers –

New Families of Molecules for Measuring Interfacial Widths

1. Introduction

The data presented in Chapter II indicated that interfacial polarity is sensitive to the equilibrium distribution of the solute at the liquid/liquid interface, but the neutral probes used provided no information about how interfacial polarity converges to bulk solution limits. This chapter describes the synthesis and characterization of new molecules that are designed to profile solvent polarity at liquid/liquid interfaces by incorporating a hydrophobic, solvatochromic probe and an ionic sulfate joined by a variable alkyl spacer. This combination gives the molecules surface specificity and makes them appropriate probes of interfacial polarity. The materials presented in this chapter form the basis of a published article in *The Journal of the American Chemical Society*.[1]

Common experience shows that oil and water don't mix and that water will wet a hydrophilic substrate but not a hydrophobic substrate. Supporting these observations are numerous experimental and theoretical investigations that demonstrate how surfaces alter the properties of an adjacent solvent from bulk solution limits.[2-6] These findings appeal to intuition. Boundaries between a solid and a liquid or two immiscible liquids create environments in which an imbalance in forces leads to large changes in long-range solvent structure, density and polarity.[7-12]

Less intuitive are the characteristic lengthscales over which these surface induced effects extend. Given that surface-mediated solvent properties control the concentration,

conformation and reactivity of adsorbed solute species, determining the width of interfacial regions has the potential to impact significantly models and mechanisms of solution-phase, surface chemistry.[13] Affected phenomena can be as simple as elementary surface reactions whose rates depend sensitively on solvent polarity[14,15] or as complex as protein recognition at cell membrane surfaces – an event that is exceedingly sensitive to local gradients in pH and ionic strength.[16] Chemical transport across liquid interfaces – the heart of solvent extraction – depends on interfacial solvent viscosity, permittivity and relaxation rates.[17]

Previous experimental studies of interfacial solvation characterized solvent polarity at the boundaries between weakly associating, immiscible liquids.[18-20] Here, the term weakly associating refers to two adjacent phases (aqueous and organic) that interact through weak dipole-dipole or dispersion forces. The model of interfacial polarity that emerges from nonlinear optical (NLO) experiments is that of an interface whose dielectric properties reflect a simple, averaged contribution from the two adjacent phases.[8] While this result may seem surprising at first, given the strong anisotropy inherent to interfacial regions, the effect can be understood in terms of a liquid/liquid interface that is both a) molecularly sharp – properties of one phase converge to those of the other in only a few solvent layers and b) microscopically flat – very little thermal roughening on the molecular scale due to capillary wave activity. Such a picture is consistent with simulations describing the interfacial properties between an aqueous solvent and a nonpolar, hydrocarbon solvent.[21-27]

Other studies, however, suggested that the "average-polarity" model breaks down when the adjacent organic solvent is polar (but aprotic). Specifically, interfacial polarity

inferred from fluorescence measurements at polar aqueous/organic interfaces was considerably less than that predicted by averaged contributions from the two adjacent phases. This result could indicate an interface that was either molecularly diffuse or thermally roughened, although simulations predict that a roughened interface should be *more polar* than a molecularly flat boundary.[20] Further complicating interpretation of the fluorescence results is the fact that the technique is not surface specific, meaning that even experiments carried out under total internal reflection conditions sample up to tens of nanometers into the phase with the lower refractive index. In contrast, nonlinear optical experiments *are* surface specific, with signals originating only within the anisotropic boundary between two isotropic phases.

While these NLO, fluorescence and molecular dynamics studies of interfacial solvation raise important questions about how interfacial anisotropy influences the local chemical environment *experienced by solutes*, the experiments themselves suffered from several limitations. First, the probes were generally large relative to the size of solvent species in each phase. In some cases, the probes consisted of fused aromatic systems containing up to seven six-membered rings and several sites with formal positive or negative charges.[19,20] Solvation around such large solutes necessarily reflects an average of the environment sampled by the solute, thus claims about the lengthscales over which solvation forces change are limited to minimum distances of the ~1.5 nm (or ~5 water layers) spanned by the solute. The smallest probe – N,N-diethyl-*para*-nitroaniline (DEPNA, see Figure I.1) – was used in nonlinear optical measurements characterizing solvent polarity at the air/aqueous and several organic/aqueous interfaces.[18] While the optically active part of the DEPNA chromophore is similar in size to the organic solvents

used, experiments were sensitive only to the equilibrium distributions and orientations of solutes at the different interfaces.[28] Missing was information about *how* the interfacial properties converged from aqueous to a nonpolar, organic limits. In order to understand the origins and extent of interfacial solvation, experiments must be able to discern how chemical solvation around a solute varies as the solute changes its equilibrium position relative to a nominal interfacial plane.

These considerations highlight the need to profile accurately solvation *across* different aqueous/organic, liquid/liquid boundaries as well as the interfaces formed between different solids and liquids. Accomplishing this goal requires tools that measure interfacial width. Described below are the methods used to create a homologous series of surfactants capable of probing changes in solvent environment on molecular length scales. These "molecular rulers" consist of hydrophobic, solvent-sensitive chromophores attached to polar or charged headgroups by means of simple, variable length alkyl spacers. At liquid surfaces, molecular rulers form monolayers that span the interfacial region, as depicted schematically in Figure III.1. The solvent-sensitive chromophore response provides a means of observing how the local solvation environment changes as a function of chromophore-headgroup separation. Implicit in this admittedly simple, schematic model is that the charged headgroup remains solvated in the aqueous phase while the hydrophobic, solvent-sensitive chromophore "floats" into the organic phase.

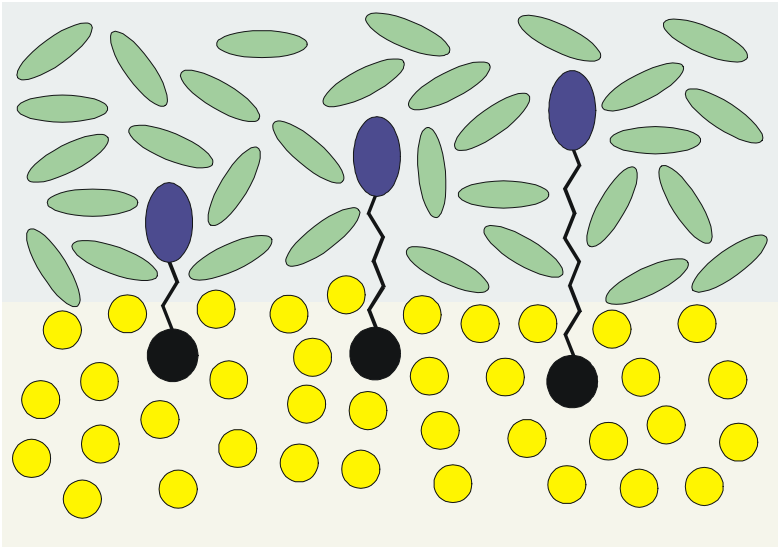

Figure III.1. A schematic representation of molecular rulers adsorbed to a liquid/liquid interface.

The "resolution" of these rulers is limited by the size of the hydrophobic chromophore – intentionally chosen to be as small as possible – and the minimum size by which the spacers can be varied – nominally a single CH_2 group or ~1.5 Å. While these rulers can not provide unambiguous information about how solvent properties and structure vary across an interface, the solvent-sensitive response of the ruler chromophore can identify how the local chemical environment surrounding a solute changes with the solute's equilibrium distribution relative to an interfacial boundary. Results from surface specific, nonlinear optical experiments show that this approach to measuring interfacial width holds tremendous potential for clarifying how surfaces impact solvation and how far into a solvent surface mediated effects extend.

Surfactants described below are but one example of a general strategy designed to measure changes in local environment on *molecular lengthscales*. The emphasis of this work is on the synthesis and characterization of a class of novel surfactants that can overcome the aforementioned limitations associated with experiments examining

interfacial solvation. This approach of altering the equilibrium distribution of solutes across an interfacial boundary promises to provide quantitative information that can spur the development of more accurate solvation models. Molecular rulers may also find applications in environmentally and biologically important systems where knowledge about changes in chemical environment on sub-nm lengthscales is essential for formulating mechanisms of interfacial reactivity. Different applications may require using chromophores having different photophysical properties. Furthermore, molecular rulers can be constructed specifically for x-ray and neutron scattering experiments by incorporating probes with sufficiently large scattering cross-sections at different positions within the ruler structure.

2. Criteria and Synthetic Overview

In order to profile solvation across different interfaces, molecular rulers must satisfy three criteria: a) rulers must exhibit measurable sensitivity to changes in local solvation; b) rulers must be surface active and c) rulers must be modular with simple synthetic methods for varying the separation between headgroup and chromophore.

2A. Solvent Sensitivity

Solute solvatochromism can serve as a sensitive probe of local solvation environment.[29] Solvatochromism describes the solvent sensitive shifts of a chromophore's transition energy and arises from the differential solvation of a solute's ground and excited states. If the chromophore's excited state dipole is larger than its ground state dipole, the excited state will be preferentially solvated, leading to a

spectroscopically observable red-shift in the solute excitation spectrum relative to its gas phase value. This red-shift becomes more pronounced with increasing solvent polarity.

Molecular rulers described in this work incorporate a derivative of *para*-nitroanisole (PNAS), a photoactive chromophore whose excitation wavelength red-shifts more than 20 nm as solvent polarity increases from that of cyclohexane to that of water.[30] The PNAS chromophore is ideal for use in molecular rulers because of its photochemical stability and its large change in permanent dipole upon excitation.[31] Furthermore, the small size of PNAS imparts finer spatial resolution to molecular rulers than would be afforded with large chromophores having extensive, delocalized electronic structures. Experiments profiling interfacial width will exploit these advantages by measuring effective excitation spectra of PNAS based molecular rulers adsorbed to different solid/liquid and liquid/liquid boundaries.

2B. Surface Activity

The pairing of a hydrophobic probe and polar or ionic headgroup ensures that molecular rulers will be surface active. Surface activity is monitored by measuring the interfacial tension at liquid/liquid interfaces. The Gibbs isotherm for soluble monolayers provides a relationship between the excess surface concentration and the interfacial pressure:[32]

$$A\pi = A(\gamma_o - \gamma) = \Gamma kT ln(c) \qquad \text{(III.1)}$$

Here, π is the interfacial pressure (the difference between the surface tensions of the neat interface (γ_o) and the system under study (γ)), A is the interfacial area, Γ is the surface excess concentration, k is Boltzmann's constant, T is temperature, and *c* is the bulk concentration of molecular ruler. At low bulk concentrations, the activity is assumed to

be equivalent to concentration. Differentiating surface pressure with respect to *ln*(c) leads to the expression:

$$\frac{\partial \pi}{\partial ln(c)} = \frac{\Gamma}{A} kT \quad \text{(III.2)}$$

The limiting terminal surface concentration of the molecular ruler monolayers can be determined by plotting π vs. *ln*(c) and determining the slope of steepest ascent.

3. Experimental methods

Scheme III.1 depicts the two-step synthesis used to create neutral and ionic molecular rulers. The starting material, *para*-nitrofluorobenzene (pNFB), is converted to the desired product **3n** by adding the 1,n–diol of desired length in the correct ratio to maximize the yield of the monomer.[33] After purification the alcohol is converted to an ionic salt upon reaction with chlorosulfonic acid according to published procedures.[34] Assuming an all-*trans* conformation, each methylene group increases the separation between the hydrophilic headgroup and hydrophobic chromophore by approximately 1.5 Å. This assumption is certain to break down with longer chains, but alkyl spacers up to five CH_2 groups in length should have either one or zero *gauche* defects.[35] The issue of alkyl chain conformation is discussed below in greater detail.

All reagents used were purchased from Aldrich and used without further purification. Diethyl ether was distilled from sodium/benzophenone ketyl. All reactions were run under an atmosphere of nitrogen. All compounds were >95% pure as determined by ^{1}H and ^{13}C NMR spectroscopy. Nuclear magnetic resonance (^{1}H and ^{13}C NMR) spectra were recorded on a 400 MHz spectrometer. Chemical shifts are reported in parts per million, relative to nondeuterated solvent peak. Coupling constant (*J* values)

are reported in hertz, and spin multiplicities are indicated by the following symbols: s (singlet), d (doublet), t (triplet), q (quartet), m (multiplet), br s (broad singlet). Infrared band positions are given in reciprocal centimeters (cm^{-1}) and relative intensities are listed as br (broad), s (strong), m (medium), or w (weak). Thin-layer chromatography (TLC) was performed with the compounds being identified in one or both of the following manners: UV (254 nm) and iodine.

Scheme 1. Molecular Ruler Synthesis. In the text, rulers are assigned notations to distinguish their functionality (neutral alcohol, 3n, or ionic sulfate, 4n) and length. The lengths of the alkyl spacers present follow this scheme: "a" designates a two-carbon spacer, "b" a three-carbon spacer, "c" a four-carbon spacer, and so on. Thus, 3a is the neutral alcohol containing a two-carbon spacer.

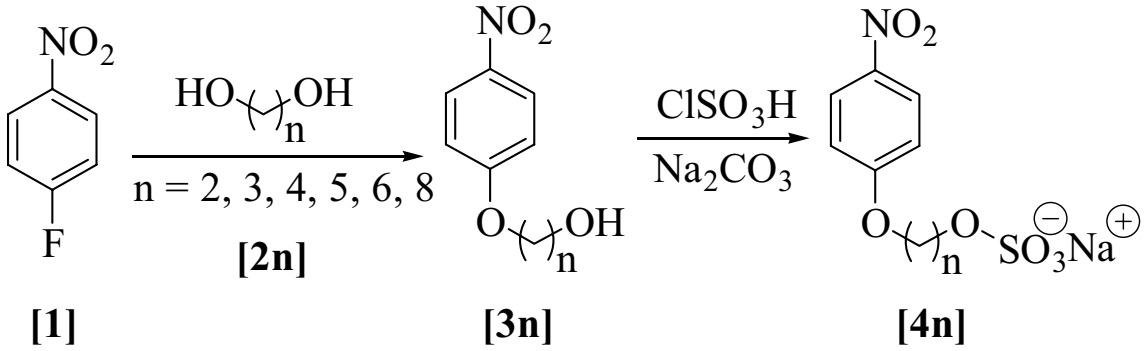

3A. Synthesis of Molecular Ruler Alcohol Precursors.

para-Nitrofluorobenzene (pNFB) was added dropwise to the mixture of diol and potassium hydroxide (KOH) at RT and stirred for 2 hours. The reaction mixture was poured into water and extracted with diethyl ether. In addition to the desired product a 1,*n*-dimer and the residual staring material were also extracted into the ether. Purification of the reaction mixture residue by flash chromatography (hexanes: EtOAc, 3:2) gave the desired alcohol and starting material. The spectral data of the individual compounds are reported below.

2-(4-nitrophenoxy)-ethanol (3a). Compound **3a** was prepared by following the general procedure employing pNFB (0.998 g, 7.07 mmol), ethylene glycol (3.51 g, 56.5 mmol), and KOH (0.500 g, 8.91 mmol). Purification of the reaction mixture gave 0.215 g (22%) of pNFB and 0.694 g (54%) of **3a** as a white solid: m.p. 83-85 °C; R_f = 0.20 (hexanes: EtOAc, 3:2); IR (KBr) 3262 (s), 3106 (w), 2947 (w), 1503 (s), 1340 (s); ^{1}H NMR ($CDCl_3$) 2.02 (s, 1H), 4.01 (t, *J* = 4.4, 2H), 4.17 (t, *J* = 4.4, 2H), 6.98 (d, *J* = 9.2, 2H), 8.20 (d, *J* = 9.2, 2H); ^{13}C NMR ($CDCl_3$) 61.1, 70.0, 114.5, 125.9, 141.7, 163.6; LRMS (EI) 183 (M^+, 66), 139 (100); HRMS (EI) calcd for $C_8H_9O_4N$ 183.0532 (M^+), found 183.0536. Supporting information in Appendix A, pp. 135 – 138.

3-(4-nitrophenoxy)-propanol (3b). Compound **3b** was prepared by following the general procedure employing pNFB (0.998 g, 7.07 mmol), 1, 3-propanediol (4.26 g, 56.0 mmol), and KOH (0.500 g, 8.91 mmol). Purification of the reaction mixture gave 0.335 g (34%) of pNFB and 0.715 g (51%) of **3b** as a yellow oil: R_f = 0.25 (hexanes: EtOAc, 3:2); IR (NaCl) 3358 (s), 3115 (w), 2952 (w), 1510 (s), 1265 (s); ^{1}H NMR ($CDCl_3$) 2.02 (dd, *J* = 6.0, 6.0, 2H), 2.33 (s, 1H), 3.80 (t, *J* = 6.0, 2H), 4.15 (t, *J* = 6.0, 2H), 6.89 (d, *J* = 9.2, 2H), 8.10 (d, 2H); ^{13}C NMR ($CDCl_3$) 31.6, 59.1, 65.7, 114.3, 125.8, 141.2, 163.9. LRMS (FAB) 198 ($(M+H)^+$, 100); HRMS (FAB) calcd for $C_9H_{12}O_4N$ 198.0766 $(M+H)^+$, found 198.0764. Supporting information in Appendix A, pp. 139 – 142.

4-(4-nitrophenoxy)-butanol (3c). Compound **3c** was prepared by following the general procedure employing pNFB (0.998 g, 7.07 mmol), 1, 4-butanediol (3.19 g, 35.4 mmol), and KOH (0.500 g, 8.91 mmol). Purification of the reaction mixture gave 0.437 g (44%) of pNFB and 0.621 g (44%) of **3c** as a white solid: m.p. 78-80 °C; R_f = 0.26 (hexanes: EtOAc, 3:2); IR (KBr) 3527 (s), 3115 (w), 2954 (w), 1508 (s), 1262, (s); ^{1}H NMR

($CDCl_3$) 1.45 (s, 1H), 1.75 (q, *J* = 6.2, 2H), 1.91 (q, *J* = 6.2, 2H), 3.72 (t, *J* = 6.2, 2H), 4.08 (t, *J* = 6.2, 2H), 6.92 (d, *J* = 9.2, 2H), 8.17 (d, *J* = 9.2, 2H); ^{13}C NMR ($CDCl_3$) 25.5, 29.1, 62.4, 68.6, 114.4, 125.9, 141.4, 164.0; LRMS (FAB) 212 ($(M+H)^+$, 100), 140 (67); HRMS (FAB) calcd for $C_{10}H_{14}O_4N$ 212.0923 $(M+H)^+$, found 212.0928. Supporting information in Appendix A, pp. 143 – 146.

5-(4-nitrophenoxy)-pentanol (3d). Compound **3d** was prepared by following the general procedure employing pNFB (2.00 g, 14.1 mmol), 1, 5-pentanediol (8.78 g, 84.3 mmol), and KOH (1.03 g, 18.3 mmol). Purification of the reaction mixture gave 0.363 g (18%) of pNFB and 2.09 g (66%) of **3d** as a yellow oil: R_f = 0.20 (hexanes: EtOAc, 3:2); IR (NaCl) 3361 (s), 3111 (w), 2940 (w), 1511 (s), 1265 (s); ^{1}H NMR ($CDCl_3$) 1.27 (t, *J* = 6.0, 1H), 1.50-1.60 (m, 2H), 1.60-1.65 (m, 2H), 1.80-1.90 (m, 2H), 3.68 (q, *J* = 6.0, 2H), 4.05 (t, *J* = 6.4, 2H), 6.92 (d, *J* = 9.2, 2H), 8.27 (d, *J* = 9.2, 2H); ^{13}C NMR ($CDCl_3$) 22.2, 28.7, 32.2, 62.6, 68.6, 114.3, 125.9, 141.3, 164.1. LRMS (FAB) 226 ($(M+H)^+$, 100), 69 (77); HRMS (FAB) calcd for $C_{11}H_{16}O_4N$ 226.1079 $(M+H)^+$, found 226.1085. Supporting information in Appendix A, pp. 147 – 150.

6-(4-nitrophenoxy)-hexanol (3e). Compound **3e** was prepared by following the general procedure employing pNFB (2.00 g, 14.1 mmol), 1, 6-hexanediol (8.30 g, 70.2 mmol), and KOH (1.03 g, 18.3 mmol) at 50 – 60 °C. Purification of the reaction mixture gave 0.321 g (16%) of pNFB and 0.213 g (63%) of **3e** as a white solid: m.p. 80-83 °C; R_f = 0.31 (hexanes: EtOAc, 3:2); IR (KBr) 3516 (s), 3115 (w), 2930 (w), 1500 (s), 1258 (s); ^{1}H NMR ($CDCl_3$) 1.28 (s, 1H), 1.40-1.65 (m, 6H), 1.80-1.85 (m, 2H), 3.65 (s, 2H), 4.03 (t, *J* = 6.4, 2H), 6.91 (d, *J* = 9.2, 2H), 8.17 (d, *J* = 9.2, 2H); ^{13}C NMR ($CDCl_3$) 25.5, 25.7, 28.9, 32.6, 62.8, 68.7, 114.4, 125.9, 141.3, 164.1; LRMS (FAB) 240 ($(M+H)^+$, 99), 55

(100); HRMS (FAB) calcd for $C_{12}H_{18}O_4N$ 240.1236 $(M+H)^+$, found 240.1233. Supporting information in Appendix A, pp. 151 – 154.

8-(4-nitrophenoxy)-octanol (3f). Compound **3f** was prepared by following the general procedure employing pNFB (0.998 g, 7.07 mmol), 1, 8-octanediol (6.20 g, 42.4 mmol), and KOH ((0.500 g, 8.91 mmol) at 50 – 60 °C. Purification of the reaction mixture gave 0.345 g (35%) of pNFB and 0.923 g (49%) of **3f** as a white solid: m.p. 86-88 °C; R_f = 0.35 (hexanes: EtOAc, 3:2); IR (KBr) 3516 (s), 3111 (w), 2929 (w), 1499 (s), 1260 (s); ^{1}H NMR ($CDCl_3$) 1.24 (t, *J* = 5.6, 1H), 1.30-1.60 (m, 10H), 1.75-1.85 (m, 2H), 3.63 (q, *J* = 5.6, 2H), 4.02 (t, *J* = 6.4, 2H), 6.91 (d, *J* = 9.2, 2H), 8.17 (d, *J* = 9.2, 2H); ^{13}C NMR ($CDCl_3$) 25.6, 25.8, 28.9, 29.2, 29.3, 32.7, 63.0, 68.8, 114.4, 125.9, 141.3, 164.2; LRMS (FAB) 268 ($(M+H)^+$, 56), 69 (100); HRMS (FAB) calcd for $C_{14}H_{22}O_4N$ 268.1549 $(M+H)^+$, found 268.1546. Supporting information in Appendix A, pp. 155 – 158.

3B. Synthesis of Molecular Rulers.

Chlorosulfonic acid was added to the solution of the corresponding alcohol in diethyl ether at RT and stirred for one hour. A 10% sodium carbonate solution was added until the pH rose to 10. The water and any remaining ether were then removed by rotary evaporation. The product is separated from mixture of solids with several acetonitrile extractions. Evaporating the acetonitrile leaves solely the product of interest as a sodium salt. The spectral data of the individual compounds are reported below.

Sodium-2-(4-nitrophenoxy)-ethylsulfate (4a). Compound **4a** was prepared following the general procedure employing chlorosulfonic acid (0.390 g, 3.35 mmol) and compound **3a** (0.471 g, 2.57 mmol). Evaporating the acetonitrile gave 0.618 g (82%) of **4a** as an off-white solid: IR (KBr) 3517 (s), 3254 (s), 3115 (w), 1494 (s), 1250 (m); ^{1}H

NMR (D_2O) 4.22 (s, 4H), 6.90 (d, J = 9.2, 2H), 8.00 (d, J = 9.2, 2H); ^{13}C NMR (D_2O) 66.8, 67.0, 114.9, 126.1, 141.2, 163.6. Supporting information in Appendix A, pp. 159 – 163.

Sodium-4-(4-nitrophenoxy)-butylsulfate (4c). Compound **4c** was prepared following the general procedure employing chlorosulfonic acid (3.12 g, 26.8 mmol) and compound **3c** (2.26 g, 10.7 mmol). Evaporating the acetonitrile gave 2.67 g (80%) of **4c** as a white solid: IR (KBr) 3498 (s), 3113 (w), 1501 (s), 1263 (m); ^1H NMR (D_2O) 1.65-1.71 (m, 4H), 3.95 (t, J = 5.6, 4H), 6.82 (d, J = 9.2, 2H), 7.95 (d, J = 9.2, 2H); ^{13}C NMR (D_2O) 24.7, 25.1, 68.5, 68.9, 114.7, 126.1, 140.8, 164.1. Supporting information in Appendix A, pp. 164 – 168.

Sodium-6-(4-nitrophenoxy)-hexylsulfate (4e). Compound **4e** was prepared following the general procedure employing chlorosulfonic acid (1.30 g, 11.2 mmol) and compound **3e** (1.34 g, 5.58 mmol). Evaporating the acetonitrile gave 1.53 g (81%) of **4e** as an off-white solid: IR (KBr) 3479 (s), 3117 (w), 1508 (s), 1259 (s); ^1H NMR (D_2O) 1.10-1.15 (s, 4H), 1.40-1.45 (m, 4H), 3.70-3.85 (m, 4H), 6.62 (d, J = 8.4, 2H), 7.77 (d, J = 8.4, 2H); ^{13}C NMR (D_2O) 24.8, 24.9, 28.2, 28.5, 69.0, 69.2, 114.5, 125.8, 140.5, 164.2. Supporting information in Appendix A, pp. 169 – 173.

The neutral alcohol species **3a-f** serve as excellent probes of hydrophilic solid/liquid interfaces. The alcohol functional group can hydrogen bond with silanol terminated quartz surfaces allowing the chromophore to probe local solvation environments different distances away from the solid/liquid boundary. Surface specific nonlinear optical measurements described elsewhere show how different length rulers

sample regions of significantly different polarities, despite the fact that the bulk dielectric properties of the solvents being studied can be quite similar.[36] In addition, preliminary studies have shown that the ionic species **4a-e** are also successful as probes of weakly interacting liquid/liquid interfaces. Data comparing results from the shortest ruler with those from the parent PNAS chromophore are discussed below. (*Vide infra*.)

4. Characterization

4A. Solvatochromic behavior

Figure III.2 displays the solvatochromic behavior of **3a**, **3d**, **3f**, and PNAS. Shown are excitation maxima plotted against the polarity function for a representative sample of protic and aprotic solvents. The Onsager polarity function,[37] f(D), is directly related to the solvent dielectric constant:

$$f(D) = \frac{2(D-1)}{2D+1} \quad \text{(III.3)}$$

where D is the solvent static dielectric constant. Typical f(D) values for common solvents range from ~0.4 (alkanes) to ~1 (water). A linear relationship between f(D) and solute excitation maxima typically indicates solute sensitivity to long range, nonspecific solvation forces.[29,38]

The solvatochromic behavior of all alcohol species is quite similar to that of the original PNAS chromophore. Data show a linear relationship across a wide range of solvents – both protic and aprotic – with the only significant deviation appearing in aqueous solution. Furthermore, excitation spectra of the different salts (**4a**, **4c**, **4e**) in aqueous solution are identical to spectra from the corresponding alcohols indicating that the second step in Scheme 1 leaves the electronic structure of the chromophore

unchanged. Consequently, ruler excitation energies provide a sensitive measure of local solvation environments in interfacial systems.

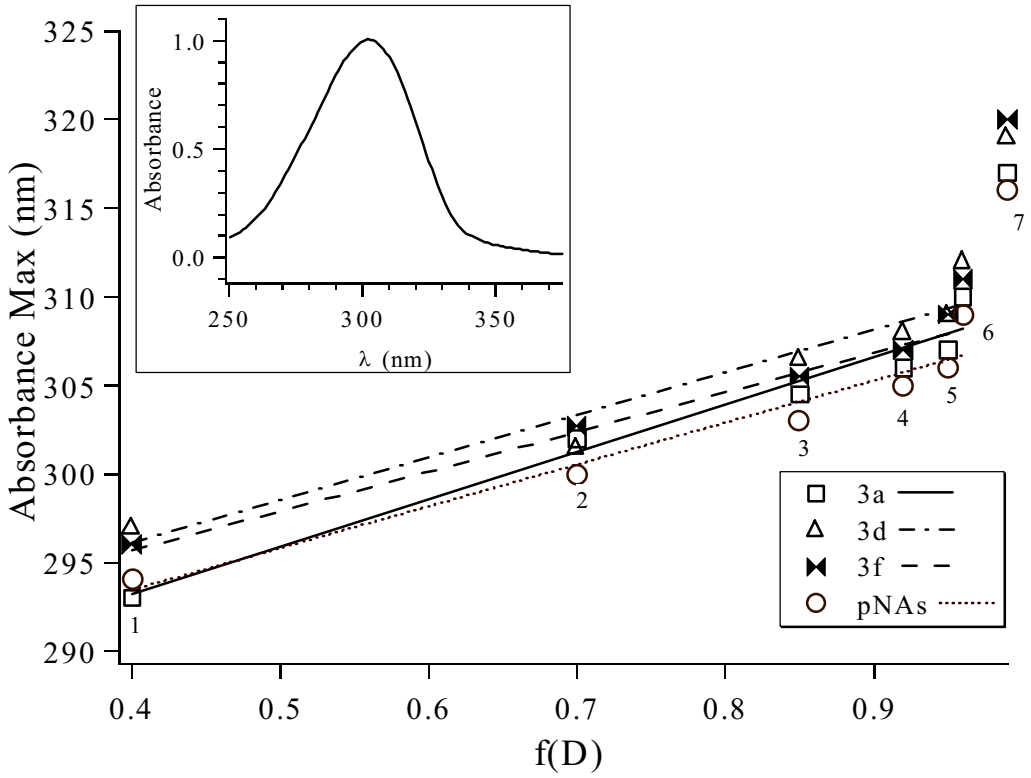

Figure III.2. Solvatochromic behavior of products 3a, 3d, and 3f, with comparison to PNAS. Data demonstrates that the alcohol species retain the solvatochromic characteristics of PNAS. UV maxima were recorded in (1) cyclohexane, (2) diethyl ether, (3) 1-octanol, (4) ethanol, (5) methanol, (6) acetonitrile, and (7) water. Inset shows a representative UV spectrum, recorded for product 3d in 1-octanol.

4B. Surface activity

The Wilhelmy Plate method[32] was used to measure the surface activity of different rulers at a water/cyclohexane interface. Figure III.3 shows the surface pressure isotherms of products **4a**, **4c**, and **4e**. Fitting the data according to Equations III.1-III.2 shows the terminal surface concentrations of species **4a**, **4c**, and **4e** to be 1.49×10^{14}, 1.66×10^{14}, and 1.89×10^{14} molecules/cm^2, respectively. These results compare favorably

to surface concentrations for other alkyl surfactants at weakly associating liquid/liquid interfaces.[39] An interesting observation is that the terminal surface concentration appears to increase slightly with increasing alkyl chain length, consistent with the idea that more hydrophobic species should exhibit greater surface activity. Choosing a specific aqueous ruler concentration sets the concentration of the interfacial monolayer formed. The well-behaved surface activity exhibited in Figure III.3 enables experiments examining interfacial solvation to be carried out with well defined ruler surface concentrations up to the reported terminal concentrations.

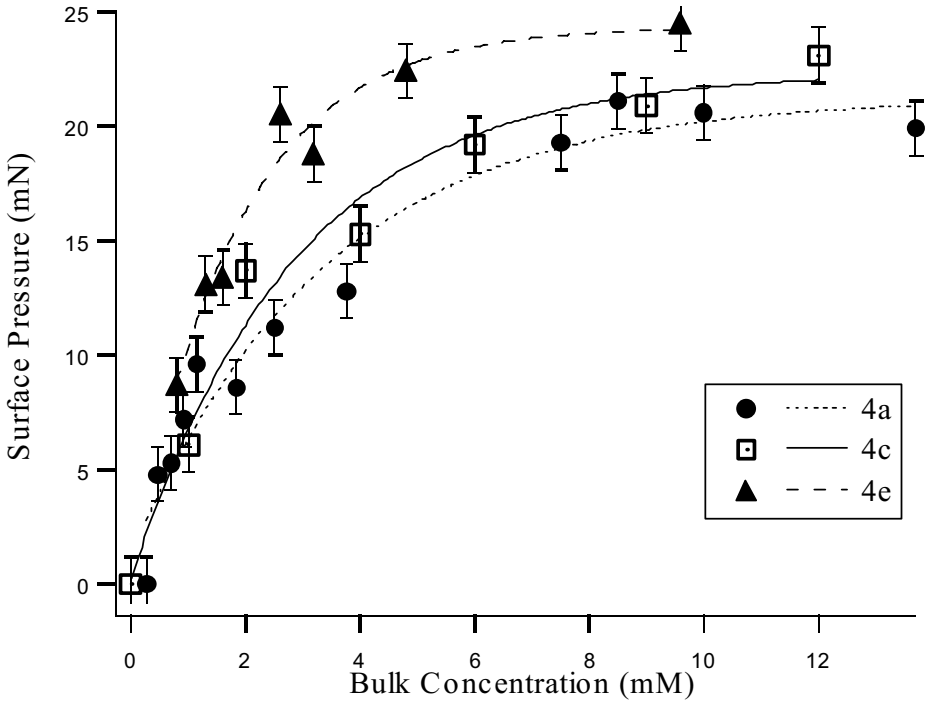

Figure III.3. Interfacial pressure isotherms for representative molecular ruler salts at the water/cyclohexane boundary. Data were fit with Langmuir isotherms which in turn were used to calculate terminal surface concentrations of products 4a, 4c, and 4e.

At aqueous/organic interfaces, rulers form anionic monolayers with surfactant separation being controlled by Coulomb repulsions between individual headgroups.

Reported surface excess concentrations correspond to areas of ~50-70 $Å^2$/molecule. This figure represents approximately three times the area occupied by *neutral* surfactants packed to their hard sphere limits (e.g. long-chain carboxylic acids).[28] The fact that these PNAS-based surfactants do not form tightly packed monolayers raises several concerns about their ability to function as molecular rulers. Issues of spacer conformation and surfactant aggregation are addressed below.

4C. Conformational considerations

Relatively low surface concentrations of adsorbed molecular rulers (compared to the tightly-packed, hard sphere limit) enable the alkyl spacers to adopt multiple conformations. *Gauche* defects in the alkyl chain will shorten the effective length of the molecular ruler and – consequently – the ruler's ability to distinguish changes in solvation across different liquid/liquid interfaces. Obviously, multiple conformations and reduced ruler effectiveness become concerns as alkyl spacers get longer. However, Raman and X-ray scattering studies of alkanes in solution show that >90% of linear alkanes up to 5 C atoms in length exist in conformations that are either all-*trans* or incorporate a single *gauche* defect.[35,40] Furthermore, nonlinear optical studies of alkyl chain structure in monolayers adsorbed to liquid/liquid interfaces show that short chain surfactants exhibit fewer *gauche* defects than long chain alkyl surfactants.[41,42] Molecular dynamics simulations suggest that the greatest propensity for *gauche* defects in surfactants adsorbed to liquid surfaces exists in the second C–C bond after the charged headgroup. The order parameter for alkyl chains then remains constant through 6 CH_2 groups.[27] Interestingly, charged surfactant monolayers exhibit less conformational order

at air/water interfaces than at liquid/liquid interfaces, a result that stands in contrast to results from neutral monolayers that can achieve higher surface concentrations.

Given the short lengths of the alkyl spacers used in the molecular rulers described above *and* the surface induced polar ordering at liquid/liquid interfaces, we anticipate that conformational disorder within adsorbed surfactants will not hamper their ability to sample changes in solvation across liquid/liquid interfaces. An empirical method for assessing conformational order within alkyl chains involves comparing relative intensities of different CH_2 infrared vibrational bands.[35] One such pair of bands are those assigned to the CH_2 symmetric stretch (at ~2850 cm^{-1}) and the CH_2 antisymmetric stretch/Fermi Resonance (at 2930 cm^{-1}). The I_{2850}/I_{2930} ratio varies from less than 1.0 in well-ordered systems of *n*-alkanes to a limiting value of ~3 for long, *n*-alkyl chains (e.g. > C_{22}) having statistical distributions of *gauche* defects.[35] Fits to IR spectra of **3e** dissolved in CCl_4 yield a I_{2850}/I_{2930} ratio of 0.7 (± 0.1). (Data not shown.) This result is further evidence that spacer flexibility should not diminish the ability of these molecular ruler surfactants to span different interfacial widths. Systems requiring rulers with longer spacers (> six carbons) will need additional characterization by surface specific, NLO vibrational spectroscopy in order to ascertain chain conformation. Alternatively, rulers can be created with rigid, nonconjugated spacers such as fused norbornane ring systems.[43]

4D. Mass Spectrometry characterizations

One unusual aspect of the characterization warrants mention here. Fast atom bombardment (FAB) mass spectrometry provides unambiguous identification of the neutral alcohol species (**3a-f**). The ionic sulfates, however, need to be identified using electrospray mass spectrometry. Mass spectra of species **4a**, **4c**, and **4e** recorded using anion detection show dominant features corresponding to the monomer anion (r^-) mass.

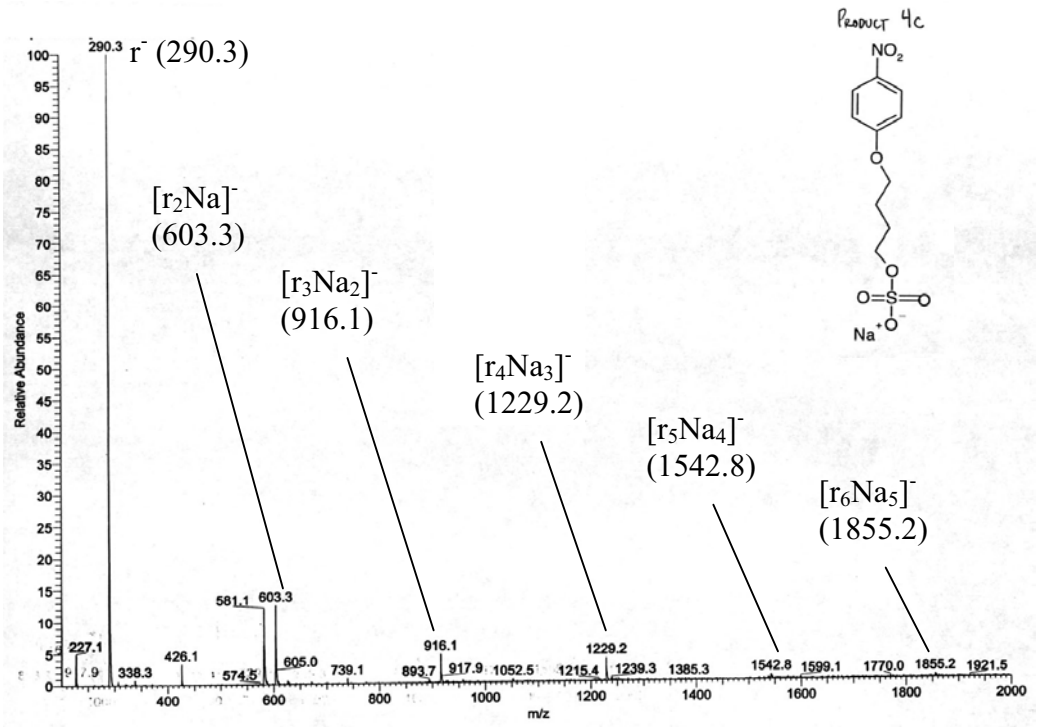

Figure III.4. Negative ion electrospray mass spectrum of 4c. The ruler anion [r^-] appears as the dominant feature (m/z = 290 amu). Aggregates [r_nNa_{n-1}]$^-$ are labeled out to the hexamer. In contrast to the positive ion spectrum, intensity in the larger aggregates drops off dramatically above the dimer, [r_2Na_1]$^-$. Negative ion spectra of 4a and 4e can be found in Appendix A.

The negative ion mass spectrum of product **4c** is shown in Figure III.4. Careful inspection of the spectra show small, additional features at higher masses corresponding to [r_2Na_1]$^-$ up to hexamer clusters ([r_6Na_5]$^-$). These aggregates provide evidence that

samples are, in fact, the sodium salt. Except for species **4a**, these larger clusters have very small intensities relative to that of the parent monomer anion. In the **4a** anion spectrum, the dimer $[r_2Na_1]^-$ has ~50% of the intensity of the monomer anion.

Spectral patterns change dramatically in the positive ion spectra. Data for the **4a**, **4c**, and **4e** show long progressions out to the detection limits of the instrument (2000 amu). The positive ion spectrum of product **4c** is shown in Figure III.5. These progressions correspond to aggregates of anion:sodium complex with an additional sodium ion $[r_nNa_{n+1}]^+$. The progression extends out to the hexamer ($[r_6Na_7]^+$) with appreciable intensity. Analysis of each band indicates that the primary component is the multimer in a +1 charge state. While the mechanism of charged aggregate formation

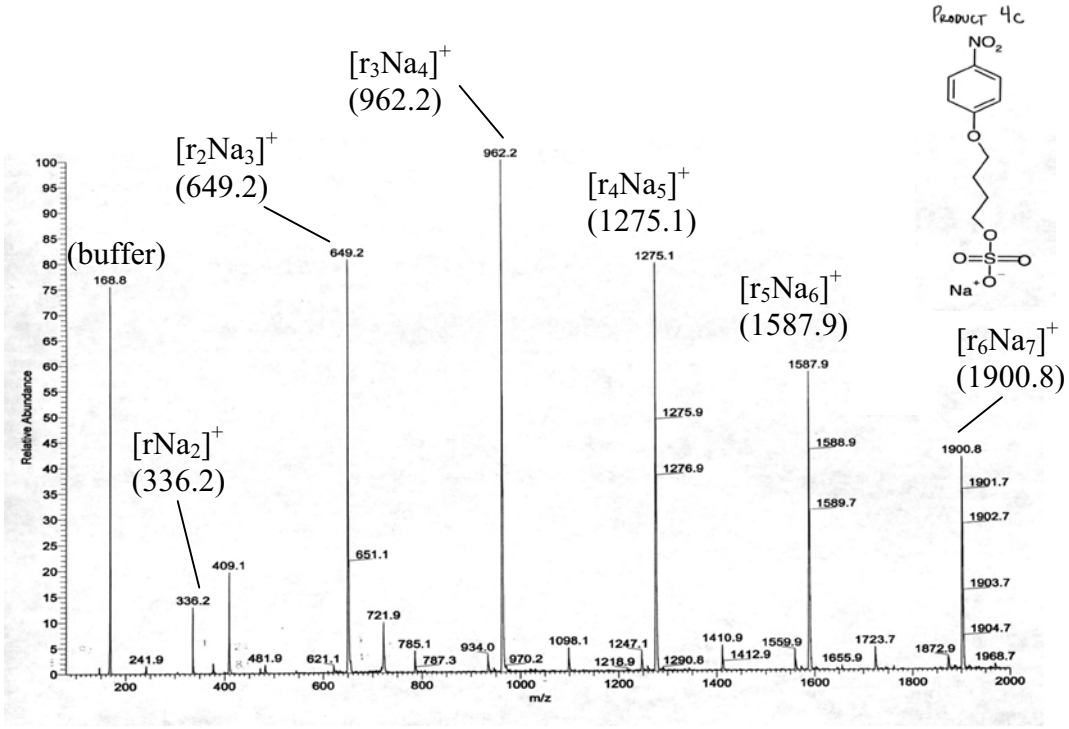

Figure III.5. Positive ion electrospray mass spectrum of 4c. The feature at 168 amu arises from the buffer used to dissolve the molecular ruler. Aggregates $[r_nNa_{n+1}]^+$ are labeled out to the hexamer. Isotopic separation of equivalently sized aggregates indicate that species are predominantly in the +1 charge state. Positive ion spectra of 4a and 4e can be found in Appendix A.

remains unclear,[44] the gas phase ions are generated from small, highly charged droplets in which the effective solute concentration has increased ~100 fold.[45] Droplets that contain excess cations or anions form the charged clusters detected by the spectrometer.

The more pronounced progressions in the cation spectra likely reflect the preferred solvation energetics associated with small cations (Na^+) compared to bulkier anions ($R\text{-}SO_4^-$).[45] In other words, droplets containing *n* ruler anions and (*n*+1) Na^+ cations are thermodynamically more stable (and prevalent) than stoichiometries leading to corresponding anionic aggregates. Similar phenomena have been observed in solutions of simple surfactants as well as numerous inorganic salts.[44,45]

The effect(s) of surfactant aggregation on the photophysical properties of the hydrophobic chromophore represents a second source of concern about the surfactants' abilities to function as molecular rulers. Aggregation-induced quenching or energy transfer between chromophores will not be important due to the reasonably large separation between chromophores (~1 nm chromophore-chromophore separation at full monolayer coverage), the narrow bandwidth of the excitation and emission bands, and the large difference in energy between chromophore absorption and emission.

Furthermore, the probe of interfacial solvation – resonant second harmonic generation – does not result in chromophore excitation. (*Vide infra.*) Of greater concern is the effect of soluble monolayer formation from anionic headgroup-cationic counterion pairing. The presence of charged species so close to the PNAS chromophore could lead to anomalously large electric fields inside of the solute cavity. If double-layer formation influences probe solvation, we would expect the data to reflect large solvatochromic shifts, consistent with the effects of electric fields measuring 10^7 V/cm. In fact, NLO

data for the shortest of the molecular rulers (**4a**) shows that the ruler probe samples a *less polar* environment than the neutral parent, PNAS chromophore. This observation supports the picture of the hydrophobic ruler chromophore interacting strongly with the organic phase, effectively screened from field effects arising from the charged headgroup and counterion interactions.[46]

4E. Nonlinear Optical Spectroscopy

Second harmonic generation (SHG) is a nonlinear optical method that can measure effective excitation spectra of species at interfaces.[4,47] Due to its origins, SHG is both surface and molecularly specific, meaning that spectra result only from solutes that experience interfacial anisotropy.[8,10] In a typical SHG experiment, a single coherent optical field with frequency ω is focused on the interface under study, and a nonlinear polarization with frequency 2ω is detected. The intensity of the 2ω field is proportional to the square of the second-order susceptibility, $\chi^{(2)}$

$$I(2\omega) \propto \left|\chi^{(2)}\right|^2 I(\omega)^2 \qquad \text{(III.4)}$$

where I (ω) is the intensity of the incident field and $\chi^{(2)}$ is a third rank tensor that under the electric dipole approximation is zero in isotropic environments. The $\chi^{(2)}$ tensor is responsible for the technique's inherent surface specificity, and contains both nonresonant and resonant contributions:

$$\chi^{(2)} = \chi^{(2)}_{NR} + \chi^{(2)}_{R} \qquad \text{(III.5)}$$

Typically, the resonant term is several orders of magnitude larger than the nonresonant contribution and can be related to microscopic hyperpolarizability:

$$\chi_R^{(2)} = \sum_{k,e} \frac{\left\langle \mu_{gk} \mu_{ke} \mu_{eg} \right\rangle}{(\omega_{gk} - \omega - i\Gamma)(\omega_{eg} - 2\omega + i\Gamma)} \qquad \text{(III.6)}$$

where $\mu_{i,j}$ is the transition matrix element between the state i and state j (where g stands for ground state, k for an intermediate, virtual state, and e for the first excited state). When 2ω is resonant with ω_{eg}, $\chi^{(2)}$ becomes large leading to a strong resonance enhancement in the observed intensity at 2ω. Thus, measuring the scaled intensity $[I(2\omega)/I^2(\omega)]$ as a function of 2ω records an *effective* excitation spectrum of solutes adsorbed to an interface.

Figure III.6 shows the SHG spectra of PNAS and **4a** adsorbed to a water/cyclohexane interface. Also shown are the excitation maxima for PNAS in both solvents. In aqueous solution, λ_{max} for PNAS, **3a**, and **4a** differ by less than 2 nm, while PNAS and **3a** share similar excitation wavelengths in cyclohexane. Cyclohexane's low dielectric constant prevents **4a** from dissolving in the organic phase. The PNAS spectrum appears in the bottom panel and shows a single, sharp feature. Fitting the data with equations III.4-III.6 (including the nonresonant contribution to $\chi^{(2)}$) leads to a transition wavelength maximum of 309 ± 2 nm. This result is consistent with aforementioned models that report interfacial polarity at liquid/liquid interfaces to represent an arithmetic mean of contributions from the two adjacent solvents.[8,13] Although noisy, the **4a** spectrum shows that the ruler chromophore also samples an interfacial polarity intermediate between that of cyclohexane and that of water. The data, however, are weighted toward the cyclohexane limit with a calculated transition wavelength maximum of 302 ± 3 nm. This large wavelength disparity between the PNAS and **4a** spectra implies that the chromophore of **4a** samples an environment that is

significantly less polar than that sampled by PNAS, consistent with the idea that **4a** spans the water/cyclohexane interface leaving the ruler chromophore more strongly solvated by the organic solvent.

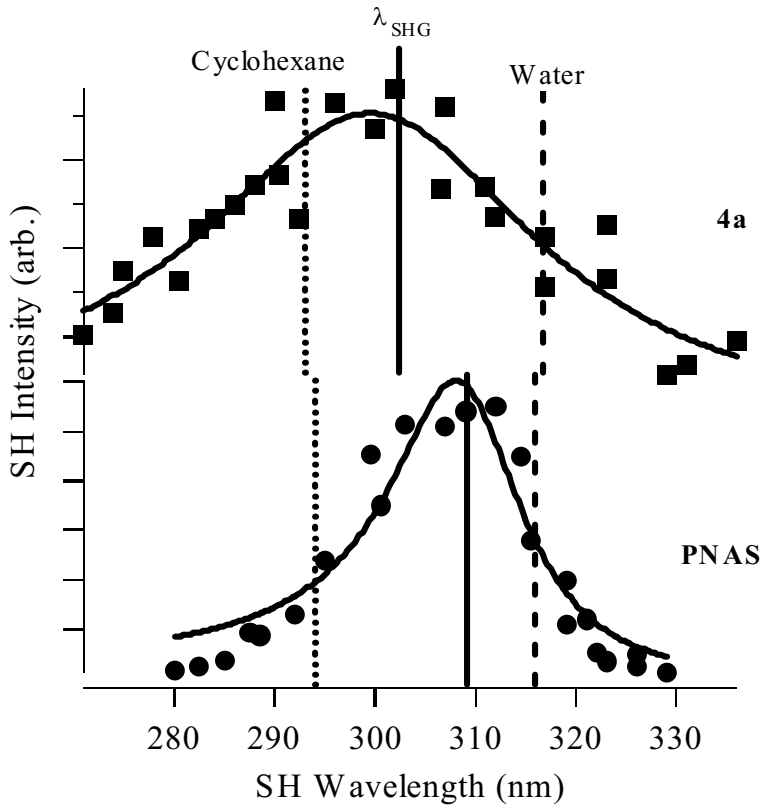

Figure III.6. Second Harmonic Generation spectra of product 4a and PNAS at the water/cyclohexane interface. The figure also shows the absorption maxima of each species in both bulk cyclohexane (dotted lines) and water (dashed lines). Solid lines represent fits of data to equations III.4-III.6.

The data in Figure III.6 provide additional evidence that surfactant aggregation is not significantly influencing ruler chromophore solvation. Strong fields such as those found within double layers strongly enhance a molecule's hyperpolarizability leading to a large enhancement in the second harmonic response. While experimental limitations prevent quantitative absolute intensity comparisons between the **4a** and bare PNAS data, the normalized signal levels of the two spectra differ by approximately a factor of two,

rather than the order of magnitude enhancement that typically results from electric field induced second harmonic generation.[31,48] The difference in normalized signal levels can easily be accounted for by the difference between the surface concentrations of ruler **4a** and PNAS, 1.5×10^{14} and 0.5×10^{14}, respectively. Furthermore, we would expect any ion related field effects to shift chromophore excitation to longer wavelengths, consistent with the solvatochromic behavior observed in Figure 4. In fact, the spectrum of ruler **4a** shifts 7 nm to *shorter wavelengths*, consistent with the idea that the **4a** chromophore samples a less polar environment than the simple, bare PNAS probe adsorbed to the aqueous/cyclohexane interface. That the adsorbed chromophore shows any resonant signal at all implies that ruler **4a** is still influenced by surface induced anisotropy. In the limit that the chromophore samples a bulk-like, isotropic environment, the $\chi^{(2)}$ tensor would be zero by symmetry and a SHG experiment would show no wavelength dependent, resonant response. If applicable, anisotropy resulting from chromophore-chromophore interactions will enhance the $\chi^{(2)}$ tensor by only ~15% over a monolayer concentration of $0.5 - 1.5\times10^{14}$ molecules/cm^2.[49] High chromophore density, however, would again create larger fields around solutes leading to a more polar environment, not less polar. Keeping these effects in mind, we can say that the ~3 Å separation between headgroup and chromophore in **4a** allows the chromophore to solvated more thoroughly by the cyclohexane than by the water. Additional experiments probing the influence of organic solvent identity, monolayer concentrations, and temperature are ongoing.

5. Conclusion

We have synthesized series of neutral and ionic surfactants consisting of hydrophobic chromophores connected to hydrophilic headgroups by *n*-alkyl spacers. Neutral and ionic rulers can be produced with moderate yields and high purity. The solvatochromic behavior of all surfactants closely mimics that of the parent, *para*-nitroanisole chromophore. The solvent sensitive chromophore and a variable separation between the chromophore and headgroup raises the possibility that these surfactants can be used to measure changes in noncovalent forces across interfaces on molecular lengthscales, thus overcoming a number of challenges faced by previous studies of interfacial solvation. Specifically, changing the length of the *n*-alkyl spacer should, in principle, change the equilibrium distribution of chromophores relative to a nominal interfacial boundary.

Preliminary surface-specific, nonlinear optical experiments with the shortest ionic surfactant and the bare, parent PNAS chromophore indicate that the surfactants do, in fact, function as molecular rulers. Separating the PNAS-based probe from the charged, sulfate headgroup by only two methylene groups (~3 Å) shifts the effective excitation spectrum at the water/cyclohexane interface by 7 nm to shorter wavelengths relative to the bare chromophore spectrum. This observation is consistent with a model that allows the surfactant chromophore to "float" into the organic phase and sample a less polar environment. Furthermore, these results support recent models of interfacial solvation that predict water/alkane liquid/liquid boundaries to be molecularly sharp and microscopically flat. Based on the generality of the synthesis and characterization of these surfactants as well as the promise from initial nonlinear optical studies, we

anticipate that molecular rulers will be powerful tools that can profile solvation across a wide variety of environmentally and biologically relevant interfaces.

References

(1) Steel, W. H.; Damkaci, F.; Nolan, R.; Walker, R. A. *J. Am. Chem. Soc.* **2002**, *124*, 4824-4831.

(2) Benjamin, I. *Chem. Rev.* **1996**, *96*, 1449-1475.

(3) Eisenthal, K. B. *J. Phys. Chem.* **1996**, *100*, 12997-13006.

(4) Richmond, G. L. *Annu. Rev. Phys. Chem.* **2001**, *52*, 357-389.

(5) Penfold, J.; Richardson, R. M.; Zarbakhsh, A.; Webster, J. R. P. *J. Chem. Soc. Faraday Trans.* **1997**, *93*, 3899-3917.

(6) Lee, S. H.; Rossky, P. J. *J. Phys. Chem.* **1994**, *100*, 3334-3345.

(7) Mitrinovic, D.; Tikhonov, A. M.; Li, M.; Huang, Z.; Schlossman, M. L. *Phys. Rev. Lett.* **2000**, *85*, 582-585.

(8) Wang, H.; Borguet, E.; Eisenthal, K. B. *J. Phys. Chem. A* **1997**, *101*, 713-718.

(9) Stanners, C. D.; Du, Q.; Chin, R. P.; Cremer, P.; Somorjai, G. A.; Shen, Y.-R. *Chem. Phys. Lett.* **1995**, *232*, 407-413.

(10) Zhang, X.; Esenturk, O.; Walker, R. A. *J. Am. Chem. Soc.* **2001**, *123*, 10768-10769.

(11) Zhang, X.; Walker, R. A. *Langmuir* **2001**, *17*, 4486-4489.

(12) Tikhonov, A. M.; Mitrinovic, D. M.; Li, M.; Huang, Z.; Schlossman, M. L. *J. Phys. Chem. B* **2000**, *104*, 6336-6339.

(13) Michael, D.; Benjamin, I. *J. Chem. Phys.* **1997**, *107*, 5684-5693.

(14) Sola, M.; Lledos, A.; Duran, M.; Bertran, J.; Abboud, J.-L. M. *J. Am. Chem. Soc.* **1991**, *113*, 2873-2879.

(15) Reichardt, C. *Solvent Effects in Organic Chemistry*; Verlag Chemie: New York, 1979; Vol. 3, Chapter 1.

(16) Safran, S. A. *Statistical Thermodynamics of Surfaces, Interfaces, and Membranes*; Addison-Wesley: Reading, MA, 1994.

(17) Freiser, H. *Chem. Rev.* **1988**, *88*, 611-616.

(18) Wang, H.; Borguet, E.; Eisenthal, K. B. *J. Phys. Chem. B* **1998**, *102*, 4927-4932.

(19) Ishizaka, S.; Satoshi, H.; Kim, H.; Kitamura, N. *Anal. Chem.* **1999**, *71*, 3382-3389.

(20) Ishizaka, S.; Kim, H.; Kitamura, N. *Anal. Chem.* **2001**, *73*, 2421-2428.

(21) Michael, D.; Benjamin, I. *J. Phys. Chem. B* **1998**, *102*, 5145-5151.

(22) Squitieri, E.; Benjamin, I. *J. Phys. Chem. B* **2001**, *105*, 6412-6419.

(23) Michael, D.; Benjamin, I. *J. Chem. Phys.* **2001**, *114*, 2817-2824.

(24) Chipot, C.; Wilson, M. A.; Pohorille, A. *J. Phys. Chem. B* **1997**, *101*, 782-791.

(25) Pohorille, A.; Wilson, M. A. *J. Chem. Phys.* **1996**, *104*, 3760-3769.

(26) Dang, L. X. *J. Phys. Chem. B* **2001**, *105*, 804-809.

(27) Berkowitz, M. L.; Schweighofer, K.; Essman, U. *J. Phys. Chem. B* **1997**, *101*, 3793-3799.

(28) Girault, H. H.; Tamburello-Luca, A. A.; Hebert, P.; Brevet, P. F. *J. Chem. Soc. Faraday Trans.* **1996**, *92*, 3079-3085.

(29) Suppan, P.; Ghoneim, N. *Solvatochromism*; The Royal Society of Chemistry: Cambridge, UK, 1997.

(30) Laurence, C.; Nicolet, P.; Dalati, M. T. *J. Phys. Chem.* **1994**, *98*, 5807-5816.

(31) Whitaker, C. M.; Patterson, E. V.; Kott, K. L.; McMahon, R. J. *J. Am. Chem. Soc.* **1996**, *118*, 9966-9973.

(32) Adamson, A. W. *Physical Chemistry of Surfaces*; John Wiley & Sons: New York, 1990.

(33) Rarick, M. J.; Brewster, R. Q.; Dains, F. B. *J. Am. Chem. Soc.* **1933**, *55*, 1289-1290.

(34) Lambrech, J. A. In *U.S. Patent 2,573,769*, 1951.

(35) Snyder, R. G.; Strauss, H. L.; Elliger, C. A. *J. Phys. Chem.* **1982**, *86*, 5145-5150.

(36) Zhang, X.; Steel, W. H.; Walker, R. A. *J. Phys. Chem. B* **2003**, *107*, 3829-3836.

(37) Onsager, L. *J. Am. Chem. Soc.* **1936**, *58*, 1486-1493.

(38) Wong, M. W.; Frisch, M. J.; Wiberg, K. B. *J. Am. Chem. Soc.* **1991**, *113*, 4776-4782.

(39) Watry, M. R.; Richmond, G. L. *J. Am. Chem. Soc.* **2000**, *122*, 875-883.

(40) Habenschuss, A.; Narten, A. H. *J. Chem. Phys.* **1990**, *92*, 5692-5699.

(41) Walker, R. A.; Gruetzmacher, J. A.; Richmond, G. L. *J. Am. Chem. Soc.* **1998**, *120*, 6991-7003.

(42) Conboy, J. C.; Messmer, M. C.; Richmond, G. L. *Langmuir* **1998**, *14*, 6722-6727.

(43) Oevering, H.; Paddon-Row, M. N.; Heppener, M.; Oliver, A. M.; Cotsaris, E.; Verhoeven, J. W.; Hush, N. S. *J. Am. Chem. Soc.* **1987**, *109*, 3258-3269.

(44) Hao, C.; March, R. E. *J. Mass Spectrom.* **2001**, *36*, 509-521.

(45) Siuzdak, G.; Bothner, B. *Angew. Chem. Int. Ed. Engl.* **1995**, *34*, 2053-2055.

(46) Pratt, L. R. *J. Phys. Chem.* **192**, *96*, 25-33.

(47) Eisenthal, K. B. *Chem. Rev.* **1996**, *96*, 1343-1360.

(48) Gragson, D. E.; Richmond, G. L. *J. Am. Chem. Soc.* **1998**, *120*, 366-375.

(49) Xu, Z.; Dong, Y. *Surf. Sci.* **2000**, *445*, L65-L70.

Chapter IV. Solvent Polarity across Weakly Associating Interfaces

1. Introduction

Chapter III described the development and characterization of new tools capable of profiling the dipolar width of liquid/liquid interfaces. This chapter covers the work done using these molecular rulers at weakly associating water/alkane interfaces. The materials presented in this chapter form the basis of an article currently under review by *The Journal of Physical Chemistry B*.

The boundaries between two immiscible liquids have been the subject of increasing scrutiny during the last decade due to their roles in solvent extraction,[1,2] phase transfer catalysis[1,2] and environmental remediation.[3] Furthermore, liquid/liquid interfaces frequently serve as biomimetic models of cell membranes[4,5] and are used to gauge anesthetic efficacy[6] as well as protein binding affinity.[4] Numerous experimental and computational techniques have been used to examine how the asymmetry inherent to interfaces affects interfacial structure and long-range order.[7-9] In addition, many of the same methods have been employed to identify how surface mediated solvent properties change interfacial solvation from bulk solution limits.[10-13] Here, solvation refers to the noncovalent interactions experienced between a solute and its surroundings. Understanding how interfaces alter solute-solvent interactions from those in bulk solution is essential for formulating quantitative, predictive models of solution phase surface chemistry.

In bulk solution a solute is subject to isotropic forces and continuum models of solvation can accurately describe solute behavior. At an interface, however, solutes

experience an anisotropic environment, especially if the solute contains both polar and nonpolar functional groups that lead to surface-induced, polar ordering. Under these circumstances, short range interactions between a solute and its interfacial surroundings can lead to dramatic changes in solute energetics, structure and reactivity. In the studies described below, we use second order nonlinear optical spectroscopy to measure solvent polarity across weakly associating liquid/liquid interfaces. The interfaces all consist of an aqueous phase in contact with an alkane, and the solutes are solvatochromic probes that have been integrated into surfactants of varying lengths, e.g. "molecular rulers".[14,15] Results show that despite having similar bulk dielectric properties, the alkanes create very different dipolar environments at the interface depending on molecular structure.

One of the most fundamental properties associated with liquid/liquid interfaces is one of interfacial width. Across liquid/liquid interfaces, properties such as density, dielectric constant and refractive index are changing on some lengthscale. This distance may be short by molecular standards, leading to abrupt changes in these solvent properties, or interfacial width may be broad with properties changing gradually over multiple solvent diameters. The most direct measure of interfacial width comes from X-ray and neutron scattering studies. These experiments explicitly identify the distance across which solvent density changes. X-ray scattering studies of different water/alkane interfaces show these boundaries to be molecularly sharp[16] in agreement with predictions based on capillary wave theory[7] as well as molecular dynamics simulations.[17] However, these data do not probe the interactions between a solute and its surroundings. Similarly, neutron scattering studies have identified how liquid/liquid interfaces induce gradients in interfacial salt concentrations and control the structure of adsorbed surfactants,[18] but

again, results identify the distribution of species across an interface, not the forces between them.

Optical spectroscopy can not measure the spatial or distance-dependent information necessary for determining interfacial width, but optical spectroscopy *does* measure solvation forces directly. When coupled with methods to ensure surface specificity, i.e. a total internal reflection geometry or a second order nonlinear response, fluorescence and nonlinear optical spectroscopy can serve as a versatile means for probing interfacial solvation across a variety of liquid/liquid interfaces. For example, using rotational anisotropy of a solute's fluorescence Kovaleski and coworkers demonstrated that interfacial viscosity depended sensitively on solvent structure in ways that could not be predicted based on bulk viscosity values.[19-21] Similarly, Eisenthal and coworkers employed resonance-enhanced second harmonic generation to show that solute isomerization rates at interfaces varied depending on the phase in which the solute was actually solvated.[22,23] More recently, these techniques have been used to examine electron and energy transfer between interfacial species, and infer how surface effects alter interfacial solvation from solvation in bulk solution.[12,24] Several of these studies suggest that liquid/liquid interfaces are molecularly sharp, but quantitative data about interfacial width remain elusive.

Of particular relevance to the work described below are a series of studies by Wang, *et al* that probed interfacial polarity at a number of liquid/liquid interfaces.[22,23] In these experiments, SHG was used to acquire effective excitation spectra of solvatochromic solutes adsorbed to different liquid/liquid interfaces. The probes themselves had excitation wavelengths that varied considerably depending on whether

the probe was solvated in a polar or nonpolar medium. Data showed that interfacial polarity could be described by an average polarity model in which the local dielectric environment contained approximately equal contributions from both bulk phases. This model can be described remarkably well by continuum-based scales of solvent polarity. At first, this result may seem surprising in light of the X-ray scattering experiments that show liquid/liquid interfaces to be molecularly sharp.[16] One might expect interfacial polarity to reflect disproportionate contributions from one phase or the other. However, in a series of molecular dynamics simulations Michael and Benjamin showed how a molecularly sharp interface could give rise to the average polarity picture if the interface was thermally roughened and the solute resided very close to the Gibbs dividing surface.[17] These simulations also suggested that results should be very sensitive to solute distribution across the interface, a conclusion that was later supported by additional SHG experiments.[13,25]

2. Experimental methods

2A. Molecular rulers

Experiments described in this dissertation couple resonance-enhanced SHG spectroscopy with surfactants created specifically to vary the equilibrium distribution of solvatochromic solutes across a liquid/liquid interface. By measuring how SHG spectra vary with surfactant length, the dipolar width of different weakly associating liquid/liquid interfaces has been measured. The alkanes used to create an interface with an aqueous subphase include cyclohexane, methylcyclohexane, octane and hexadecane. All of these interfaces appear to be molecularly sharp, namely, solvent polarity converges to bulk

alkane limits on sub-nm lengthscales, but there exist qualitative differences between the different systems that can not be described by differences in bulk solvent properties. These findings are discussed in terms of the molecular structure of the individual solvents themselves and recent simulations that expose the role of interfacial roughness on solvation dynamics and interfacial polarity.

As described in Chapter III, molecular rulers are surfactants containing an ionic headgroup attached to a hydrophobic nitrobenzene chromophore via an alkoxy spacer whose length can be varied by controlling the number of methylene groups present. Surfactants have been produced with spacers ranging from two to eight methylene groups, primarily in even increments. A more complete description of synthetic conditions and characterization of the molecular rulers can be found in Chapter III.

After ruler surfactants had been synthesized and purified, their solvatochromic behavior and surface activity were characterized. By measuring the excitation maxima (λ_{max}) of the family of molecular rulers in a variety of solvents having different polarities we concluded that their solvatochromic behavior closely matches that of the model chromophore, *para*-nitroanisole (PNAS). PNAS is an ideal probe for the study of interfacial polarity for a number of reasons. It contains a single chromophoric benzene ring, meaning experiments detect signal from a single source, rather than the averaged signal from multiple chromophores that are present in a number of dyes used in previous studies of interfacial polarity. PNAS exhibits a single electronic excitation in the wavelength region between 270 and 350 nm. This excitation is accompanied by a large change in the molecule's permanent dipole. As a result, PNAS has a broad solvatochromic window - its excitation maximum red shifts by more than 20 nm from its

value in nonpolar, organic solvents to that in water. Finally, PNAS contains a polar nitro group and a nonpolar methoxy group, imparting an affinity for both the polar and nonpolar solvent phases at water/alkane liquid/liquid interfaces.

The Wilhelmy plate method was used to measure the surface activity of different length molecular rulers at different water/alkane interfaces. From these data, using procedures described in Chapter III, terminal surface concentrations ranged from 1.5×10^{14} and 1.9×10^{14} molecules/cm^2 for different families of molecular rulers. Surface activities of two neutral chromophores used in SHG studies were also measured. PNAS was found to have a terminal surface concentration of only 4.1×10^{13} molecules/cm^2 at the water/cyclohexane interface. As expected, *para*-nitrophenol (PNP) was found to be more surface active at weakly associating water/alkane interfaces, forming monolayers with terminal surface concentrations between 1.9×10^{14} and 2.4×10^{14} molecules/cm^2. Both of the neutral species were found to excellent probes of solvation at water/alkane interfaces. Representative surface pressure isotherms for C_2 rulers and PNP adsorbed to the water/cyclohexane interface are shown in Figure IV.1.

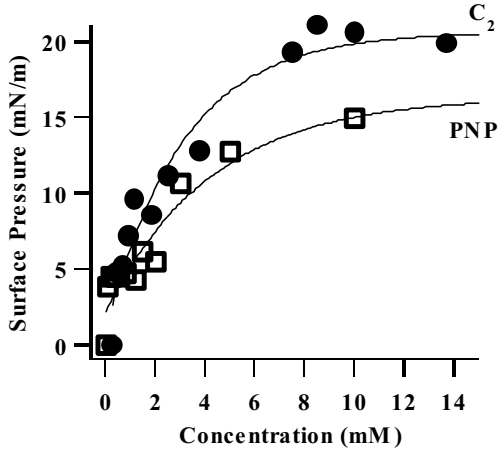

Figure IV.1. Surface pressure isotherms for C_2 rulers (circles) and PNP (squares) adsorbed to a water/cyclohexane interface. Other water/alkane interfaces led to quantitatively similar isotherms. Interfacial tensions were collected using the Wilhelmy plate method for these species and others studied in this work.

2B. Partitioning of neutral chromophores

Motivated by a need to better understand molecular ruler behavior at liquid surfaces we measured the neutral chromophore partitioning across various weakly associating water/alkane liquid/liquid interfaces. Ideally, the solvatochromic probe of molecular ruler surfactants would be hydrophobic enough so that it would solvate itself as much as possible in the lower dielectric, organic phase. Opposing this tendency is the affinity of the polar nitro group for the higher dielectric, aqueous phase, possibly causing the molecular rulers to tilt towards the interfacial plane. As the data in Table IV.1 show, PNP partitioned to the water layer preferentially. With the exception of the water/hexadecane system, PNP was approximately 100 times more soluble in water than the organic phase. In contrast, PNAS displayed a preference for the organic layer over the aqueous phase, with a partitioning ratio of ~20:1 (organic:aqueous). The chromophore incorporated into ruler surfactants more closely resembles PNAS than PNP, thus we feel confident that at water/alkane interfaces the ruler probe will attempt to solvate itself in the organic phase. (Specific partitioning experiments with the ionic molecular ruler species were not feasible as the anionic sulfate group prohibits surfactant solvation in the nonpolar, alkane phase.)

2C. Experimental details

Resonance-enhanced SHG was used to acquire effective excitation spectra of molecular rulers adsorbed to different water/alkane, liquid/liquid interfaces. Because of its origins, the resonance-enhanced response is both surface and molecularly specific, meaning that spectra result only from solutes influenced by interfacial anisotropy.[22,26] In

Table IV.1. Partitioning results of PNP and PNAS in several water/alkane systems characterized as ratio of concentrations of solute in each phase.

Solute	System	Partitioning Ratio (Water:Organic)
PNP	Water: Cyclohexane	113:1
PNP	Water: m-cyclohexane	104:1
PNP	Water: Octane	121:1
PNP	Water: Hexadecane	42:1
PNAS	Water: Cyclohexane	1:23
PNAS	Water: Octane	1:18

a typical experiment, a single coherent optical field of frequency ω is incident upon an interface having a sub-monolayer coverage of a given ruler surfactant. A nonlinear polarization of frequency 2ω and intensity $I(2\omega)$ is detected, where the intensity of this second harmonic is proportional to the square of the second-order susceptibility, $\chi^{(2)}$

$$I(2\omega) \propto |\chi^{(2)}|^2 I^2(\omega) \quad \text{(IV.1)}$$

and $\chi^{(2)}$ is a third rank tensor that under the electric dipole approximation is zero in isotropic environments. The $\chi^{(2)}$ tensor, then, imparts to the technique its inherent surface specificity. The tensor itself contains both resonant and nonresonant contributions:

$$\chi^{(2)} = \chi_R^{(2)} + \chi_{NR}^{(2)} \quad \text{(IV.2)}$$

For dielectric systems, such as the water/alkane interfaces considered here, the resonant term is typically several orders of magnitude larger than the nonresonant contribution and can be related to the microscopic hyperpolarizability:

$$\chi_R^{(2)} = \sum_{k,e} \frac{\langle \mu_{gk} \mu_{ke} \mu_{eg} \rangle}{(\omega_{gk} - \omega - i\Gamma)(\omega_{eg} - 2\omega + i\Gamma)} \qquad \text{(IV.3)}$$

where μ_{ij} is the transition matrix element between state i and state j (where g stands for the ground state, k for an intermediate, virtual state, and e for the first excited state). The ω_{ij} refer to the transition energies between the ground state and states k and e, and Γ is the transition's line width. When 2ω is resonant with ω_{eg}, $\chi^{(2)}$ becomes large, leading to a strong resonance enhancement in the observed intensity at 2ω. Thus, measuring the scaled intensity ($I(2\omega)/I^2(\omega)$) as a function of 2ω records an *effective* excitation spectrum of solutes adsorbed to an interface. With the exception of data recorded to determine solute orientations, spectra in this work were acquired under $P_\omega P_{2\omega}$ polarization conditions, where P polarized light describes light that is polarized vertically perpendicular to the direction it travels. Varying the incident and detected polarizations enabled us to determine the average chromophore orientation using methods described previously. Different polarizations did not lead to qualitatively different SHG spectra.

To record spectra, aqueous solutions of solutes were prepared between 0.5 and 2 mM. These concentrations lead to surface coverages of less than 20% of a full monolayer according to adsorption isotherms recorded for rulers at the water/cyclohexane and water/octane interfaces. Liquid/liquid interfaces were generated by first placing aqueous solutions into a cylindrical kel-F cell having a reservoir 4 cm in diameter. Then an application of a thin layer (~1-3 mm) of organic solvent atop the aqueous solution creates the aqueous/organic interface. A trapezoidal fused silica prism (50 x 50 x 30 mm, JDSU Casix) is secured atop the reservoir, preventing evaporation of the solvent. Prior to use the prism is cleaned in a 50:50 mixture (by volume) of concentrated sulfuric and

fuming nitric acid. Prisms cleaned in this way have been shown to be hydrophilic, as demonstrated by complete wetting of the surface. All liquid/liquid interfaces and SH spectra were acquired at room temperature, 22 $\pm$ 1.5 °C.

The SHG apparatus is built around a Ti:sapphire regeneratively amplified, femtosecond laser (Clark-MXR CPA 2001) that produces 130 fs pulses with energies of ~700 μJ at a wavelength of 775 nm and a repetition rate at 1 kHz. The output of the Ti:sapphire laser pumps a commercial optical parametric amplifier (OPA, Clark-MXR). The visible output of the OPA is tunable from 550 to 700 nm, with a bandwidth of 2.5 ± 0.5 nm. The polarization of the incident beam is controlled using a Glan-Taylor polarizer and a half-wave plate. A series of filters block the fundamental 775 nm and any second harmonic light generated from the preceding optical components. Second harmonic photons are detected in the reflected direction using photon-counting electronics. Typical signal levels average 0.01 – 0.1 photon per shot. A second polarizer selects the polarization of the SH signal and a short pass filter and monochromator serve to separate the second harmonic signal from background radiation.

Because the visible OPA cannot be synchronously tuned, acquisition of a complete SHG spectrum requires multiple hours. A typical procedure entails letting the liquid/liquid system equilibrate followed by manual tuning of ω_{vis} to each desired wavelength. System alignment is reoptimized at every wavelength to account for the wavelength-dependent refractive indices of the prism and collection optics. At each wavelength, SH data are collected for four 10 s intervals and normalized for incident power. Although tedious, this procedure ensures that spectra are reproducible. A single wavelength might be sampled three separate times several hours apart (beginning,

middle, and end of an acquisition sequence). If the normalized SH signal from each of these three samples does not fall within experimental uncertainty (typically $\pm$ 15%), data acquisition is halted and the spectrum discarded. In addition, data at the same wavelength were often acquired using several different incident powers and then normalized to confirm quadratic dependence of SH signal intensity on the incident field intensity predicted by Equations IV.1 – IV.3. Predicted quadratic behavior was always observed.

3. Results

3A. Molecular Rulers at the Water/Cyclohexane Interface

Figure IV.2 shows the composite SHG spectra of four different solutes adsorbed to the water/cyclohexane interface: PNAS, C_2 ruler, C_4 ruler, and C_6 ruler. Each spectrum is the composite of two or more individual spectra for the system under study (i.e. PNAS at the water/cyclohexane interface). Individual spectra for each system were normalized and combined; Equations IV.1 – IV.3 were used to fit the data and the composite excitation maximum always closely matched that of the individual spectra. Overlaid on the plots are dotted and dashed lines to denote the excitation maximum of each species in bulk aqueous and organic solutions, respectively. (Due to solubility limits of the ionic rulers in alkane solvents, neutral molecular rulers containing a terminal hydroxyl group in place of the ionic sulfate group were used to determine excitation maxima these nonpolar solvents. When maxima for both neutral and ionic species could be collected (in more polar solvents) they were found to be equivalent.) The solid vertical line on each panel indicates the fitted interfacial maximum of each species

(including the nonresonant contribution). Note that interference effects between the resonant and nonresonant contributions to $\chi^{(2)}$ can lead to a calculated SH maximum that does not coincide with the apparent spectral maximum. (For example, see the bottom panel of Figure IV.2, depicting the SHG spectrum of the C_6 ruler at the water/cyclohexane interface.)

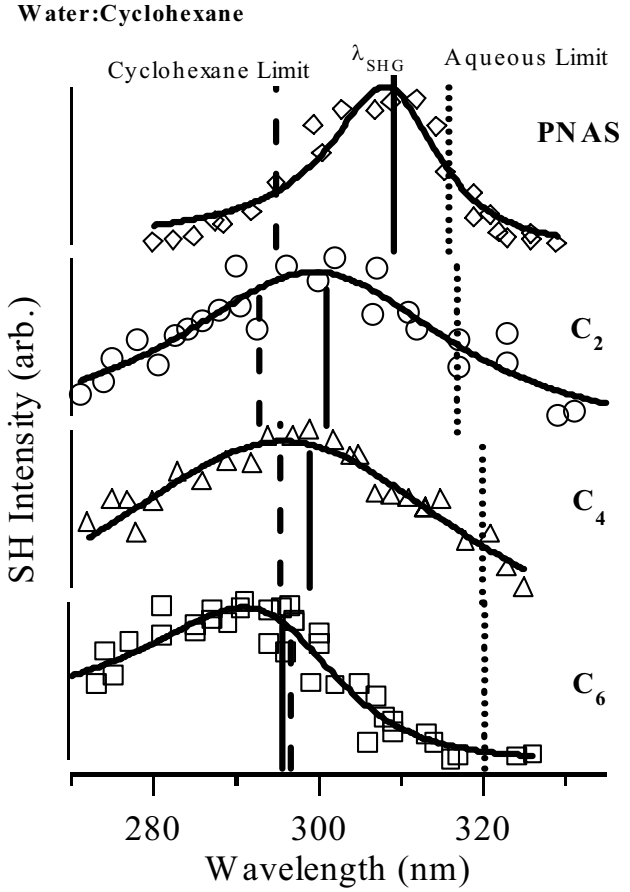

Figure IV.2. Resonance-enhanced SHG spectra of (top to bottom) *p*-nitroanisole (PNAS), C_2 rulers, C_4 rulers, and C_6 rulers adsorbed to a water/cyclohexane interface. Dashed and dotted vertical lines denote excitation maxima in bulk cyclohexane and water, respectively. Solid vertical lines correspond to SHG maxima (λ_{SHG}) as determined by fitting the data to equations IV.1 – IV.3. Note that SHG maxima do not always correspond to the wavelengths with the highest SHG intensity, owing to the nonresonant contribution to $\chi^{(2)}$ in equation 2.

Data clearly show that the chromophores of each ruler species experience unique solvation environments. The transition maximum for PNAS at the water/cyclohexane

interface is 309 $\pm$ 2 nm, compared to its bulk water and organic limits of 316 and 294 nm, respectively. This result is close to the energetic arithmetic mean of the aqueous and organic limits and is consistent with previous studies of interfacial polarity across different weakly associating interfaces.[23] As the chromophore of each subsequent species is allowed to "float" into the organic solvent we observe dramatic changes in the measured transition maximum and excitation bandwidth. The chromophore experiences an increasingly nonpolar environment as the alkyl spacer lengthens from C_2 to C_4 to C_6. This nonpolar environment is reflected by an excitation wavelength that blue shifts from 302 nm (C_2) to 296 nm (C_6). The bulk solution limits of these ruler species are 318 $\pm$ 2 nm in water and 295 $\pm$ 2 nm in cyclohexane. In earlier work, we attributed these results to a gradual convergence of the local dielectric character to the organic limit.[13] The alkyl spacer separating the chromophore from the ionic headgroup of the C_6 ruler has a maximum length of 9 Å, or approximately three water diameters. This value reflects an upper limit to the interfacial dipolar width and would decrease if there were conformational defects in the alkyl spacers or a net tilt of the adsorbed surfactant. Experiments examining the orientation of adsorbed molecular rulers suggest that disorder in alkyl chains is not an issue with rulers of increasing length.

A second striking feature that stands out in the four spectra is the marked change in linewidth as the length of the alkyl spacer increases. In bulk solution, the fullwidth, half-maximum (FWHM) of the excitation spectrum varies between approximately 44 nm in cyclohexane and 68 nm in water. In a given solvent, excitation bandwidths of different species (e.g. C_2, C_4, C_6, etc.) vary by less than 10%. While there is little variation in the measured linewidth of each bulk solution spectrum, the interfacial spectra are marked by

dramatic changes in their widths. The FWHM of the PNAS spectrum is 15 nm, the sharpest of the four species. This value increases for the C_2 and C_4 rulers, to 39 and 52 nm, respectively, before decreasing to a linewidth of 25 nm for the C_6 ruler. Interfacial linewidths that are narrower than bulk solution limits imply a more homogeneous distribution of solvation environments at the interface relative to bulk solution. Narrow linewidths are expected given that chromophores at liquid/liquid interfaces are "anchored" to the boundary by the ionic headgroup and should share a common "float depth" and average orientation. Thus we would interpret linewidth changes to indicate that the chromophores of the C_2 and C_4 rulers experience a more heterogeneous environment in the interfacial region, producing a broader spectrum than the C_6 ruler.

3B. Molecular Rulers at the Water/Methylcyclohexane Interface

Figure IV.3 shows the SH spectra of three species adsorbed to the water/methylcyclohexane (m-cyclohexane) interface. We have probed chromophore excitation at the liquid/liquid interface using PNP, and the C2 and C6 Rulers. As in the water/cyclohexane case the dotted and dashed lines denote the excitation maxima of the species in bulk water and m-cyclohexane, respectively. Again, the neutral species, PNP in this case, experiences an interfacial polarity that is intermediate between the aqueous and organic limits. The fitted excitation maximum of 304 nm represents the energetic average of the water and m-cyclohexane limits of 318 and 290 nm, respectively. However, unlike at the water/cyclohexane interface, the C_2 ruler experiences a local polarity that is equivalent to that of bulk m-cyclohexane. The chromophore of the C_6 ruler also experiences bulk organic-like solvation at this interface. The only significant difference between the C_2 and C_6 spectra is the linewidths of the SHG features. This

quantity decreases from 46 nm for the C_2 ruler to 22 nm for the C_6 ruler, again implying that the probe of the shorter surfactant experiences a more heterogeneous environment than the probe of the longer surfactant.

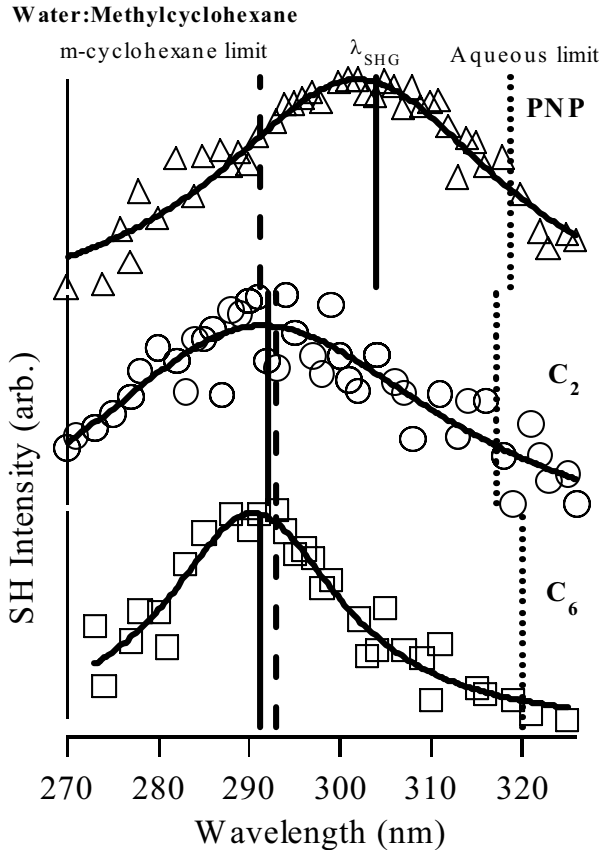

Figure IV.3. Resonance-enhanced SHG spectra of (top to bottom) *p*-nitrophenol (PNP), C_2 rulers, and C_6 rulers adsorbed to a water/m-cyclohexane interface. Dashed, dotted, and solid vertical lines have the same significance as in Figure IV.2.

Despite similarities in the spectral linewidths from the water/cyclohexane and water/m-cyclohexane systems – C_2 spectra are broad, C_6 spectra are narrow – the solvatochromic response of molecular rulers adsorbed to these two interfaces show clear differences in interfacial polarity. Polarity changes gradually across the water/cyclohexane interface, but this transition appears much more abrupt at the water/m-cyclohexane interface. In fact, a C_2 ruler separates headgroup and chromophore by ~3 Å,

or less than one water diameter. Despite this short separation from a headgroup that can only be solvated in the aqueous phase, the chromophore of a C_2 ruler samples an alkane-like, low polarity environment at the water/m-cyclohexane interface.

This comparison represents the first experimental evidence that a slight alteration of organic solvent structure results in a quantitatively sharper liquid/liquid interface. The dramatic difference between the two systems is somewhat surprising, considering the similarities between bulk cyclohexane and m-cyclohexane. Both solvents have similar dielectric constants (2.0), bulk excitation maxima for the C_2 ruler (293 nm), densities (0.770 and 0.779 g/ml, respectively), and indices of refraction (1.426 and 1.422, respectively). Additionally, the solubility of water in cyclohexane is very similar to that in m-cyclohexane – approximately 0.012% by weight at 20°C.[27]

One possible source of the observed difference between the systems might arise from differences in the orientation of adsorbed chromophores with respect to each interface. Polarization-dependent SHG measurements have been used to determine the average orientation of the chromophore relative to the surface normal in a manner similar to that described in Reference 30. For similar concentrations of C_2 ruler at the water/cyclohexane and water/m-cyclohexane interfaces, the chromophore adopts different orientations. At the water/m-cyclohexane interface the pseudo C_2 axis of the C_2 chromophore is oriented approximately 37° off the interfacial normal, while at the water/cyclohexane interface the pseudo C_2 axis is tilted further off-axis (47°). This difference leads to a difference in the projection of the PNAS transition moment onto the surface normal. Assuming the PNAS chromophore to be ~7 Å long these tilt angles lead to projections that differ by ~ 1 Å (5.5 Å at the water/m-cyclohexane interface and 4.5 Å

at the water/cyclohexane interface). In other words, at the water/cyclohexane interface the molecular ruler chromophore is more susceptible to the solvating influence of the adjacent aqueous phase. A difference of 1 Å may seem quite small, but previous experimental studies and simulations of solvation at weakly associating liquid/liquid interfaces have shown that even small changes in a solute equilibrium distribution can have a dramatic effect on the resulting solvation experienced by the solute.[25,28] At the water/m-cyclohexane interface the more upright geometry may expose the chromophore to a more alkane-like environment, while at the water/cyclohexane the chromophore may remain more readily solvated by water. The net result is that the water/m-cyclohexane interface has a more abrupt transition from bulk water to alkane than the water/cyclohexane interface.

3C. Molecular Rulers at the Water/Octane Interface

Results similar to those from the water/m-cyclohexane interface are observed at the water/octane interface. Figure IV.4 shows the SH spectra of PNP, PNAS, C_2 ruler, and C_6 ruler at the water/octane interface. Again, the dotted and dashed lines indicate the excitation maxima of each species in bulk water and octane. We see from the PNP spectrum that the chromophore experiences a surrounding solvation that appears to represent averaged contributions from the two adjacent solvent layers. Just as in the water/m-cyclohexane system we observe a striking transition to an alkane-like dielectric environment with very short molecular rulers. In fact, even the neutral PNAS chromophore experiences an environment suggesting bulk octane solvation. Subsequent spectra of the C_2 and C_6 rulers indicate that these species, too, experience an octane-like solvation. While the spectra indicate that each chromophore samples a low-polarity

environment, the interfacial linewidth of the C_2 spectrum is much broader, 50 nm, than that of the C_6 spectrum, 28 nm. The data suggest that although the chromophores of both ionic ruler surfactants are surrounded by an alkane environment, the C_2 ruler chromophore experiences a less homogeneous environment at the water/octane interface than the C_6 ruler chromophore.

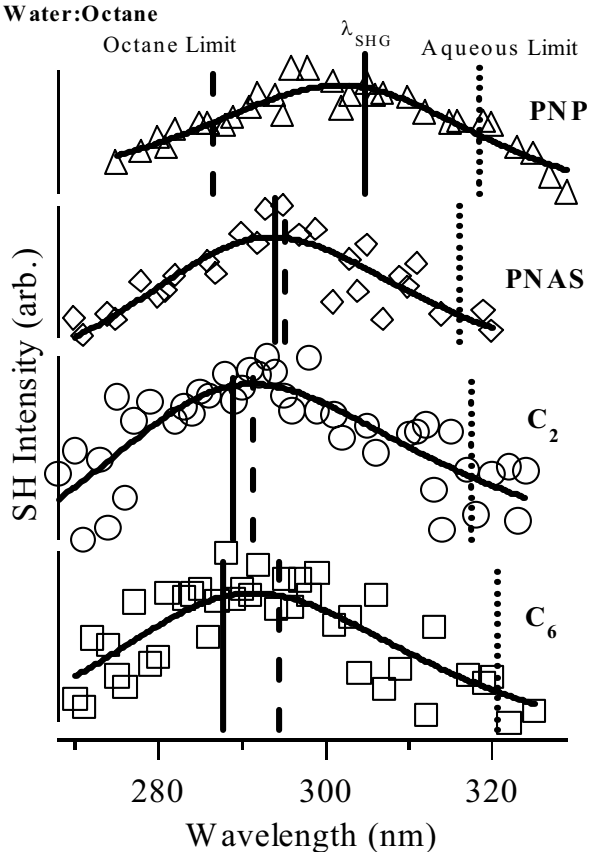

Figure IV.4. Resonance-enhanced SHG spectra of (top to bottom) PNP, PNAS, C_2 rulers, and C_6 rulers adsorbed to a water/octane interface. Dashed, dotted, and solid vertical lines have the same significance as in Figure IV.2.

In each of the previous systems discussed (and the system to follow), interfacial solvation of the adsorbed neutral chromophores generally reflected averaged contributions from the two adjacent solvent phases. One might be surprised, then, that PNAS experiences an octane-like solvation at the water/octane interface. The change

from a hydrophilic hydroxyl group (PNP) to a hydrophobic methoxy group (PNAS) alters the overall hydrophobic/hydrophilic balance in two solutes that otherwise share similar solvation behavior. Water/octane partitioning data were collected for both PNP and PNAS and are shown in Table IV.1. We observed that PNP partitioned to the aqueous phase relative to the organic phase with an equilibrium constant of more than 100. Conversely, PNAS preferentially partitioned to the octane layer by a ratio of almost 20:1 (octane:water), a difference in K_{eq} of more than 3 orders of magnitude. PNAS, then, is more likely to be solvated by octane molecules at the water/octane interface, accounting for the rapid transition to the nonpolar solvation reported by the bare, adsorbed PNAS chromophores. Similar behavior has been observed previously and predicted by simulation.[25,28] This observation emphasizes that subtle variations in solute structure can impact significantly the equilibrium distribution of solutes across interfaces, leading to markedly different local environments experienced by solutes *at the same interface.*

Additionally, we might expect that because PNAS exhibits an increased affinity for the organic phase, the molecules will be drawn more into the organic layer, thus adopting a more upright orientation with respect to the interfacial plane. Polarization-dependent SHG measurements were collected for PNP and PNAS at the water/octane interface, and indicate that PNP is tilted 49° off of normal, while PNAS leans only 34° off of normal, a significant difference. The PNAS adopts a more upright orientation, meaning the chromophore is more effectively solvated by the organic phase than is PNP. Presumably, the structure of PNP induces the molecule to lie further off of surface normal in order to solvate both polar functional groups.

3D. Molecular Rulers at the Water/Hexadecane Interface

The SHG spectra in Figure IV.5 show the behavior of PNP, C_2 ruler, C_6 ruler, and C_8 ruler adsorbed to the water/hexadecane interface. The data are not as clean as in other weakly associating systems, raising some concerns about our interpretation. Specifically, the C_2 and C_6 ruler spectra are noteworthy because they contain large nonresonant contributions that shift the spectral maxima far from the observed intensity maxima and cause the intensity to "leak" to shorter wavelengths in the C_2 ruler spectrum and to longer wavelengths in the C_6 ruler spectrum. Two sources could account for the observed distortions on the SH spectra: a large nonresonant term or a broad distribution of local environments (leading to extreme inhomogeneous broadening). The origins of this large nonresonant contribution are not immediately clear, yet the return to a well-defined spectrum for the C_8 ruler makes us confident that these spectra represent real behavior of ruler surfactants adsorbed to the liquid/liquid interface.

Examining the fitted intensity maxima of the series of spectra, we observe that the neutral chromophore experiences a local polarity that is intermediate between the two bulk limits. In contrast to the behavior observed at the water/octane interface, the C_2 ruler also reflects such intermediate solvation. The excitation wavelength maximum of the C_2 ruler at the water/hexadecane interface is 303 nm. The spectrum of the C_6 ruler is fitted to an interfacial maximum of 290 nm, which indicates a polarity slightly lower than that of the C_6 ruler in bulk hexadecane (294 nm). Unlike at the three previous interfaces, the C_6 ruler spectrum at the water/hexadecane interface is broad (43 nm) and comparable to the linewidths of 42 and 50 nm for PNP and C_2 ruler at this interface. We see in the bottom panel of Figure IV.5 that the C_8 ruler spectrum is much sharper (FWHM = 23 nm)

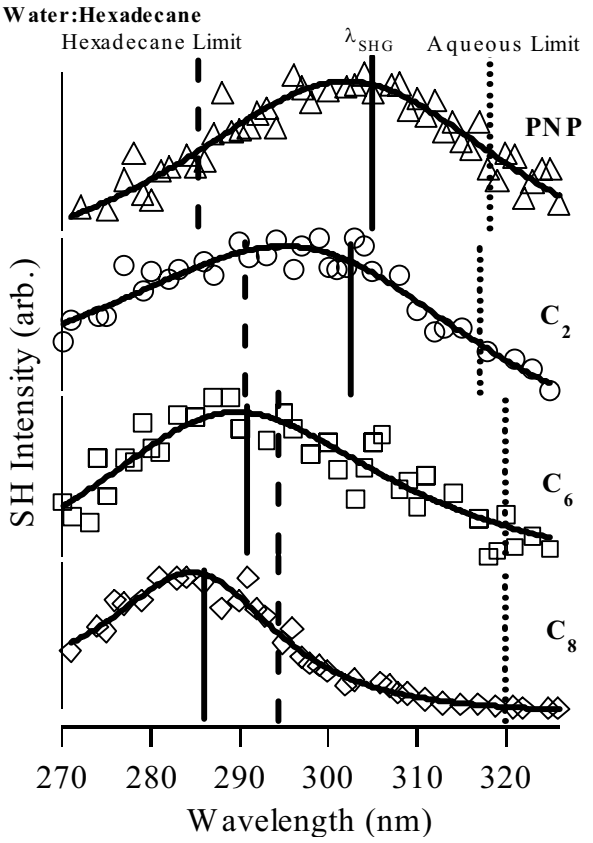

Figure IV.5. Resonance-enhanced SHG spectra of (top to bottom) PNP, C_2 rulers, C_6 rulers, and C_8 rulers adsorbed to a water/hexadecane interface. Dashed, dotted, and solid vertical lines have the same significance as in Figure IV.2.

and reflects a transition maximum of 286 nm, a curious value because it would indicate a surrounding solvation that is much less polar than bulk hexadecane. The linewidth data suggest that solutes sample a broader distribution of environments at the water/hexadecane interface than at other weakly associating interfaces.

4. Discussion

A common feature of the weakly associating interfaces examined in this work is that they are all molecularly sharp – in each case the solvatochromic probe of the C_6 ruler experiences a solvation representative of the bulk organic solvent. This sets an upper

limit on the dipolar width of these weakly associating interfaces; as previously mentioned, a fully extended C_6 spacer oriented perpendicular to the interface stretches 9 Å between the oxygen on the chromophore and the oxygen on the sulfate headgroup. However, qualitative differences do exist between the four alkane solvents studied. The transition to bulk alkane solvation across the water/cyclohexane and water/hexadecane interfaces is more gradual than it is across the water/m-cyclohexane and water/octane interfaces. This behavior is evidenced by two experimental observables, excitation wavelength and spectral linewidth. Figures IV.6 and IV.7 summarize wavelength and linewidth data for different length rulers adsorbed to different water/alkane interfaces. In Figure IV.6 the decrease in excitation wavelength is more gradual at the water/cyclohexane and water/hexdecane interfaces and more abrupt at the water/m-cyclohexane and water/octane interfaces. Figure IV.7 demonstrates that the shorter interfacial probes produce broader spectral bands, and that the longest probe used to examine each system always produced the narrowest linewidth. To further clarify these trends, a summary table including interfacial SHG maxima, linewidth, and orientation data for the species and interfaces discussed appears in Table IV.2.

Any analysis of the differences arising at different water/alkane interfaces should begin by considering the different molecular structures of the alkanes. Of the alkane solvents used in these studies, two are cyclic (cyclohexane and m-cyclohexane) and two are linear (octane and hexadecane). Within each pairing the molecular ruler data suggest that one interface is sharper than the other. In this section, we will examine different factors that can influence interfacial width and speculate on the origins of the observed differences.

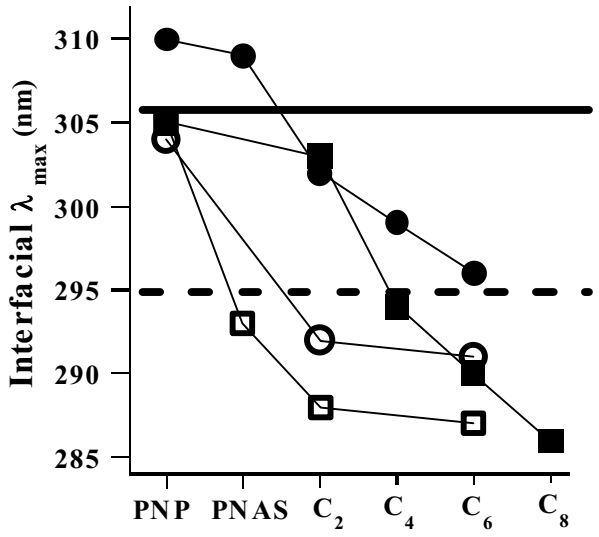

Figure IV.6. Fitted interfacial SHG maxima for species adsorbed to weakly associating liquid/liquid, water/alkane interfaces. The dashed horizontal line denotes the average excitation wavelength of the species in bulk organic solvents (~295 nm). The solid horizontal line denotes the energetic average of the aqueous and organic excitation wavelengths. Two of the interfaces feature a gradual transition from an average polarity to a bulk organic polarity: cyclohexane (filled circles) and hexadecane (filled squares). Two interfaces have abrupt transitions from average polarity to bulk organic solvation: m-cyclohexane (open circles) and octane (open squares).

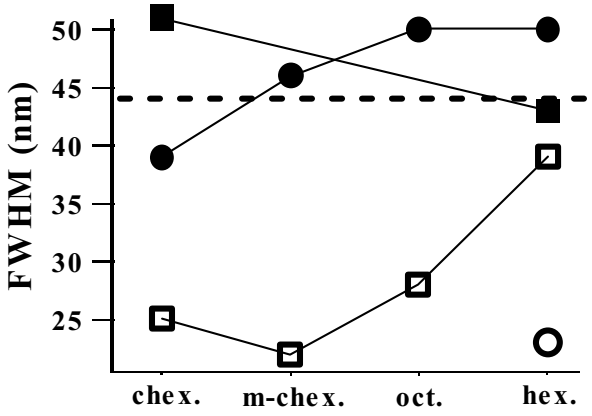

Figure IV.7. Linewidth data for SHG spectra of molecular rulers adsorbed to liquid/liquid interfaces between water and cyclohexane, m-cyclohexane, octane, and hexadecane. The horizontal dashed line denotes the average linewidth of excitation spectra of molecular rulers in bulk organic solvents (~44 nm). The four species shown include C_2 (filled circles), C_4 (filled squares), C_6 (open squares), and C_8 (open circle). At each interface the longest species produced the spectrum with the narrowest linewidth.

Table IV.2. Summary of data collected for species adsorbed to liquid/liquid water/alkane interfaces. The average excitation wavelength of species is ~295 nm in bulk organic solvents and ~318 nm in bulk water. Interfacial Max. refers to the fitted excitation maximum as determined by fitting spectra with Equations IV.1 – IV.3. Fullwidth, half-maximum (FWHM) describes the linewidth of SHG spectra collected at liquid/liquid interfaces. Tilt angle refers to the orientation of the species chromophore at liquid/liquid interfaces relative to surface normal.

Solute	Organic Solvent	Interfacial Max. (nm)	FWHM (nm)	Tilt Angle (°)
PNP	Cyclohexane	310	33	53
PNAS	Cyclohexane	309	15	
C2Ruler	Cyclohexane	302	39	47
C4Ruler	Cyclohexane	299	52	51
C6Ruler	Cyclohexane	296	25	45
PNP	M-cyclohexane	304	35	42
C2Ruler	M-cyclohexane	292	46	37
C6Ruler	M-cyclohexane	291	22	44
PNP	Octane	305	42	49
PNAS	Octane	293	44	34
C2Ruler	Octane	288	50	42
C6Ruler	Octane	287	28	
PNP	Hexadecane	305	42	44
C2Ruler	Hexadecane	303	50	
C6Ruler	Hexadecane	290	43	43
C8Ruler	Hexadecane	286	23	

4A. Cyclic alkanes

In the case of the cyclic solvents, spectra in Figures IV.2 and IV.3 (and in Figures IV.6 and IV.7) indicate that the water/m-cyclohexane interface is sharper than that of the water/cyclohexane system. Based on solvent packing considerations and attractive intermolecular forces – cyclohexane has a smaller surface area, molecular volume and higher melting point than m-cyclohexane – intuition might lead one to guess the opposite to be true. Cyclohexane experiences stronger intermolecular interactions and greater long-range order than m-cyclohexane. Thus we might expect cyclohexane to become more ordered at the water/cyclohexane interface leading to an abrupt transition from an aqueous solvation environment to an organic limit. In contrast, m-cyclohexane would be more disordered adjacent to a water boundary and one might anticipate a more gradual transition from the aqueous to organic limit. However, solvation across liquid/liquid interfaces will not necessarily reflect bulk solution properties, and there exist several considerations that contradict bulk solvent-based intuition and, instead, support findings presented here.

Theoretical and statistical models of interfaces express the interfacial width as the combination of an intrinsic profile width and a capillary wave contribution that is inversely proportional to the surface tension of the interface.[29] The water/cyclohexane interfacial surface tension is 50.2 mN/m while the water/m-cyclohexane has an interfacial tension of 51.5 mM/m as measured with the Wilhemy plate method in our lab. The higher surface tension for the water/m-cyclohexane interface implies a smaller capillary wave contribution to surface roughness and thus a narrower interfacial region separating bulk water from bulk alkane. This interpretation should be viewed cautiously, however,

given that Schlossman and coworkers found that the capillary wave contribution was fairly constant across a broad range of water/alkane interfaces having interfacial tensions that varied by more than 3 mN/m.[7]

Of greater significance to our interpretation are a series of molecular dynamics simulations of water/alkane interfaces performed by Vieceli and Benjamin. In these simulations the authors varied interfacial properties between water and an alkane monolayer by altering the length of the alkane chains present and attaching chlorine atoms to some or all alkanes. In doing so they generated a series of interfaces having varying character: smooth or rough; methyl-terminated, chlorine-terminated or mixed. The interface could also be varied in terms of whether the terminal methyl group or chlorine atom (when present) was "in" or "out" with respect to the interfacial plane. The local environment was then examined by placing a dipolar probe at each interface and evaluating different contributions to the probe's solvation energy. (Figure IV.8 shows a schematic representation of these interfacial topographies.)

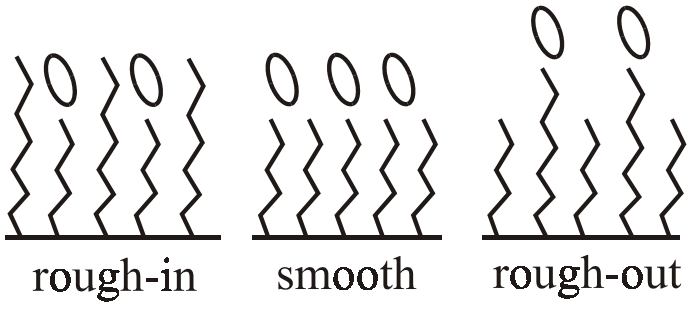

Figure IV.8. Schematic representation of 3 liquid/monolayer interfaces simulated by Vieceli and Benjamin. Water molecules would be placed above the alkane regions shown. The probe molecules (ovals) can be adsorbed in an "in" or "out" orientation at the rough interfaces, resulting in unique interfacial polarities for all three surfaces.

The simulations generated electronic absorption spectra of the probe molecule at these interfaces, and therefore serve as a useful guide for interpreting our studies of solute excitation at liquid/liquid interfaces. Vieceli and Benjamin were able to summarize the polarity of their series of interfaces as follows:

$$\text{rough-in-}CH_3 < \text{smooth-}CH_3 < \text{rough-out-}CH_3$$

All systems containing chlorine (rough-in, rough-out, and smooth) were more polar than the alkane systems. From this hierarchy one sees that the polarity scales with a solute's solvent accessible area. Not surprisingly, greater exposure to the aqueous phase leads to a more polar interfacial environment.

These findings can, in part, be used to interpret the results shown in Figures IV.2 and IV.3. At the water/alkane interface each solvent will pack in a way that is determined by its molecular structure. Based on its compact geometry, small surface area, and relatively high melting point, we expect the symmetric cyclohexane solvent at the interface to arrange itself in a manner more ordered than in bulk. In fact, this surface enhanced density has been proposed as the origin of non-additive solvent polarity at solid/liquid interfaces,[30] and such a surface induced structure in the organic phase is likely to resemble the "smooth" interface simulated by Vieceli and Benjamin.

The additional methyl group on m-cyclohexane breaks the symmetry found in cyclohexane, and creates additional volume between molecules. Additional "free volume" could allow the molecular ruler probe to be more easily solvated in the organic phase. This picture of the interface resembles the "rough-in" interface in the molecular dynamics simulations carried out by Vieceli and Benjamin. In effect, the probe is less exposed to the solvating influence of water and simulations predict that the "rough-in"

interface is less polar than the "smooth" interface. The spectra in Figures IV.2 and IV.3 support this picture, with the chromophore of the shortest ruler (C_2) sampling alkane-like solvation at the water/m-cyclohexane interface, but an intermediate polarity at the water/cyclohexane interface. For the water/cyclohexane system polarity across the well-ordered "smooth" interface converges to that of bulk cyclohexane on a longer lengthscale than for the "rough" water/m-cyclohexane system. These geometric considerations provide a strong motivation to further characterize these interfaces structurally using techniques such as sum frequency generation (SFG) and X-ray and neutron scattering. SFG can report on absolute orientation of solvent species and the degree of solvation at different liquid/liquid interfaces.[31,32] X-ray reflectivity studies may observe the transition from water to alkane manifested as an abrupt exponential decay in reflectivity for sharp interfaces and a more gradual decay for broader interfaces. Information about solvent orientation and conformation at liquid/liquid interfaces will allow further refinement of models of interfacial solvation.

4B. Linear alkanes

Similar to the cyclic alkanes studied, one of the linear alkanes (octane) created a sharper interface than the other (hexadecane). The spectra in Figures IV.4 and IV.5 indicate that solvent polarity converges from an intermediate polarity to that of the bulk alkane more abruptly at the water/octane interface than at the water/hexadecane interface. We begin by noting that Schlossman and co-workers examined a number of water/n-alkane interfaces using X-ray reflectivity to measure the density profile the interfacial region. Their work focused on linear alkanes, and found that as alkane chain length increased the interfacial width increased. Although the widths reported in these

scattering studies measure a different physical property (solvent density) then the one measured in this work (solvent polarity), both sets of results *are* internally consistent. X-ray reflectivity studies measure interfacial width as a function of the density profile across an interface and describe how rapidly the solvent density converges from bulk water to bulk alkane. The interfacial density reflects the physical composition of the interface. In our studies, the interfacial width is a function of the electronic forces between the solute and its surroundings at the boundary between adjacent phases. Nevertheless, despite the differences between the quantities probed by these two experimental techniques, we find it encouraging that the results presented here agree with those from previous studies.

For the data shown in Figures IV.4 and IV.5, differences in solvent molecular structure again suggest why octane and hexadecane create different interfacial environments. Solvent packing is an important factor in the ability of octane and hexadecane to solvate the probe. The molecular volume of hexadecane is 488 $Å^3$ and that of octane is 271 $Å^3$. Obviously, hexadecane is larger than octane, but it is not twice as large. In fact, the molecular volume of hexadecane is only 90% of that of two octane molecules. This discrepancy arises from hexadecane's additional conformational flexibility relative to octane. Due to its longer length, hexadecane can bend and adopt more compact conformations. At an interface, these efficient, space filling geometries mean less free volume to solvate the probe of adsorbed molecular rulers. The interface created by hexadecane compared to octane, then may be similar to that of cyclohexane compared to m-cyclohexane. As in the case of the cyclic alkanes, we would expect solvents possessing less free volume to produce broader interfaces.

5. Conclusion

We have used molecular rulers to probe solute excitation at several weakly associating water/alkane liquid/liquid interfaces. The data suggest that all these interfaces are sharp, featuring an abrupt transition (< 9 Å) from the aqueous to the organic phase. However, our findings suggest that some weakly associating interfaces are sharper than others. Differences in dipolar width depend sensitively on solvent structure and appear to correlate with free volume within the organic phase. These findings agree well with predictions from molecular dynamics simulations predicting that interfacial solvent polarity should scale with a solute's solvent accessible area. Ongoing studies will continue to explore the relationship between solvent molecular structure and interfacial width.

References

(1) Volkov, A. G.; Deamer, D. W.; Tanelian, D. L.; Markin, V. S. *Liquid Interfaces in Chemistry and Biology*; John Wiley & Sons: New York, 1998.

(2) Volkov, A. G., Ed. *Liquid Interfaces in Chemical, Biological, and Pharmaceutical Applications*; Marcel Dekker: New York, 2001; Vol. 95.

(3) Chhabra, V.; Free, M. L.; Kang, P. K.; Truesdail, S. E.; Shah, D. O. *Tenside, Surfactants, Detergents* **1997**, *34*, 156.

(4) Safran, S. A. *Statistical Thermodynamics of Surfaces, Interfaces, and Membranes*; Addison-Wesley: Reading, MA, 1994; Vol. 90.

(5) Chipot, C.; Wilson, M. A.; Pohorille, A. *J. Phys. Chem. B* **1997**, *101*, 782.

(6) Sangster, J. *Octanol-Water Partition Coefficients*; John Wiley and Sons: New York, 1997; Vol. 2.

(7) Mitrinovic, D.; Tikhonov, A. M.; Li, M.; Huang, Z.; Schlossman, M. L. *Phys. Rev. Lett.* **2000**, *85*, 582.

(8) Stanners, C. D.; Du, Q.; Chin, R. P.; Cremer, P.; Somorjai, G. A.; Shen, Y.-R. *Chem. Phys. Lett.* **1995**, *232*, 407.

(9) Tikhonov, A. M.; Mitrinovic, D. M.; Li, M.; Huang, Z.; Schlossman, M. L. *J. Phys. Chem. B* **2000**, *104*, 6336.

(10) Girault, H. H.; Tamburello-Luca, A. A.; Hebert, P.; Brevet, P. F. *J. Chem. Soc. Faraday Trans.* **1996**, *92*, 3079.

(11) Eisenthal, K. B. *J. Phys. Chem.* **1996**, *100*, 12997.

(12) Kitamura, N.; Ishizaka, S.; Kim, H. *Anal. Chem.* **2001**, *73*, 2421.

(13) Steel, W. H.; Walker, R. A. *Nature* **2003**, *424*, 296.

(14) Steel, W. H.; Damkaci, F.; Nolan, R.; Walker, R. A. *J. Am. Chem. Soc.* **2002**, *124*, 4824.

(15) Beildeck, C. L.; Steel, W. H.; Walker, R. A. *Langmuir* **2003**, *19*, 4933.

(16) Schlossman, M. L.; Li, M.; Mitrinovic, D. M.; Tikhonov, A. M. *High Perform. Polym.* **2000**, *12*, 551.

(17) Michael, D.; Benjamin, I. *J. Phys. Chem. B* **1998**, *102*, 5145.

(18) Penfold, J.; Richardson, R. M.; Zarbakhsh, A.; Webster, J. R. P. *J. Chem. Soc. Faraday Trans.* **1997**, *93*, 3899.

(19) Wirth, M. J.; Burbage, J. D. *J. Phys. Chem.* **1992**, *96*, 9022.

(20) Sassaman, J. L.; Wirth, M. J. *Coll. & Surf. A* **1994**, *93*, 49.

(21) Kovaleski, J. M.; Wirth, M. J. *J. Phys. Chem.* **1995**, *99*, 4091.

(22) Wang, H.; Borguet, E.; Eisenthal, K. B. *J. Phys. Chem. A* **1997**, *101*, 713.

(23) Wang, H.; Borguet, E.; Eisenthal, K. B. *J. Phys. Chem. B* **1998**, *102*, 4927.

(24) Piron, A.; Brevet, P. F.; Girault, H. H. *J. Electroanal. Chem.* **2000**, *483*, 29.

(25) Steel, W. H.; Walker, R. A. *J. Am. Chem. Soc.* **2003**, *125*, 1132.

(26) Zhang, X.; Esenturk, O.; Walker, R. A. *J. Am. Chem. Soc.* **2001**, *123*, 10768.

(27) Englin, B. A.; Plate, A. F.; Tugolukov, V. M.; Pryanishnikova, M. A. *Chem. & Tech. Fuel & oil* **1965**, *10*, 722.

(28) Michael, D.; Benjamin, I. *J. Chem. Phys.* **2001**, *114*, 2817.

(29) Weeks, J. D. *J. Chem. Phys.* **1977**, *67*, 3106.

(30) Zhang, X.; Cunningham, M. M.; Walker, R. A. *J. Phys. Chem. B* **2003**, *107*, 3183.

(31) Scatena, L. F.; Brown, M. G.; Richmond, G. L. *Science* **2001**, *292*, 908.

(32) Scatena, L. F.; Richmond, G. L. *J. Phys. Chem. B* **2001**, *105*, 11240.

Chapter V. Solvent Polarity across Strongly Associating Interfaces

1. Introduction

Chapter IV addressed profiling solvent polarity across weakly associating liquid/liquid interfaces. Molecular rulers were used to measure the dipolar widths of four interfaces between water and alkane solvents. This chapter focuses on the same issues for interfaces that are strongly associating. The materials presented in this chapter form the basis of an article currently under review in *The Journal of Physical Chemistry B*.

Strongly associating liquid/liquid interfaces describe boundaries where strong dipolar forces control the structure and dynamics of two immiscible liquids. These surfaces are characterized by low interfacial tensions[1,2] and can contain significant electric potential gradients.[3,4] Accordingly, these interfaces figure prominently in electrochemistry studies as well as in efforts to mimic biophysical systems.[5-8] In particular, strongly associating liquid/liquid interfaces have proven to be valuable systems for determining drug efficacy and have served as effective models of cell membranes.[9] Several experimental and theoretical studies have investigated the structures of liquid/liquid interfaces in a variety of manners, including molecular dynamics simulations,[10,11] X-ray scattering experiments,[12] and non-linear optical spectroscopy.[13-15] Numerous experimental and theoretical studies of weakly associating liquid/liquid interfaces have provided considerable information about the forces controlling the structure and dynamics of the boundaries between two phases with no affinity for one another.[11,16-18] In contrast, fewer studies have investigated how long-range order and interfacial structure are influenced by the strong asymmetric forces

inherent to strongly associating interfaces.[19-21] Even less clear is how anisotropic boundaries control interfacial solvation. Here, solvation refers to the noncovalent interactions experienced between a solute and its surroundings. Understanding how interfaces alter solute-solvent interactions from those in bulk solution is essential for formulating quantitative, predictive models of solution phase surface chemistry.

In bulk solution a solute is subject to isotropic forces and continuum models of solvation can accurately describe solute behavior. At an interface, however, solutes experience an anisotropic environment, especially if the solute contains both polar and nonpolar functional groups that lead to surface-induced, polar ordering. Under these circumstances, short range interactions between a solute and its interfacial surroundings can lead to dramatic changes in solute energetics, structure and reactivity. In the studies described below, we use second order nonlinear optical spectroscopy to measure solvent polarity across strongly associating liquid/liquid interfaces. The interfaces all consist of an aqueous phase in contact with an alcohol, and the solutes are solvatochromic probes that have been integrated into surfactants of varying lengths, e.g. "molecular rulers".[22,23] Results show that interfacial properties depend sensitively on the structure of the alcohol, with all strongly associating interfaces containing a region of reduced polarity between the adjacent solvent layers. This result is important because it emphasizes how interphase interactions between two solvents can create an environment having completely different properties from either bulk solution.

On some lengthscale interfacial properties must converge to bulk solution limits. Quantifying changes in properties such as density, dielectric constant, or refractive index can lead to the determination of the interfacial width. This distance may be short by

molecular standards, leading to abrupt changes in these solvent properties, or interfacial width may be broad with properties changing gradually over multiple solvent diameters. Several experimental techniques currently exist for investigating the properties of interfaces, each observing a different characteristic feature of these inhomogeneous regions. X-ray[24] and neutron scattering experiments[25] provide the most direct measure of interfacial width by recording profiles of solvent density at liquid/liquid interfaces along the interfacial normal. Such techniques have been used successfully to probe interfacial width at weakly associating water/alkane interfaces, and determined these boundaries to molecularly sharp.[12] This finding is in agreement with molecular dynamics simulations[26-28] and non-linear optical second harmonic generation studies[29] of these interfaces.

Unlike the scattering techniques described above, optical spectroscopy is not a direct measure of changes in solvent properties. Techniques such as total internal reflection fluorescence (TIRF) and second harmonic generation (SHG) probe the interactions between solvent and solute molecules at the interface. These studies have been broadly applied to interfaces, including air/liquid, solid/liquid, and liquid/liquid boundaries in attempts to investigate a variety of solvent sensitive properties of solute probe molecules.[30-37] For example, Kitamura and co-workers have used TIRF to investigate the energy transfer between two fluorescent dyes at weakly associating liquid/liquid interfaces.[30,38] Eisenthal and co-workers have used SHG extensively to study solvent polarity at liquid/liquid interfaces, producing some of the earliest quantitative models of interfacial polarity.[39,40] Recent experiments using SHG to probe interfacial excitation of solvatochromic surfactants adsorbed to weakly associating

interfaces have shown these boundaries to be molecularly sharp,[29] in agreement with scattering studies and molecular dynamics simulations mentioned above.[26-28]

The success of SHG as a probe of solvent polarity at weakly associating liquid/liquid interfaces has led us to believe it will also be a suitable probe of such behavior at strongly associating interfaces. While there exists a growing body of work focused on interfacial properties at weakly associating boundaries, little has been done to probe solvent properties at interfaces between water and organic solvents capable of interacting through strong dipolar forces.[19,21,41] These strongly associating interfaces play prominent roles in chemistry and warrant thorough investigation. To this point, the majority of work examining strongly associating liquid/liquid interfaces has focused on the vibrational structure of the organic solvent at the interface. For example, sum frequency generation (SFG) has been used to probe the structures of pentadecanoic acid at the water surface,[42] long chain alcohols at the liquid/vapor interface (Shen (CPL),[21] and surfactant chains at the air/water interface.[43-45] Emerging from these studies are a variety of conclusions about the structure of the adsorbed surfactants and alkyl chains. Briefly, the presence of *gauche* defects was determined to be related to surface coverage[42] and chain length of the adsorbed species.[21,43] Finally, Cramb and Wallace reported using SHG to investigate the orientation of octanol molecules at the water/octanol interface.[6] They determined that the adsorbed octanol molecules exhibited a net tilt off of the surface normal.

In addition to the vibrational studies mentioned above, several simulations have been performed that provide information about the structure of strongly associating interfaces. Michael and Benjamin investigated the fluorescence of probes adsorbed to a

water/octanol interface and determined that the relaxation times were strongly dependent on the solute's position relative to the interface.[10] Their results also implied that the water/octanol interface was composed of a low polarity region that contained no water molecules, a conclusion that is supported by the findings presented in this work.

Experiments described in this chapter used SHG to investigate the interfacial excitation of surfactants adsorbed to strongly associating liquid/liquid interfaces between water and various alcohols. By observing the solvent sensitve excitation response we are able to infer the polarity of the interface. As surfactant length increases, interfacial polarity converges to bulk solution limits, and each family of excitation spectra represents a profile of the changes in solvent polarity across the liquid/liquid interface. These experiments represent the first attempts to probe dipolar width of water/alcohol interfaces, and as such, much of the analysis presented herein is speculative in nature.

2. Experimental methods

Experiments described in this thesis couple resonance-enhanced SHG spectroscopy with surfactants created specifically to vary the equilibrium distribution of solvatochromic solutes across a liquid/liquid interface. By measuring how SHG spectra vary with surfactant length, the dipolar width of different strongly associating liquid/liquid interfaces has been measured. The alcohols used to create an interface with an aqueous subphase include 1-octanol, 1-decanol, 3-octanol, and 2,6-dimethyl-4-heptanol. While similar experiments at interfaces between water and alkanes found such weakly associating interfaces to be sharp,[29] these strongly interfaces appear to be broader and contain a region of reduced polarity between the two phases. These findings are

discussed in terms of the molecular structure of the individual solvents themselves and recent simulations that expose the role of interfacial roughness on solvation dynamics and interfacial polarity.

As described in Chapter III, molecular rulers are surfactants containing an ionic headgroup attached to a hydrophobic nitrobenzene chromophore via an alkoxy spacer whose length can be varied by controlling the number of methylene groups present. Surfactants have been produced with spacers ranging from two to eight methylene groups, primarily in even increments. A more complete description of synthetic conditions and characterization of the molecular rulers can be found in Chapter III.

Resonance-enhanced SHG was used to acquire effective excitation spectra of molecular rulers adsorbed to different water/alcohol, liquid/liquid interfaces. Because of its origins, the resonance-enhanced response is both surface and molecularly specific, meaning that spectra result only from solutes influenced by interfacial anisotropy.[39,46] In a typical experiment, a single coherent optical field of frequency ω is incident upon an interface having a sub-monolayer coverage of a given ruler surfactant. A nonlinear polarization of frequency 2ω and intensity $I(2\omega)$ is detected, where the intensity of this second harmonic is proportional to the square of the second-order susceptibility, $\chi^{(2)}$

$$I(2\omega) \propto |\chi^{(2)}|^2 I^2(\omega) \qquad \text{(V.1)}$$

and $\chi^{(2)}$ is a third rank tensor that under the electric dipole approximation is zero in isotropic environments. The $\chi^{(2)}$ tensor, then, imparts to the technique its inherent surface specificity. The tensor itself contains both resonant and nonresonant contributions:

$$\chi^{(2)} = \chi^{(2)}_{R} + \chi^{(2)}_{NR} \qquad \text{(V.2)}$$

For dielectric systems, such as the water/alcohol interfaces considered here, the resonant term is typically several orders of magnitude larger than the nonresonant contribution and can be related to the microscopic hyperpolarizability:

$$\chi_R^{(2)} = \sum_{k,e} \frac{\left\langle \mu_{gk} \mu_{ke} \mu_{eg} \right\rangle}{(\omega_{gk} - \omega - i\Gamma)(\omega_{eg} - 2\omega + i\Gamma)} \qquad (V.3)$$

where μ_{ij} is the transition matrix element between state i and state j (where g stands for the ground state, k for an intermediate, virtual state, and e for the first excited state). The ω_{ij} refer to the transition energies between the ground state and states k and e, and Γ is the transition's line width. When 2ω is resonant with ω_{eg}, $\chi^{(2)}$ becomes large, leading to a strong resonance enhancement in the observed intensity at 2ω. Thus, measuring the scaled intensity $[I(2\omega)/I^2(\omega)]$ as a function of 2ω records an *effective* excitation spectrum of solutes adsorbed to an interface. With the exception of data recorded to determine solute orientations, spectra in this work were acquired under $P_\omega P_{2\omega}$ polarization conditions, where P polarized light describes light that is polarized in the plane defined by the surface normal and the direction of propagation. Varying the incident and detected polarizations enabled us to determine the average chromophore orientation using methods described previously. Different polarizations did not lead to qualitatively different SHG spectra.

The experimental methods used for acquiring spectra of molecular rulers adsorbed to strongly associating liquid/liquid interfaces are similar to those described in Reference 29. One difference between the two systems is the solubility of the molecular rulers in the organic phase. Due to slight surfactant solubility in the alcohols used in the present studies, only one spectrum was usually collected from each prepared sample before it was

discarded due to decreased signal intensity. Over the course of several hours molecular rulers were able to transfer across the aqueous/organic interface from the water phase into the alcohol. Rulers in the alcohol phase will absorb the second harmonic signal produced by those chromophores adsorbed to the interface, thus apparent intensity of the detected SH signal diminishes slightly over time. At weakly associating interfaces multiple spectra could be recorded from the same system and compared for internal consistency and reproducibility. In the current studies, spectra of surfactants adsorbed to strongly associating interfaces were acquired within three hours of cell assembly. Spectra acquired during this window demonstrated reproducible behavior and results were normalized to produce the composite spectra shown in Figures 1 through 4.

3. Results

3A. Molecular Rulers at the Water/1-Octanol Interface

Figure V.1 shows the composite SH spectra of four molecular ruler species (C_2 ruler, C_4 ruler, C_6 ruler, and C_8 ruler) adsorbed to the water/1-octanol interface. The SH data are fit according to Equations V.1 – V.3. Overlaid on the plots are dashed and dotted lines to denote the excitation maximum of each species in bulk aqueous and organic solutions, respectively. The solid vertical line on each panel indicates the fitted interfacial maximum of each species (including the nonresonant contribution). Note that interference effects between the resonant and nonresonant contributions to $\chi^{(2)}$ can lead to a calculated SH maximum that does not coincide with the apparent spectral maximum. (For example, see the bottom panel of Figure 1, depicting the SHG spectrum of the C_8 ruler at the water/1-octanol interface.)

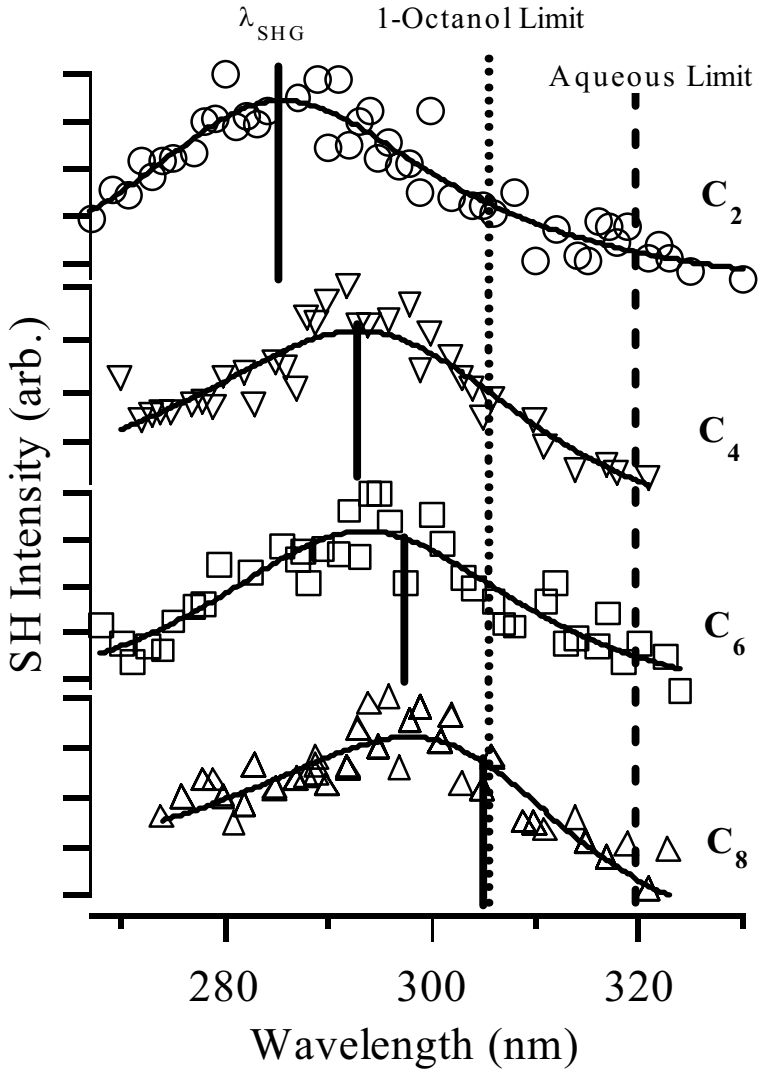

Figure V.1. Resonance-enhanced SHG spectra of (top to bottom) C_2 rulers, C_4 rulers, C_6 rulers, and C_8 rulers adsorbed to a water/1-octanol interface. Dotted and dashed vertical lines denote excitation maxima in bulk 1-octanol and water, respectively. Solid vertical lines correspond to SHG maxima (λ_{SHG}) as determined by fitting the data to Equations V.1 – V.3. Note that SHG maxima do not always correspond to the wavelengths with the highest SHG intensity, owing to the nonresonant contribution to $\chi^{(2)}$ in Equation V.2.

The data show that the solvatochromic probe of each solute samples a unique solvation environment. Of greater interest is the local polarity sampled by each probe. The excitation maximum of the C_2 ruler at the water/1-octanol interface is 285 $\pm$ 3 nm,

compared to maxima of 317 nm in bulk water and 306 nm in 1-octanol. An excitation maximum of 285 nm suggests a solvation environment that is even less polar than that of a bulk alkane having a static dielectric constant of ~2.0. As the alkyl spacer in the molecular rulers lengthens from C_2 to C_4 to C_6 to C_8, the chromophores can "float" further into the bulk organic phase. The resulting interfacial excitation maxima reflect increasingly polar solvation environments. This change is detected as a red shift in the fitted interfacial excitation maxima from 285 nm for the C_2 ruler to 305 nm for the C_8 ruler. The 305 nm interfacial excitation maximum of the C_8 ruler is similar to the excitation maximum of the C_8 ruler in bulk 1-octanol (306 nm).

While molecular rulers adsorbed to weakly associating interfaces reflected solvation environments that could be described by appropriately weighted additive effects from the two adjacent solvents,[29] here rulers adsorbed to strongly associating interfaces sample dielectric environments that are considerably less polar than bulk 1-octanol. This result can not be explained by an additive model. The series of spectra imply that the interfacial polarity gradually converges from a nonpolar, alkane-like solvation to one reflecting a solvation similar to bulk 1-octanol – that is, there is a region of reduced polarity between the very polar water phase and the 1-octanol phase of intermediate polarity. In contrast, when adsorbed to weakly associating interfaces, the same species of probes displayed a monotonic blue-shift in interfacial excitation maxima, implying a transition from a more polar to a less polar solvation environment. The length of the alkyl spacer in the C_8 ruler is approximately 1.2 nm, assuming no *gauche* defects in the chain. This length represents an upper limit to the width of the reduced polarity region

between the two phases. All weakly associating interfaces were found to converge to bulk organic limits over a distance of less than 9 Å.

Another feature distinguishing this series of spectra from similar series collected at weakly associating interfaces is the stability of the linewidth of each spectrum as the alkyl spacer lengthens. At weakly associating interfaces the spectrum of the molecular ruler with the longest alkyl spacer had the narrowest full-width half-maximum (FWHM). Here, there is little change in the linewidth of the spectra, as they range from 35 nm (C_8) to 38 nm (C_2 and C_6). Excitation spectra of molecular rulers in bulk solutions of water and 1-octanol have FWHM of 68 nm and 56 nm, respectively. A narrower linewidth for adsorbed species indicates a solvation environment that is more homogeneous than bulk solution.[47,48] Interestingly, excitation spectra of molecular rulers in bulk alkanes have an average linewidth of 44 nm. This observation would indicate that ruler species adsorbed to the water/1-octanol interface sample a solvation environment more homogeneous than bulk alkanes. Polarization-dependent SHG measurements have been used to determine the average orientation of molecular ruler chromophores relative to the surface normal.[49] The data indicate that all molecular ruler species adsorbed to the water/1-octanol interface adopt similar orientations, ranging from 34º off of normal (C_2) to 37º off of normal (C_4 and C_8). This finding suggests that the chromophores of each ruler species experience similar, homogeneous environments at the water/1-octanol interface. Spectral linewidth and orientation data will be discussed in more detail in section 4. A summary of the data collected at the water/1-octanol interface appears in Table V.1. The table includes interfacial maxima, linewidth, and orientation data.

Table V.1. Summary of data collected for species adsorbed to water/1-octanol liquid/liquid interface. The average excitation wavelength of species is ~305 nm in bulk organic solvents and ~318 nm in bulk water. Interfacial Max. refers to the fitted excitation maximum as determined by fitting spectra with Equations V.1 – V.3. Fullwidth, half-maximum (FWHM) describes the linewidth of SHG spectra collected at liquid/liquid interfaces. Tilt angle refers to the orientation of the species chromophore at liquid/liquid interfaces relative to surface normal.

Solute	Interfacial Max. (nm)	FWHM (nm)	Tilt Angle (°)
C_2 Ruler	285	36	34
C_4 Ruler	295	36	37
C_6 Ruler	297	38	36
C_8 Ruler	305	35	37

3B. Molecular Rulers at the Water/1-Decanol Interface

The same four molecular ruler surfactants were used to probe interfacial polarity at the water/1-decanol interface. SH spectra for the water/1-decanol interface are shown in Figure V.2, where once again the dashed and dotted lines denote excitation maxima of each species in bulk water and 1-decanol, respectively. As at the water/1-octanol interface, the chromophore of the shortest ruler species, C_2, experiences the least polar solvation environment at the water/1-decanol interface. The interfacial maximum of 295 nm for the C_2 ruler is shared by the chromophore of the C_4 ruler before, as at the water/1-octanol interface, it red shifts to 300 nm for the chromophore of the C_8 ruler. The C_8 ruler has an excitation maximum of 306 nm in bulk 1-decanol, implying that the interfacial polarity is still less polar than bulk 1-decanol. The difference in the water/1-octanol versus water/1-decanol as sampled by the C_2 ruler remains unexplained, but qualitative similarities between the two systems are reassuring. Both linear alcohols create regions of reduced polarity between the bulk water and alcohol phases. That the chromophore of the C_8 ruler does not experience solvation similar to the bulk alcohol at

the water/1-decanol interface, like it does at the water/1-octanol interface suggests that the water/1-decanol interface is broader. In general, the data suggest that the width of strongly associating interfaces between water and linear alcohols is related to the length of the alcohol involved.

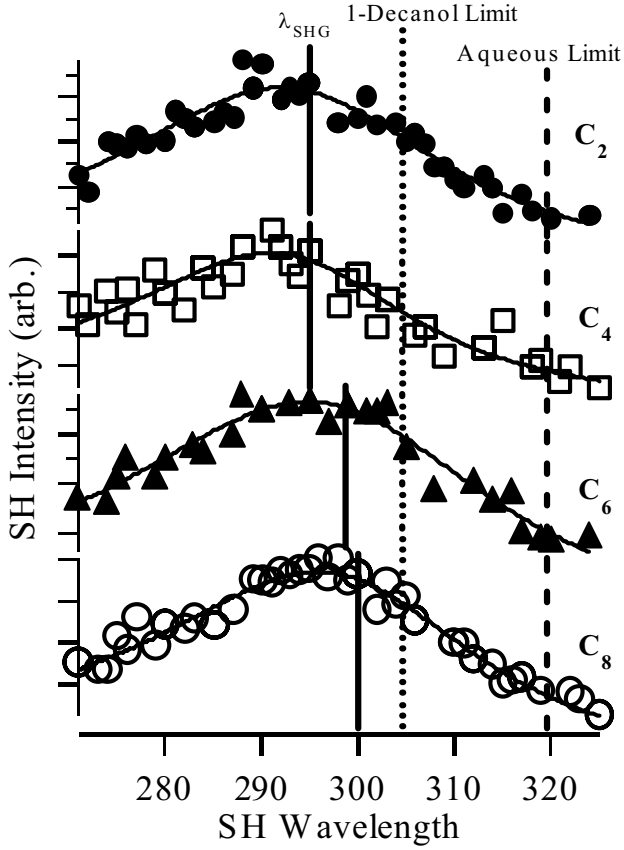

Figure V.2. Resonance-enhanced SHG spectra of (top to bottom) C_2 rulers, C_4 rulers, C_6 rulers, and C_8 rulers adsorbed to a water/1-decanol interface. Dotted, dashed, and solid vertical lines have the same significance as in Figure V.1.

The linewidth data for the spectra collected at the water/1-decanol interface are similar to those from the water/1-octanol interface, although the widths cover a slightly broader range: 35 nm to 41 nm. Even with this increased range, these data fall within the limits of the uncertainty in the linewidth calculations ($\pm$ 3 nm), implying that the two

interfaces are likely very similar in structure. Orientation measurements also reflect this trend. The tilt of the chromophore of the C_2 ruler is 37º off of normal. This value decreases to 32º off of normal for the C_8 ruler. Again, given the uncertainty in these values ($\pm$ 3º), these can be considered to be equivalent to the tilts observed at the water/1-octanol interface. Table V.2 summarizes the data from the four spectra shown in Figure V.2.

Table V.2. Summary of data collected for species adsorbed to water/1-decanol liquid/liquid interface. The average excitation wavelength of species is ~305 nm in bulk organic solvents and ~318 nm in bulk water. Quantities represent the same values as in Table V.1.

Solute	Interfacial Max. (nm)	FWHM (nm)	Tilt Angle (°)
C_2 Ruler	295	40	37
C_4 Ruler	295	35	32
C_6 Ruler	299	41	
C_8 Ruler	300	36	32

3C. Molecular Rulers at the Water/3-Octanol Interface

Figure V.3 shows the SH spectra for three molecular ruler species adsorbed to the water/3-octanol interface: C_2, C_4, and C_6. As was observed at the interfaces between water and the two linear alcohols, the chromophores of the shorter probes experience a solvation that is less polar than bulk 3-octanol. The C_2 ruler has an interfacial maximum of 297 nm, while the C_4 displays a maximum at 294 when adsorbed to the water/3-octanol interface. The slight blue shift observed in the excitation wavelength between the C_2 and C_4 ruler chromophores is a surprising result, but does not contradict the picture that emerged from the water/linear alcohol systems. Unlike in the previous systems

though, at the water/3-octanol interface the chromophore of the C_6 ruler has an interfacial excitation maximum equivalent to that of the chromophore in bulk 3-octanol. The chromophore of the C_8 ruler also experiences a polarity similar to that of bulk 3-octanol (see Table 1), although again, the non-resonant contribution is larger than for the shorter species. The conclusion to be drawn from this family of spectra is that the branched 3-octanol has created a more abrupt interface with water than either linear alcohol. The C_6 molecular ruler contains an alkyl spacer that is, at most, 9 Å long, setting the upper limit of the dipolar width of the water/3-octanol interface.

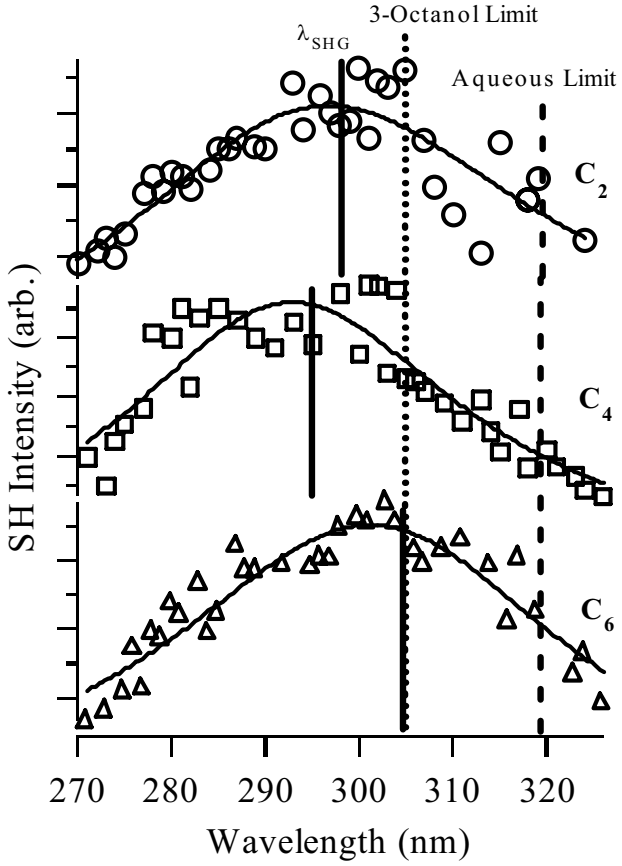

Figure V.3. Resonance-enhanced SHG spectra of (top to bottom) C_2 rulers, C_4 rulers, and C_6 rulers adsorbed to a water/3-octanol interface. Dotted, dashed, and solid vertical lines have the same significance as in Figure V.1.

Additional differences between this system and the two linear alcohol systems can be found when examining the linewidth data. Here the linewidths of the spectra from the water/3-octanol interface are ~25% broader than from the complementary systems with the linear alcohols. Furthermore, the linewidth values from the water/3-octanol interface (43 – 51 nm) are very close to those found in bulk solutions of 3-octanol (49 nm). These observations suggest that the water/3-octanol interface is more heterogeneous than interfaces formed between water and linear alcohols and that interfacial polarity converges to the bulk 3-octanol limit over a shorter lengthscale than for the linear alcohol systems. Table V.3 summarizes the interfacial maxima and linewidth data for the water/3-octanol interface.

Table V.3. Summary of interfacial maxima and linewidth data collected for species adsorbed to water/3-octanol liquid/liquid interface. The average excitation wavelength of species is ~305 nm in bulk organic solvents and ~318 nm in bulk water.

Solute	Interfacial Max. (nm)	FWHM (nm)	Tilt Angle (°)
C_2 Ruler	297	51	34
C_4 Ruler	294	43	32
C_6 Ruler	305	48	

3D. Molecular Rulers at the Water/2,6-dimethyl-4-heptanol Interface

Figure V.4 shows the SH spectra of the three shortest molecular rulers adsorbed to the water/2,6-dimethyl-4-heptanol interface. Once again, the interface between water and the branched alcohol appears to be more abrupt than those between water and the linear alcohols. The chromophore of the C_2 ruler experiences the least polar solvation, as

indicated by its interfacial excitation maximum of 293 nm. The C_4 ruler has its maximum at 297 nm, implying a local dielectric environment that is less polar than bulk 2,6-dimethyl-4-heptanol. The chromophore of the C_6 ruler absorbs at 307 nm at this interface, a value that is slightly greater than its excitation maximum in bulk 2,6-dimethyl-4-heptanol. The series of spectra are similar to those generated at the water/3-octanol interface, and indicate that the interfacial region is no wider than 9 Å, the length of the alkyl spacer in the C_6 ruler. The data from Figure V.4 are summarized in Table V.4.

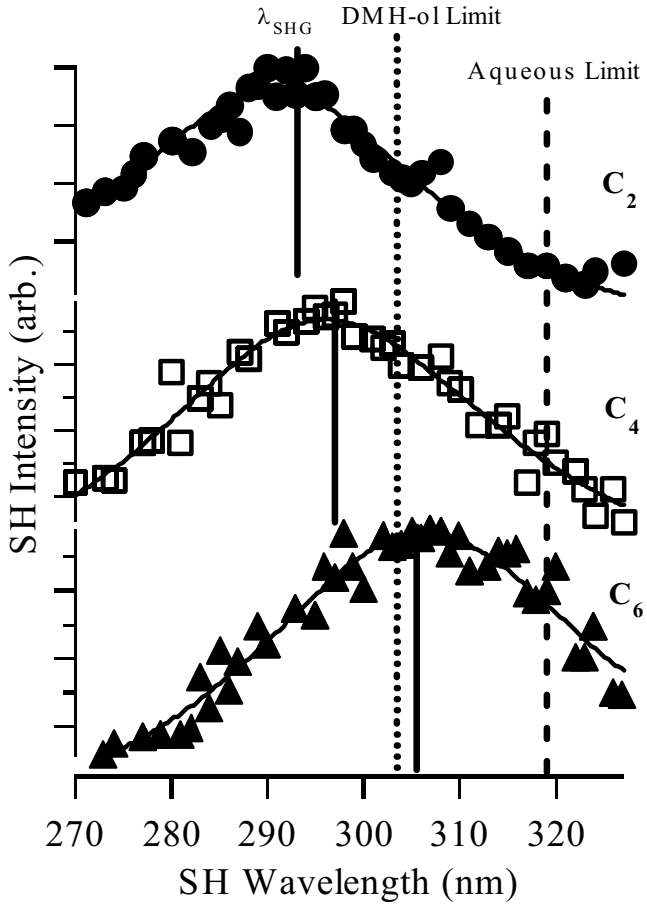

Figure V.4. Resonance-enhanced SHG spectra of (top to bottom) C_2 rulers, C_4 rulers, and C_6 rulers adsorbed to a water/2,6-dimethyl-4-heptanol interface (DMH-ol). Dotted, dashed, and solid vertical lines have the same significance as in Figure V.1.

Table V.4. Summary of interfacial maxima, linewidth, and orientation data collected for species adsorbed to water/2,6-dimethyl-4-heptanol (DMH-ol) liquid/liquid interface. The average excitation wavelength of species is ~305 nm in bulk organic solvents and ~318 nm in bulk water.

Solute	Interfacial Max. (nm)	FWHM (nm)	Tilt Angle (°)
C_2 Ruler	293	42	33
C_4 Ruler	297	46	
C_6 Ruler	307	45	32

The linewidths of the spectra collected at the water/2,6-dimethyl-4-heptanol interface all lie between 42 and 46 nm. These values are slightly larger than those recorded at the water/1-octanol and water/1-decanol interfaces. While the range is not as wide as that for the linewidths of the same species at the water/3-octanol interface, the magnitude of these FWHM data is similar, and suggests that the chromophores of the molecular rulers are exposed to interfacial solvation environments that are similar to bulk 2,6-dimethyl-4-heptanol (FWHM = 50 nm). Polarization-dependent SHG measurements were again used to calculate the average orientations of the chromophores relative to the surface normal at the water/2,6-dimethyl-4-heptanol interface. The chromophore of the C_2 ruler lies 33º off of normal while that of the C_6 ruler lies 32º off of normal.

4. Discussion

A feature common to all the strongly associating interfaces examined in this work is a region of reduced polarity between the water and alcohol phases. This observation emphasizes the non-additive nature of interfacial properties at strongly associating boundaries. In contrast, at weakly associating interfaces molecular rulers sampled

polarities that represented weighted contributions from the adjacent solvents.[29] The excitation spectra of molecular rulers adsorbed to strongly associating interfaces indicate that the interfaces between water and linear alcohols are broader than those between water and branched alcohols. Despite the contrasts between weakly and strongly associating interfaces, the relationship between solvent structure and interfacial width at strongly associating interfaces shares similarities with trends previously observed at weakly associating interfaces. Specifically, free volume considerations based on organic solvent molecular structure appear to control interfacial abruptness.

In this work two clear patterns emerge in the data from strongly associating interfaces (Figures V.5 and V.6). Figure V.5 plots the average interfacial maxima observed by each molecular ruler as a function of ruler length for the linear and branched alcohols. The shifts in excitation wavelength (and thus polarity) are more gradual at interfaces between water and the linear alcohols. Figure V.6 shows the averaged linewidth data, again as a function of ruler length for the linear and branched alcohols. Overlaid on the plot is a horizontal line denoting the average linewidth of excitation spectra of molecular rulers in bulk alkanes (44 nm). As with the excitation wavelength data, the linewidth data indicate differences between the two types of systems. In general, the spectra recorded at interfaces with branched alcohols have broader FWHM.

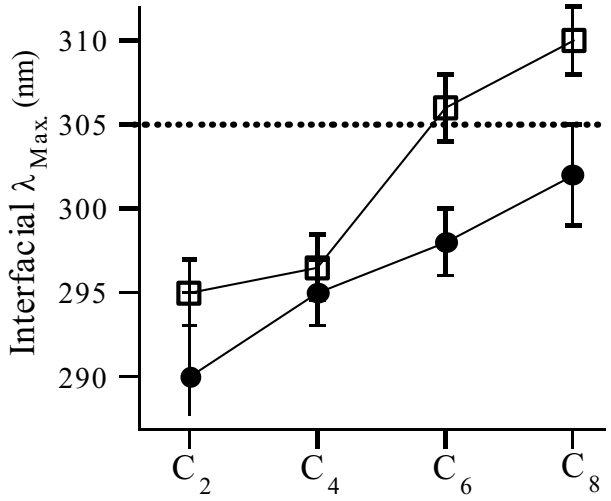

Figure V.5. Average fitted interfacial SHG maxima for species adsorbed to strongly associating liquid/liquid, water/alcohol interfaces. The dotted horizontal line denotes the average excitation wavelength of the species in bulk organic solvents (~305 nm). Excitation wavelength shifts more gradually from a non-polar limit towards the bulk alcohol limit for interfaces with the linear alcohols (circles) than it does for the branched alcohols (squares).

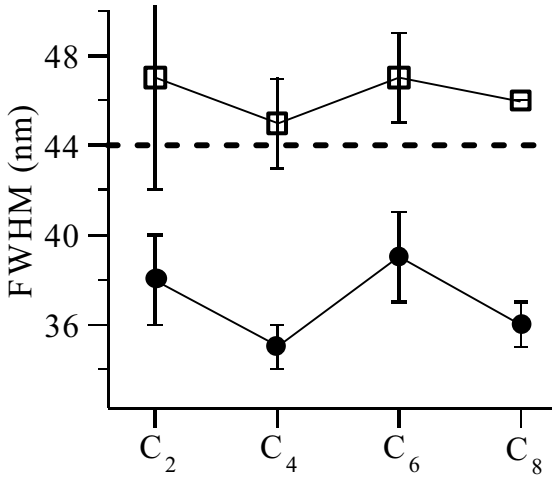

Figure V.6. Average linewidth data for SHG spectra of molecular rulers adsorbed to strongly associating liquid/liquid water/alcohol interfaces. The horizontal dashed line denotes the average linewidth of excitation spectra of molecular rulers in bulk alkane solvents (~44 nm). Linewidths for molecular rulers adsorbed to interfaces between water and linear alcohols (circles) are narrower than those for rulers adsorbed to interfaces between water and branched alcohols (squares).

4A. Linear Alcohols

In the case of the two linear solvents, spectra shown in Figures V.1 and V.2 indicate that interfacial polarity converges gradually from some nonpolar limit to a dielectric environment reflecting solvation in the bulk alcohol. In earlier work, we attributed this region of reduced polarity to close packing of the alkyl chains of the alcohol molecules at the water/alcohol interface.[50] This picture is consistent with recent X-ray scattering experiments that show the alignment of long chain surfactants adsorbed to water/hexane interfaces.[12] In addition, Shen and coworkers conducted vibrational sum frequency generation (VSFG) studies of linear alcohols at the liquid/vapor interface and found that the polar OH groups of these alcohols interact strongly with themselves and the alkyl chains point away from the liquid.[21] It is likely that a similar orientation occurs at the water/1-octanol interface, with the hydrophilic OH group hydrogen bonding with the adjacent water molecules and the alkyl chains pointing away from the water. Such a picture is supported by recent VSFG studies of monolayers of 1-octanol and 3-octanol at water surfaces.[51] This arrangement could produce a region of reduced polarity between the polar water and bulk alcohol.

Figure V.1 shows that at the water/1-octanol interface, a solvation similar to bulk 1-octanol is experienced by the chromophore of the longest ruler used, C_8. From this series of spectra we conclude that the width of the water/1-octanol interface is, at most, 1.2 nm, the length of a fully extended C_8 spacer in the all-*trans* conformation. Any *gauche* defects in the alkyl spacer of the ruler surfactant would lead to a shorter projection of the spacer onto the surface normal and reduce the dipolar interfacial width. Molecular dynamics simulations by Berkowitz and coworkers examined the

conformational structure of long chain surfactants (sodium dodecyl sulfate) at the water/vapor and water/carbon tetrachloride interfaces.[52] The simulations predict *gauche* defects to be present in surfactant chains and indicate that the most defects should occur close to the anionic headgroup of the surfactant. If true, this picture suggests a more narrow liquid/liquid interface between water and 1-octanol and the chromophore of the C_8 molecular ruler should sample a dielectric environment reflecting a reduced polarity. In fact, this is not observed, meaning that other factors should be considered in the analysis of this system.

At the water/1-octanol interface the C_8 ruler probe samples a bulk 1-octanol environment even with possible *gauche* defects. If such defects exist, then the solvent molecules can not be fully extended and parallel to the surface normal. VSFG studies of Shen and coworkers mentioned above found that long-chain alcohols tended to contain such *trans-gauche* defects at the liquid/vapor interface, and also exhibited a net tilt that decreases their projection onto the surface normal.[21] However, alcohol films at the air/water interface show little conformational disorder and a net upright orientation.[19] Our data suggests that, while the C_8 ruler probe may have a *gauche* defect decreasing its length, the long alkyl chains of the 1-octanol molecules are likely tilted off normal at the interface with water, effectively decreasing the width of the nonpolar alkyl region between the water and bulk 1-octanol. The result of these two considerations is that the "shortened" C_8 ruler still spans the water/1-octanol interface, and the chromophore of the longest ruler experiences a surrounding solvation similar to bulk 1-octanol.

Geometric considerations of interfacial solvent tilt and conformational disorder within adsorbed surfactants support the findings in this work. The molecular dynamics

simulations of sodium dodecyl sulfate at the water/carbon tetrachloride interface predicted the chains of the amphiphile to be oriented approximately 42° off of normal.[52] The VSFG studies of alcohols at the liquid/vapor interface determined the average orientation of the long alkyl chains of the alcohols to be approximately 40° off of normal.[21] This value agrees well with second harmonic generation studies performed by Cramb and Wallace that found the long axis of the alkyl chins of 1-octanol to be tilted approximately 39° off of normal.[6] Examining the geometric structure of the molecular ruler probes, a *gauche* defect near the sulfate ion would cause the dipole moment of the chromophore to be oriented approximately 7° off of the long axis of the alkyl chain. This tilt of 7° relative to the long axis of the alkyl chains of the ruler probes could result in an average chromophore orientation of either approximately 33° or 47° relative to surface normal, assuming an average chain tilt of 40°. Orientation measurements reveal the chromophore to be tilted approximately 36° off of surface normal for the family of ruler probes at the water/1-octanol interface. This agreement should not be surprising, as we expect excellent registry between the 8-membered alkyl chains of both the 1-octanol and the C_8 ruler probes. The two should pack very efficiently at the water/1-octanol interface with the chromophore tilting off axis slightly to the observed orientation.

Previous SHG studies performed in our labs have examined the excitation of solutes adsorbed to weakly associating liquid/liquid interfaces.[15,29,50] Orientation measurements included in these studies yielded chromophore orientations ranging from 34° to 51° off of surface normal, depending on the solute and specific system studied. Uncertainties in calculating orientation angles are typically $\pm$ 3° assuming that the microscopic hyperpolarizability elements in Equation 3 have been calculated accurately.

Figure V.7 shows a representative plot of SH intensity as a function of incident polarization angle for a molecular ruler surfactant adsorbed to a strongly associating interface. The data have been fit according to procedures described elsewhere in order to determine the two nonzero hyperpolarizability elements required to determine the orientation angle of the adsorbed chromophores.

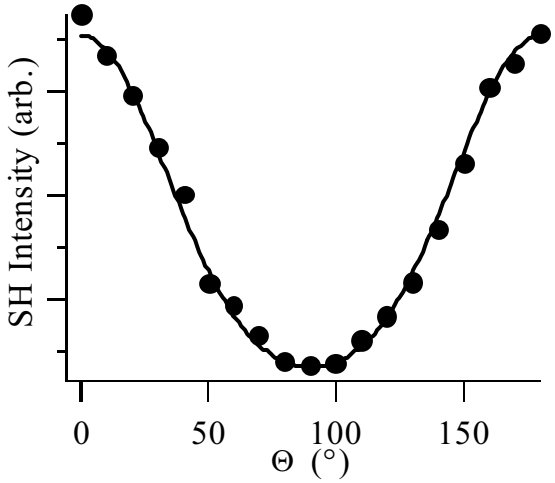

Figure V.7. Polarization dependent SHG spectra of C_6 molecular rulers adsorbed to the water/1-octanol interface. SH intensity is plotted as a function of the incident polarization angle. The data are fit to determine the nonzero elements of the hyperpolarizability found in Equation 3.

On average, molecular ruler surfactants adsorbed to weakly associating interfaces adopted orientations between 45° and 50°, while at strongly associating interfaces the same chromophores have been found to tilt between 32° and 37° off of normal. Several years ago Rowlen and Simpson determined that a SHG "magic angle" of 39° existed.[53] They predicted that, given any average orientation and a broad enough distribution about that average, orientation measurements determined by SHG would converge to 39° for a roughened surface. This result stands in contrast with previous SHG studies that assumed distributions described by a single, unique orientation with no distribution about it.

Considering the uncertainty in the measurements presented in this work ($\pm$ 3°) the orientations of molecular rulers adsorbed to the water/1-octanol interface are very close to this magic angle. However, as mentioned above, other orientations determined in our lab have differed significantly from 39°, including those of *para*-nitrophenol (55°) and 2,6-dimethyl-*para*-nitrophenol (43°), two solutes similar to the PNAS probe, at the water/cyclohexane interface.[15] In our measurements we assume two nonzero hyperpolarizability elements and a single orientation angle with no distribution.[33] While these assumptions necessarily introduce uncertainty into our reported measurements, we can state with confidence that molecular ruler surfactants adopt a more upright orientation at strongly associating interfaces than at weakly associating interfaces.

Further support of the proposed water/1-octanol interfacial structure comes from the linewidth data of the family of spectra recorded at the interface (Table V.1). The narrow FWHM (~36 nm) of each spectrum indicates that the chromophore is surrounded by a solvation environment that is much more homogeneous than bulk 1-octanol, where broader linewidths are observed (~56 nm). The alignment of the alkyl chains of the interfacial 1-octanol molecules could generate such an environment. Spectra of molecular rulers in bulk alkanes have linewidths of approximately 44 nm, meaning that probe solvation at the water/1-octanol interface is more homogeneous than bulk alkanes. This observation is not surprising given that interfacial probes and interfacial solvents all share similar orientations, as well as dielectric environments.

In the case of the water/1-decanol interface, Figure V.2 shows that a polarity indicative of bulk 1-decanol is not observed by the chromophore of the C_8 ruler. The family of spectra shows the excitation maxima shifting from a nonpolar limit of 295 nm

towards 300 nm, which is still approximately 5 nm away from the average excitation maximum displayed in bulk 1-decanol. We conclude from this that the water/1-decanol interface is broader than the water/1-octanol interface, and that dipolar width at interfaces between water and linear alcohols is directly related the length of the alkyl chains on the alcohol.

A fully extended 1-decanol molecule in an all-*trans* conformation is approximately 1.5 nm. Even with a net molecular tilt at the water/1-decanol interface the resulting nonpolar region appears to extend beyond the length of the C_8 ruler probe, as evidenced by the spectra in Figure V.2. Adding to the effect of the additional length of the 1-decanol molecules is the finding by Cramb and Wallace that the alkyl chains of longer linear alcohols were less likely to tilt off normal at the water/alcohol interface.[6] The longer alkyl chain and a more upright orientation at the water/1-decanol interface could combine to produce a broader interfacial region as sampled by the molecular ruler probes.

Again, orientation measurements support this view. The shortest ruler probe, C_2, was found to tilt 37° off of normal while the longer probes were oriented only 32° off of normal. If we were to consider surface roughness as the source of any distribution in orientations we would not expect any appreciable change in the observed tilt angles, as we see for ruler surfactants at the water/1-decanol interface. The chromophore of the C_2 ruler probe is closest to the interface and more likely to be surrounded by an interfacial structure that is directly susceptible to the interactions between water and the OH groups of the interfacial 1-decanol molecules. As the alkyl spacer of the ruler probes lengthens

the chromophore floats further into the nonpolar region where surfactant chains can adopt more easily the registry of surrounding solvent molecules.

4B. Branched Alcohols

The spectra shown in Figures V.3 and V.4 indicate that the interfaces between water and the branched alcohols are more abrupt than those between water and the linear alcohols. In each case the chromophore of the C_6 ruler probe experiences a solvation similar to that of the bulk alcohol. This finding is not unexpected. Studies of dipolar width at weakly associating water/cyclohexane and water/methylcyclohexane interfaces found the branched alkane interface to be more abrupt.[29] These results were evaluated in terms of solvent packing ability and free molar volumes. Our interpretation of the data from branched alcohol interfaces adopts similar ideas. Unfortunately, few studies of solvents or surfaces have focused on branched alcohols, thus our evaluation of the data is necessarily more speculative.

While the spectra in Figures V.3 and V.4 clearly indicate the interfacial solvation environment converges to that of the bulk alcohol more abruptly than at interfaces with linear alcohols, they also suggest a structure for the nonpolar region between the adjacent bulk solvent layers. The FWHM of the spectra of molecular rulers adsorbed to interfaces with the branched alcohols are always broader than those at the water/linear alcohol interfaces (Figure V.6). The average linewidths at the water/3-octanol and water/2,6-dimethyl-4-heptanol interfaces are 47 nm and 44 nm, respectively. Each of these is larger than the corresponding values at the water/1-octanol (36 nm) and water/1-decanol (38 nm) interfaces, and is also closer to the average linewidth of spectra of molecular rulers in bulk solutions of branched alcohols (49 nm). We can make two conclusions

based on these data. First, because the linewidths of spectra recorded at interfaces with branched alcohol are broader, the interfaces between water and the branched alcohols are more heterogeneous than those between water and the linear alcohols. Second, the local polarity experienced by chromophores at these interfaces is very similar to that of the bulk branched alcohols themselves. This observation represents a clear distinction from the trend observed at the interfaces between water and linear alcohols.

In our studies of solvation at weakly associating interfaces, we proposed that the molecular structure of the organic solvent played a large role in the resulting dipolar width of the aqueous/organic boundary.[29] This relationship appears to be a dominant factor at the strongly associating interfaces presented in this work as well. At weakly associating interfaces the amount of free volume present in an organic solvent was directly related to the dipolar width measured at the water/alkane interface. As intermolecular packing ability of the alkane decreased there was a greater ability of the solvent to solvate the chromophore of the molecular ruler probes. Consequently, bulk alkane solvation was observed over a shorter lengthscale at water/branched alkane interfaces than at those interfaces between water and the linear alkanes that packed more efficiently. Figure V.8 depicts a schematic representation of the differences in structure that arise from these considerations. The chromophore of the probe molecule is surrounded by a more homogeneous environment at the interface with the linear alcohol, thus it experiences a more alkane-like solvation and its SH spectrum has a narrower linewidth.

At strongly associating interfaces, branched alcohols will pack less efficiently than their linear counterparts. The increased free volume amongst the interfacial branched alcohols can lead to improved solvation of the molecular ruler chromophores.

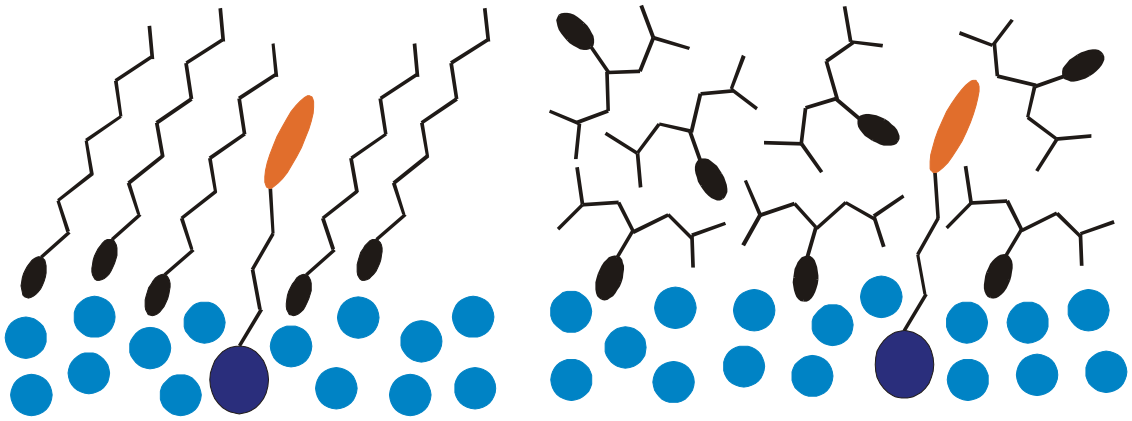

Figure V.8. A schematic representation of the solvation a molecular ruler probe at two strongly associating interfaces. In the cartoon in the top panel, the probe samples is surrounded by a homogeneous, alkane-like environment at the interface between water and 1-octanol. In the bottom panel, the same probe is exposed to a less homogeneous solvation, and samples a polarity indicative of the bulk alcohol at the water/2,6-dimethyl-4-heptanol interface.

The effect of free volume is likely to be most pronounced at the water/2,6-dimethyl-4-heptanol interface. The molecular volume of 2,6-dimethyl-4-heptanol is 330 $Å^3$, the largest of the four solvents in this work. For comparison, the molecular volume of 1-nonanol is 290 $Å^3$. The molecular volume of 3-octanol is significantly less than that of 2,6-dimethyl-4-heptanol, only 264 $Å^3$. The spectra in Figure V.4 show that the chromophores of both the C_4 and C_6 rulers sample slightly more polar environments at the water/2,6-dimethyl-4-heptanol interface than they do at the water/3-octanol interface. The reduced packing ability of the larger 2,6-dimethyl-4-heptanol molecules appears to allow for better solvation of the chromophores of the longer ruler species than is possible

at the water/3-octanol interface. This interpretation necessarily assumes that water plays little or no role in the interfacial solvation of the chromophores.

Free volume considerations do not appear to be a major factor when examining the results from the water/1-octanol and water/3-octanol interfaces. The molecular volume of 1-octanol, 260 $Å^3$, is nearly equal to that of 3-octanol. While this slight difference is not likely to result in a dramatic difference in packing in bulk solution, at an interface it can result in significant differences between the packing ability of the two solvents. Poor packing of 3-octanol at the water/3-octanol interface is supported by surface tension measurements of the air/3-octanol interface and interfacial tension measurements of a 3-octanol monolayer at the air/water interface.[51] A more likely cause of the reduced dipolar width observed at the water/3-octanol interface is the placement of the OH group on the alcohol solvent. Attaching the OH group to the third carbon in the chain of eight divides the molecule into two shorter segments, one of two methylene groups and one of five. The longer of these is only approximately 7.5 Å in length, a distance easily spanned by the longer molecular ruler species, especially when we consider the net tilt these chains may have.

An additional piece of evidence to consider is the orientation data recorded at the interfaces between water and the branched alcohols. The chromophores adopt, on average, a slightly more upright orientation, approximately 32° off of normal, than at the interfaces between water and the linear alcohols (36°). The uncertainty in the orientation calculations ($\pm$3°) means that there could be little difference between the two sets of orientations. However, given the additional free volume within branched alcohols, the chromophores of the ruler probes sampling the water/branched alcohol interfaces could

very well be oriented closer to the surface normal. At the water/1-octanol interface, for example, there is a strong driving force for the alignment of the alkyl chain of the ruler to adopt the same orientation of the interfacial 1-octanol molecules. The ruler probes are constrained by this surrounding solvation. Assuming that the water/3-octanol interface is much less structured than its water/1-octanol counterpart, this driving force should decreased at the water/3-octanol interface and thus the chromophores of the ruler probes could adopt alternative average orientations.

5. Conclusion

We have used molecular ruler surfactants to probe solute excitation at several strongly associating water/alcohol liquid/liquid interfaces. The data suggest that all of these interfaces contain a region of reduced polarity between the polar water phase and the bulk alcohol. We attribute this region to the alignment of the alkyl chains of the interfacial alcohol molecules. Our findings suggest that some interfaces are sharper than others. Those interfaces comprised of water and a branched alcohol converged to bulk alcohol-like solvation over a shorter lengthscale than those between water and a linear alcohol. These differences correlate well with the solute accessible free volume within the alcohols. The width of the interfaces between water and the linear alcohols appears to be directly related to the length of the alkyl chain on the alcohol. Ongoing studies will continue to explore the relationship between solvent structure and interfacial width.

References

(1) Donahue, D. J.; Bartell, F. E. *J. Phys. Chem.* **1952**, *56*, 480.

(2) Girifalco, L. A.; Good, R. J. *J. Phys. Chem.* **1957**, *61*, 904.

(3) Josserand, J.; Lagger, G.; Jensen, H.; Ferrigno, R.; Girault, H. H. *J. Electroanal. Chem.* **2003**, *546*, 1.

(4) Dang, L. X. *J. Phys. Chem. B* **1999**, *103*, 8195.

(5) Antoine, R.; Bianchi, F.; Brevet, P. F.; Girault, H. H. *J. Chem. Soc. Faraday Trans.* **1997**, *93*, 3833.

(6) Cramb, D. T.; Wallace, S. C. *J. Phys. Chem. B* **1997**, *101*, 2741.

(7) Cheng, Y.; Corn, R. M. *J. Phys. Chem. B* **1999**, *103*, 8726.

(8) Conboy, J. C.; Messmer, M. C.; Richmond, G. L. *J. Phys. Chem.* **1996**, *100*, 7617.

(9) Sangster, J. *Octanol-Water Partition Coefficients*; John Wiley and Sons: New York, 1997; Vol. 2.

(10) Michael, D.; Benjamin, I. *J. Phys. Chem.* **1995**, *99*, 16810.

(11) Dang, L. X. *J. Phys. Chem. B* **2001**, *105*, 804.

(12) Schlossman, M. L.; Li, M.; Mitrinovic, D. M.; Tikhonov, A. M. *High Perform. Polym.* **2000**, *12*, 551.

(13) Richmond, G. L. *Annu. Rev. Phys. Chem.* **2001**, *52*, 357.

(14) Eisenthal, K. B. *Chem. Rev.* **1996**, *96*, 1343.

(15) Steel, W. H.; Walker, R. A. *J. Am. Chem. Soc.* **2003**, *125*, 1132.

(16) Mitrinovic, D.; Tikhonov, A. M.; Li, M.; Huang, Z.; Schlossman, M. L. *Phys. Rev. Lett.* **2000**, *85*, 582.

(17) Tikhonov, A. M.; Mitrinovic, D. M.; Li, M.; Huang, Z.; Schlossman, M. L. *J. Phys. Chem. B* **2000**, *104*, 6336.

(18) Chipot, C.; Wilson, M. A.; Pohorille, A. *J. Phys. Chem. B* **1997**, *101*, 782.

(19) Braun, R.; Casson, B. D.; Bain, C. D. *Chem. Phys. Lett.* **1995**, *245*, 326.

(20) Michael, D.; Benjamin, I. *J. Chem. Phys.* **1997**, *107*, 5684.

(21) Stanners, C. D.; Du, Q.; Chin, R. P.; Cremer, P.; Somorjai, G. A.; Shen, Y.-R. *Chem. Phys. Lett.* **1995**, *232*, 407.

(22) Steel, W. H.; Damkaci, F.; Nolan, R.; Walker, R. A. *J. Am. Chem. Soc.* **2002**, *124*, 4824.

(23) Beildeck, C. L.; Steel, W. H.; Walker, R. A. *Langmuir* **2003**, *19*, 4933.

(24) Mitrinovic, D. M.; Zhang, Z.; Williams, S. M.; Huang, Z.; Schlossman, M. L. *J. Phys. Chem. B* **1999**, *103*, 1779.

(25) Penfold, J.; Richardson, R. M.; Zarbakhsh, A.; Webster, J. R. P. *J. Chem. Soc. Faraday Trans.* **1997**, *93*, 3899.

(26) Michael, D.; Benjamin, I. *J. Phys. Chem. B* **1998**, *102*, 5145.

(27) Squitieri, E.; Benjamin, I. *J. Phys. Chem. B* **2001**, *105*, 6412.

(28) Michael, D.; Benjamin, I. *J. Chem. Phys.* **2001**, *114*, 2817.

(29) Steel, W. H.; Lau, Y. Y.; Beildeck, C. L.; Walker, R. A. *submitted*.

(30) Ishizaka, S.; Satoshi, H.; Kim, H.; Kitamura, N. *Anal. Chem.* **1999**, *71*, 3382.

(31) Bessho, K.; Uchida, T.; Yamauchi, A.; Shioya, T.; Teramae, N. *Chem. Phys. Lett.* **1997**, *264*, 381.

(32) Lagugne-Labarthet, F.; Yu, T.; Barger, W. R.; Shenoy, D. K.; Dalcanale, E.; Shen, Y. R. *Chem. Phys. Lett.* **2003**, *381*, 322.

(33) Higgins, D. A.; Abrams, M. B.; Byerly, S. K.; Corn, R. M. *Langmuir* **1992**, *8*, 1992.

(34) Yamaguchi, A.; Kato, R.; Nishizawa, S.; Teramae, N. *Chem. Lett.* **2003**, *32*, 798.

(35) Uchida, T.; Yamaguchi, A.; Ina, T.; Teramae, N. *J. Phys. Chem. B* **2000**, *104*, 12091.

(36) Perrenoud-Rinuy, J.; Brevet, P. F.; Girault, H. H. *Phys. Chem. Chem. Phys.* **2002**, *4*, 4774.

(37) Naujok, R.; Higgins, D. A.; Hanken, D. G.; Corn, R. M. *J. Chem. Soc. Faraday Trans.* **1995**, *91*, 1411.

(38) Ishizaka, S.; Kim, H.; Kitamura, N. *Anal. Chem.* **2001**, *73*, 2421.

(39) Wang, H.; Borguet, E.; Eisenthal, K. B. *J. Phys. Chem. A* **1997**, *101*, 713.

(40) Wang, H.; Borguet, E.; Eisenthal, K. B. *J. Phys. Chem. B* **1998**, *102*, 4927.

(41) Wolfrum, K.; Laubereau, A. *Chem. Phys. Lett.* **1994**, *228*, 83.

(42) Guyot-Sionnest, P.; Hunt, J. H.; Shen, Y. R. *Phys. Rev. Lett.* **1987**, *59*, 1597.

(43) Bell, G. R.; Bain, C. D.; Ward, R. N. *J. Chem. Soc. Faraday Trans.* **1996**, *92*, 515.

(44) Walker, R. A.; Gruetzmacher, J. A.; Richmond, G. L. *J. Am. Chem. Soc.* **1998**, *120*, 6991.

(45) Watry, M. R.; Richmond, G. L. *J. Am. Chem. Soc.* **2000**, *122*, 875.

(46) Zhang, X.; Esenturk, O.; Walker, R. A. *J. Am. Chem. Soc.* **2001**, *123*, 10768.

(47) Chang, R. *Basic Principles of Spectroscopy*; McGraw-Hill Book Co.: New York, 1971.

(48) Suppan, P.; Ghoneim, N. *Solvatochromism*; The Royal Society of Chemistry: Cambridge, UK, 1997.

(49) Zhang, X.; Cunningham, M. M.; Walker, R. A. *J. Phys. Chem. B* **2003**, *107*, 3183.

(50) Steel, W. H.; Walker, R. A. *Nature* **2003**, *424*, 296.

(51) Esenturk, O.; Walker, R. A. *submitted*.

(52) Schweighofer, K.; Essman, U.; Berkowitz, M. L. *J. Phys. Chem. B* **1997**, *101*, 3793.

(53) Simpson, G. J.; Rowlen, K. L. *J. Am. Chem. Soc.* **1999**, *121*, 2635.

Chapter VI. Conclusions and Future Directions

1. Conclusions

This thesis has examined solvent polarity at liquid/liquid interfaces. By using the nonlinear optical technique of resonance enhanced second harmonic generation we have successfully probed the interfacial polarity of a variety of interfaces. The technique allows us to record effective excitation spectra of species adsorbed to an interface, and from the fitted interfacial excitation maximum we can infer the local polarity experienced by each solute.

1A. Solute Effects on Interfacial Polarity

The first part of this research studied the dependence of the observed polarity on the solute used to probe the interface. Slight changes in the functionality of the solute are thought to alter the equilibrium distribution of the probe molecules at the interface. Nonlinear optical spectroscopy was used to record effective excitation spectra of three probes at the water/cyclohexane interface: *para*-nitrophenol, *para*-nitroanisole, and 2,6-dimethyl-*para*-nitrophenol. The results showed that each solute sampled a unique polarity at the *same* interface. The results imply that the interfacial environment is determined as much by the identity of the solute as by gradients in the solvent properties across the interfacial boundary and supports predictions that dramatic changes in solvation should accompany small changes in solute position relative to a sharp boundary.

1B. Molecular Ruler Design and Synthesis

In the second part of this dissertation we described the development and characterization of new solvatochromic surfactants called molecular rulers. These molecules incorporated a hydrophobic chromophore connected to an ionic headgroup, separated by a *n*-alkyl spacers. The solvatochromic behavior of these molecules closely matched that of the target chromophore, *para*-nitroanisole (PNAS). The variable separation between the chromophore and the headgroup allows us to alter the position of the chromophore relative to the interfacial plane. By systematically increasing the separation between the chromophore and the interface we can profile how solvation changes across liquid/liquid interfaces and determine the dipolar widths of these regions. After a thorough characterization of the molecular rulers, including NMR and IR spectroscopy and mass spectrometry, second harmonic generation (SHG) was used to record an effective excitation spectrum of the molecular ruler containing a two carbon spacer adsorbed to the water/cyclohexane interface. Results indicated the chromophore was surrounded by a solvation less polar than the bare PNAS molecule at the same interface. This finding indicates that these molecular rulers should function as intended, and that they will prove useful tools for measuring interfacial widths.

1C. Solvation at Weakly Associating Interfaces

The final two chapters of this dissertation have described the use of these molecular rulers to profile solvent polarity across weakly and strongly associating liquid/liquid interfaces, respectively. At weakly associating water/alkane interfaces, results indicated that these boundaries were sharp. SHG spectra of molecular rulers adsorbed to four interfaces between water and cyclohexane, methylcyclohexane, octane,

and hexadecane were recorded. Spectra indicate that interfacial polarity at all of these boundaries was comprised of contributions from the two adjacent solvent layers – additive effects could be used to describe the interfacial polarity. At each interface, the chromophore of the interfacial probe experienced alkane-like solvation at a distance no more than 9 Å from the water-solvated headgroup. Two of these interfaces were found to be more abrupt (water/methylcyclohexane and water/octane), while two featured a more gradual transition in solvent polarity between the aqueous and organic phases (water/cyclohexane and water/hexadecane). Interfacial width was found to depend sensitively on solvent structure and appears to correlate with free volume within the organic phase. These findings agree well with predictions from molecular dynamics simulations predicting that interfacial solvent polarity should scale with a solute's solvent accessible area.

1D. Solvation at Strongly Associating Interfaces

As in the study of solvation at weakly associating interfaces, molecular rulers were used to probe interfacial polarity at four strongly associating interfaces between water and 1-octanol, 1-decanol, 3-octanol, and 2,6-dimethyl-4-heptanol. In contrast to the additive nature of interfacial polarity observed at weakly associating interfaces, SHG spectra of molecular rulers adsorbed to strongly associating interfaces indicate these boundaries contain a region of reduced polarity between the adjacent solvent phases. At two of the interfaces, between water and 1-octanol and 1-decanol, the width of this region of reduced polarity was related to the length of the alkyl chain on the alcohol. Also at the boundaries between water and the linear alcohols solvent polarity shifted gradually from the nonpolar limit experienced by the shortest molecular ruler species towards the bulk

alcohol limit. At the other two strongly associating interfaces, between water and 3-octanol and 2,6-dimethyl-4-heptanol, the dipolar width was found to be more abrupt. The collection of SHG spectra of molecular rulers adsorbed to strongly associating interfaces revealed a relationship between dipolar width and solvent structure similar to the one that was proposed at weakly associating liquid/liquid interfaces. As solvent accessible free volume increases within the alcohol solvent a more abrupt transition to an alcohol-like solvation is experienced by the adsorbed molecular rulers.

2. Future directions

2A. Remaining Questions

The results presented in this thesis represent significant advancement in elucidating the role solvents play in determining the dipolar width of aqueous/organic interfaces. However, there remain many questions yet to be resolved. These include:

1. What role does the functionality of the organic solvent play in altering the observed interfacial width? By altering the ability of the organic phase to hydrogen bond with the aqueous phase we can determine what, if any, functional groups cause the most abrupt or broadest interfaces. Solvents containing ketones, aldehydes, or carboxylic acids can help clarify the role that hydrogen bonding plays in interfacial width.
2. How is interfacial width related to temperature? Experiments profiling liquid/liquid interfacial width at various temperatures could lead to energetic and entropic information about these surfaces. Of particular interest is determining whether or not changes in temperature can disrupt the proposed alignment of alkyl

chains at strongly associating interfaces. For example, will raising the temperature cause interfaces such as water/1-octanol and water/1-decanol to become indistinguishable?

3. How do specific solvation forces vary across interfaces? By designing new molecular rulers that are sensitive to hydrogen bonding we can observe changes in the hydrogen bonding ability of solvents across liquid/liquid interfaces.
4. How is the width of a liquid/liquid interface sensitive to any electric fields present at the interface? By varying the ionic strength of the aqueous solution or applying an external electric field can we alter the interfacial solvent structure and observed dipolar width?
5. How do solvation dynamics at interfaces differ from bulk solution limits? The SHG experiments described in this thesis examined the static solvation environment at liquid/liquid interfaces. Time resolved experiments that can probe dynamic solvation could be combined with the SHG technique to examine solvation dynamics and relaxation at surfaces.

2B. Experimental Directions

There are a number of experiments that can address the issues raised above. Using the same set of molecular rulers we can elucidate the role that solvent functionality plays in determining the interfacial width. In order to study interfaces between water and solvents that are more dense than water, such as halogenated hydrocarbons, a new cell must be designed to allow the incident light from the OPA in the experimental setup to be transitted to the liquid/liquid interface through the organic phase. Further, the synthesis

of longer molecular rulers, containing up to 10, 12, or 14 carbon spacers, would allow for the investigation of solvents containing long alkyl chains in their structures.

In order to study the effects of temperature on interfacial polarity and width a new cell needs to be designed that allows for the variable control of the temperature of the system. Once the sample temperature can be controlled, SHG spectra can be collected at temperatures above and below ambient temperature in the same manner as described in this dissertation.

By incorporating structural components that are sensitive to hydrogen bonding into a family of surfactants we can observe the variation in specific solvation forces across liquid/liquid interfaces. Some of the likely functional groups include amines, ketones, and carboxylic acids. New synthetic procedures would be required to incorporate these components in such a way to insure that they interact with the bulk solvents rather than just the interface. This could be achieved by placing the appropriate protecting groups around the intended hydrogen bond "detector".

The presence of electric fields may alter the polarity observed at liquid/liquid interfaces, as well as the roughness of these regions. Electric fields can be brought into these studies in multiple ways. By adding ionic salts to the aqueous phase we can create short range fields near the interface that may affect the solvent organization near the liquid/liquid interface. We can also apply an external electric field to the system if we design a new cell that incorporates two electrodes.

There are, of course, other possibilities that could be considered. This dissertation is hopefully only the first of many investigations of solvation at liquid/liquid interfaces by means of SHG spectroscopy. The combination of SHG and molecular rulers has

proven a very effective tool in these studies, and will undoubtedly continue to be an significant means of investigating these important regions. As I move on in my own academic career, I look forward to following future developments in the field that may address these and other questions about solvation at liquid/liquid interfaces and wish those conducting such experiments the greatest success.

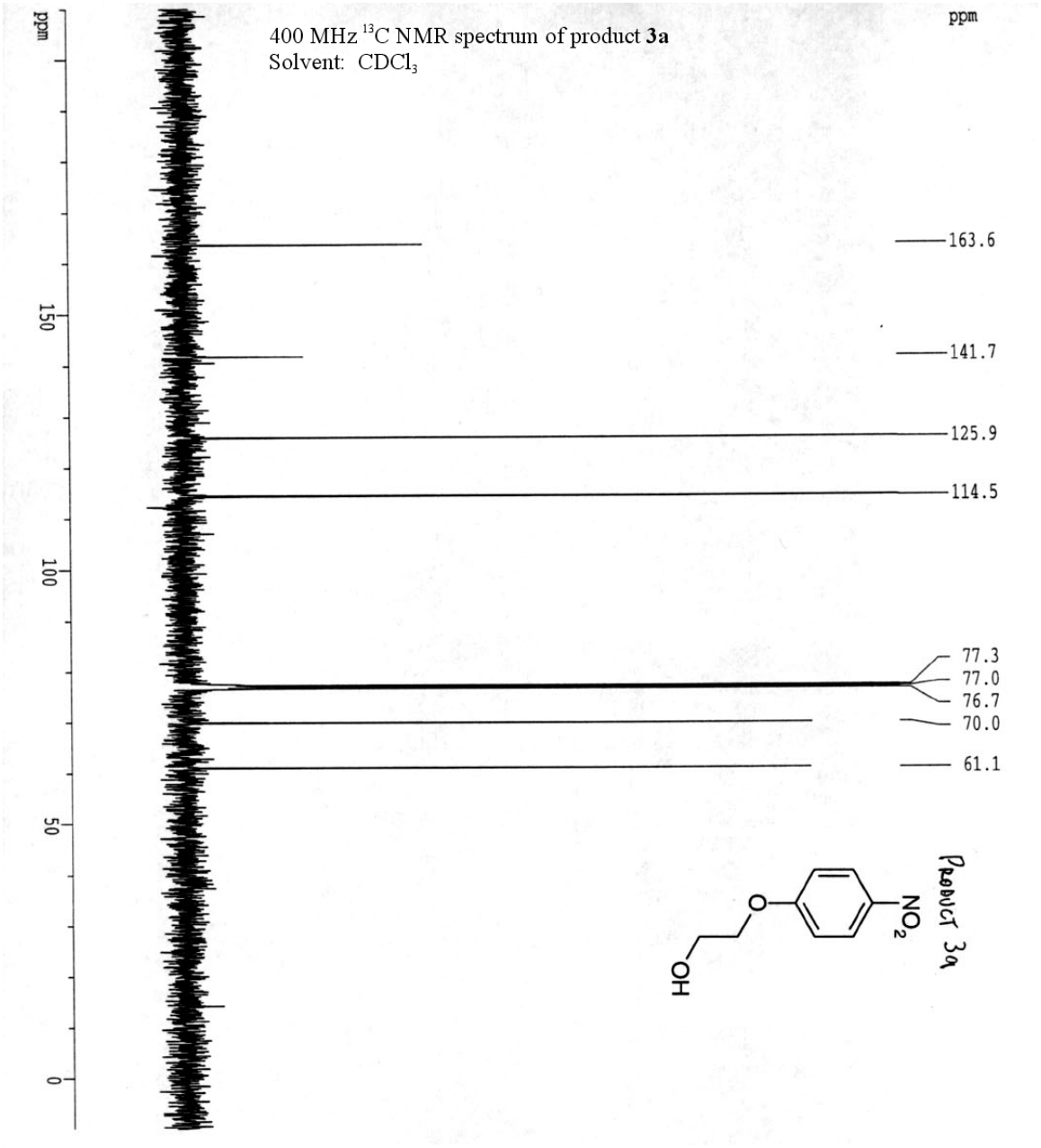

Figure A.1. ^{13}C NMR spectrum of product 3a.

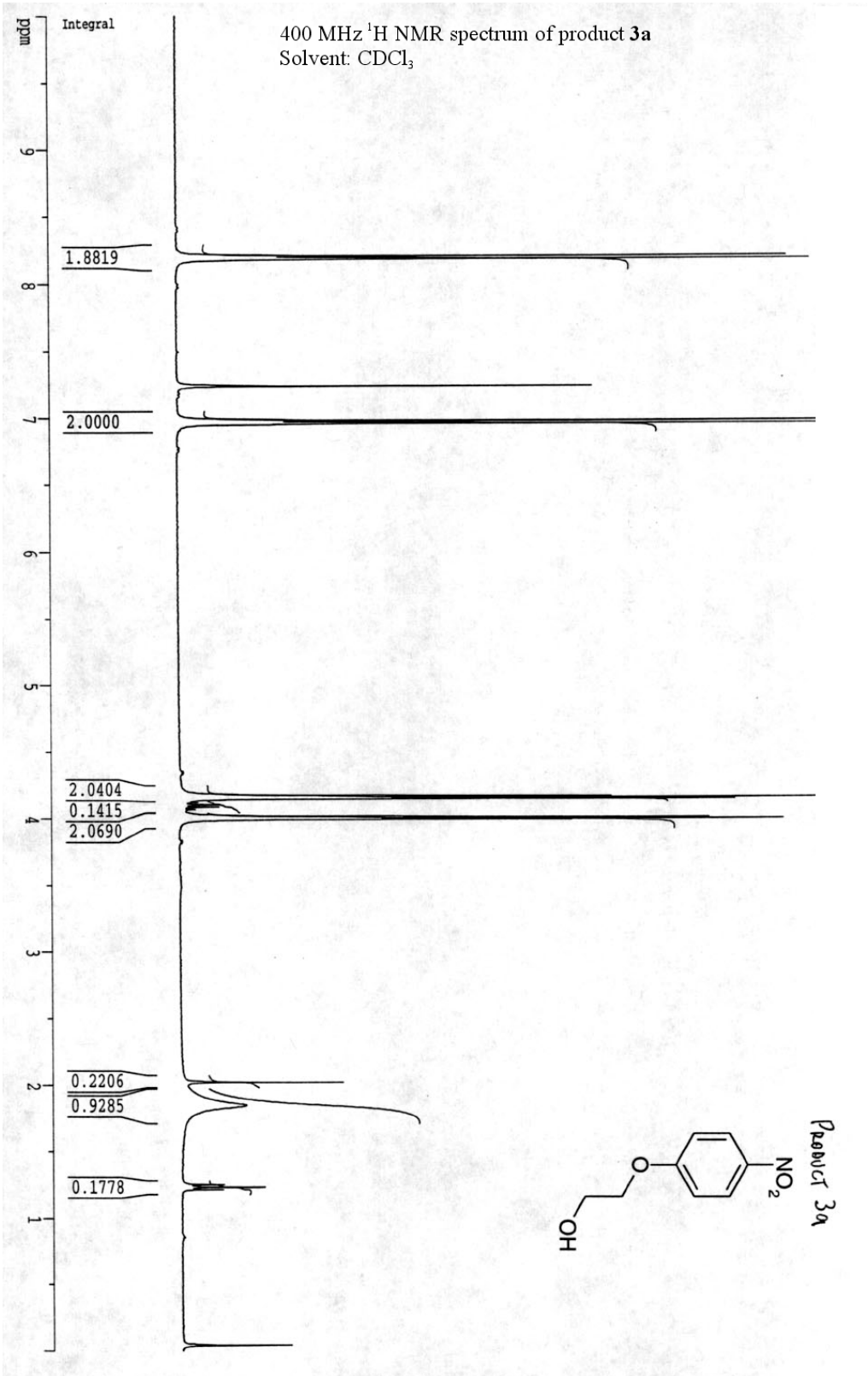

Figure A.2. ^{1}H NMR spectrum of product 3a.

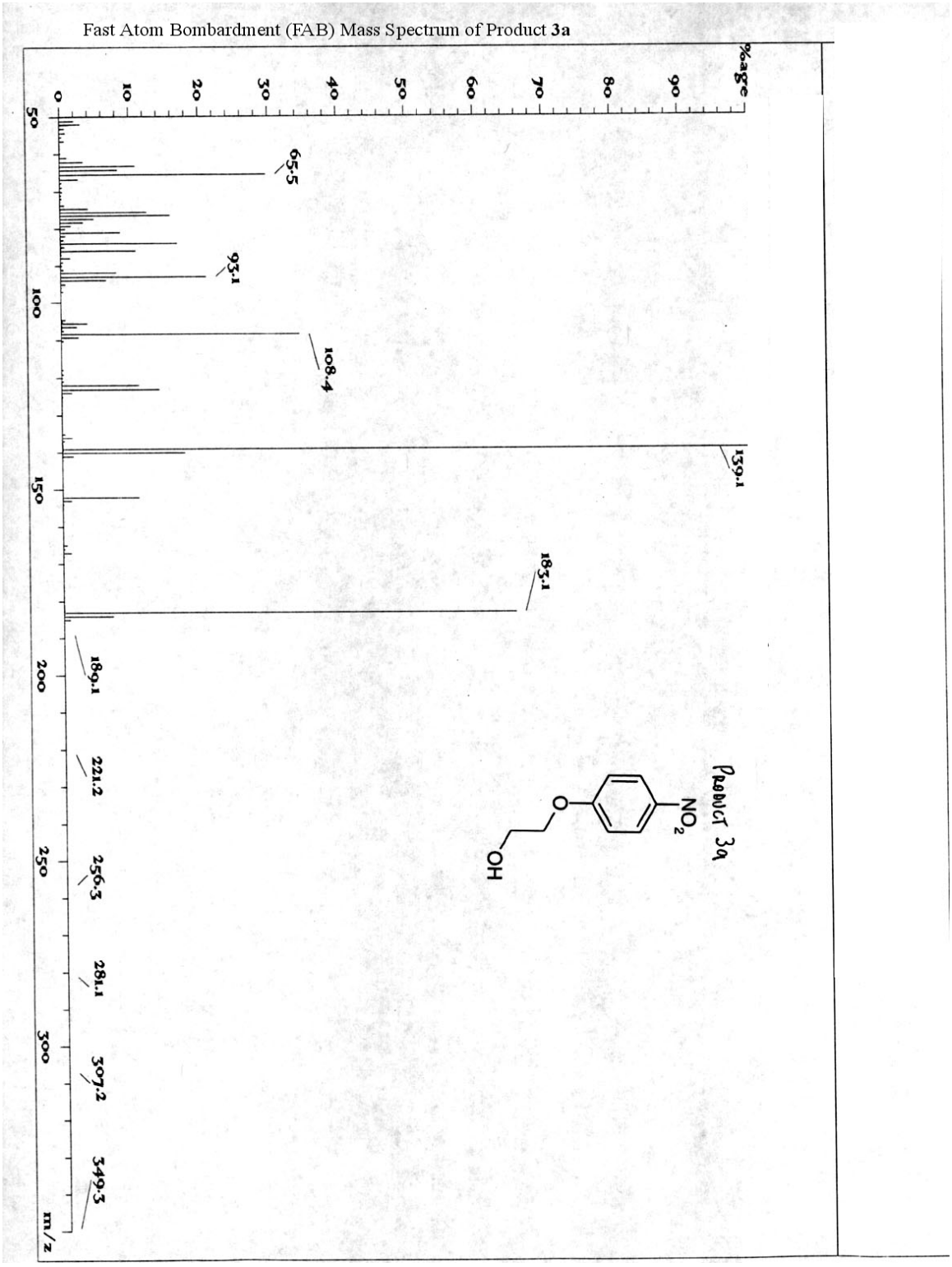

Figure A.3. Fast atom bombardment (FAB) mass spectrum of product 3a.

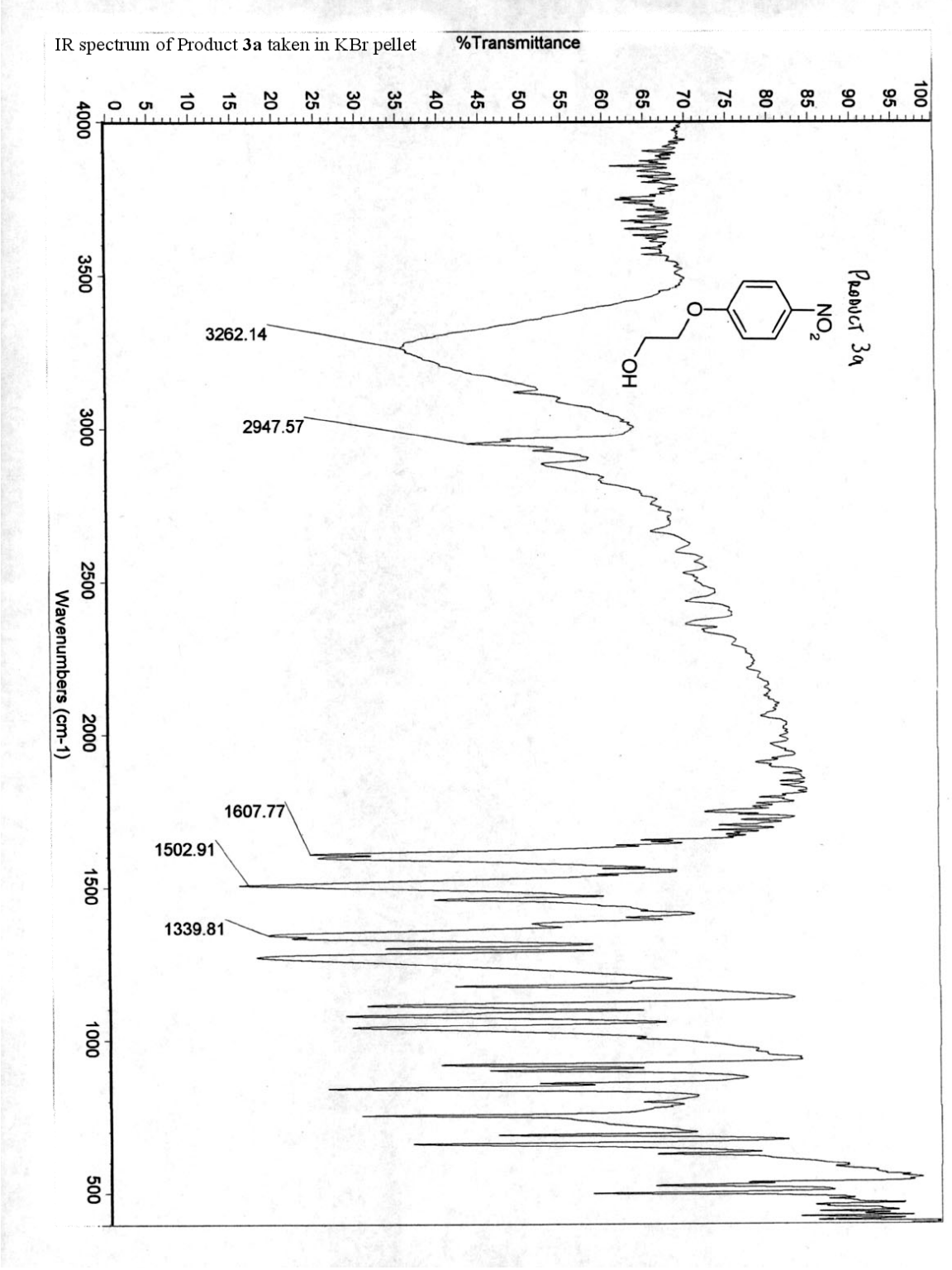

Figure A.4. IR spectrum of product 3a taken in KBr pellet.

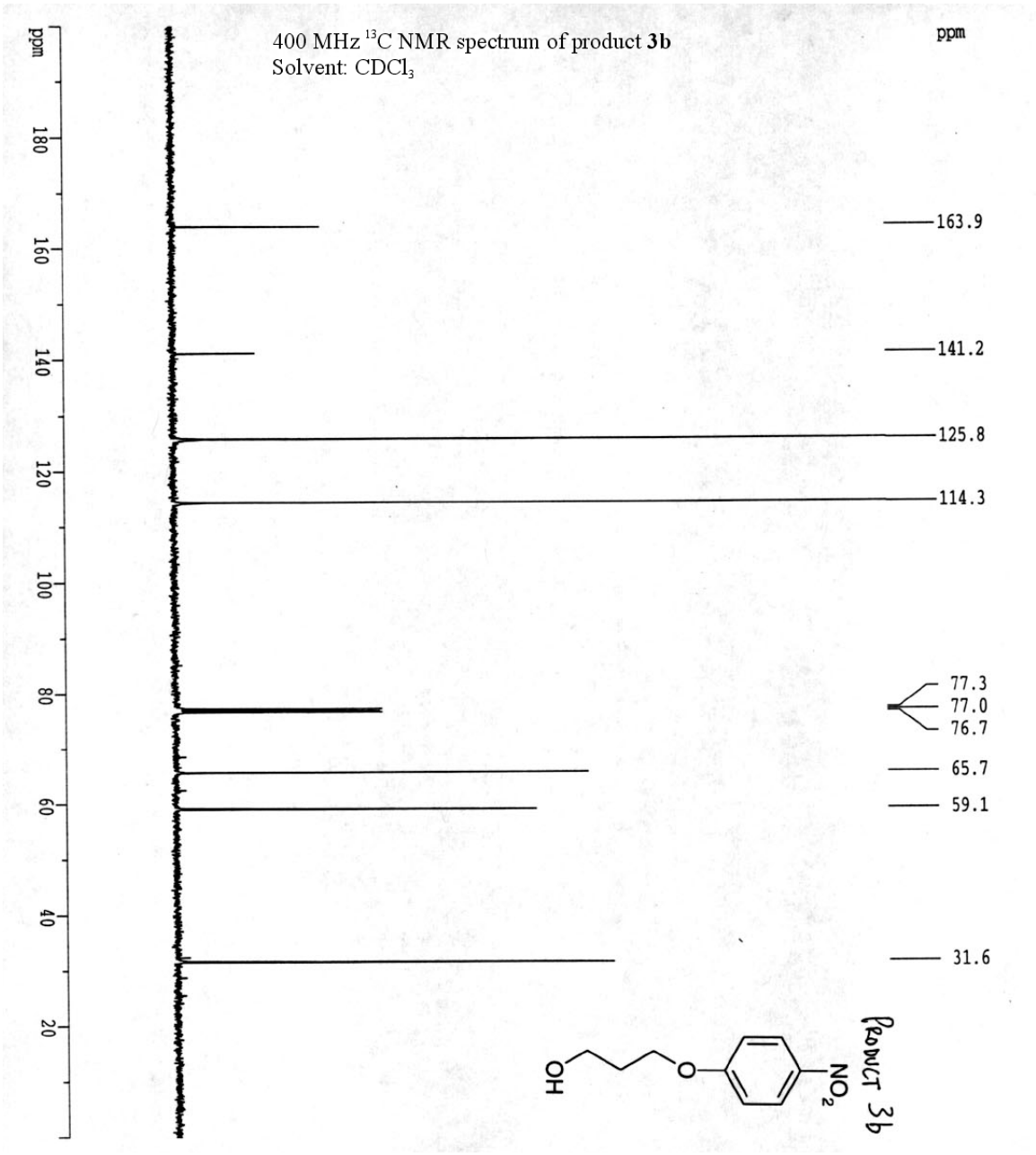

Figure A.5. ^{13}C NMR spectrum of product 3b.

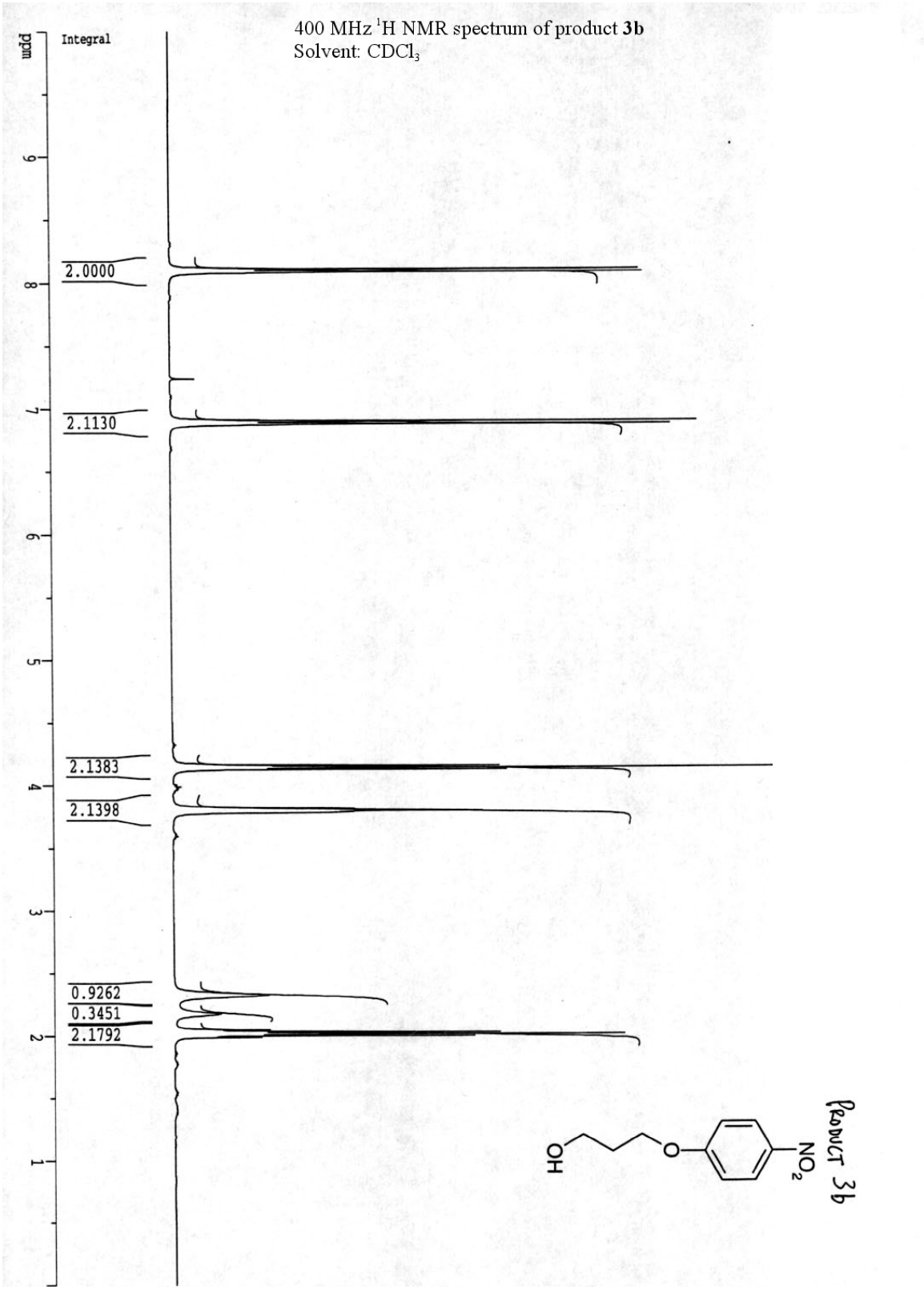

Figure A.6. ^{1}H NMR spectrum of product 3b.

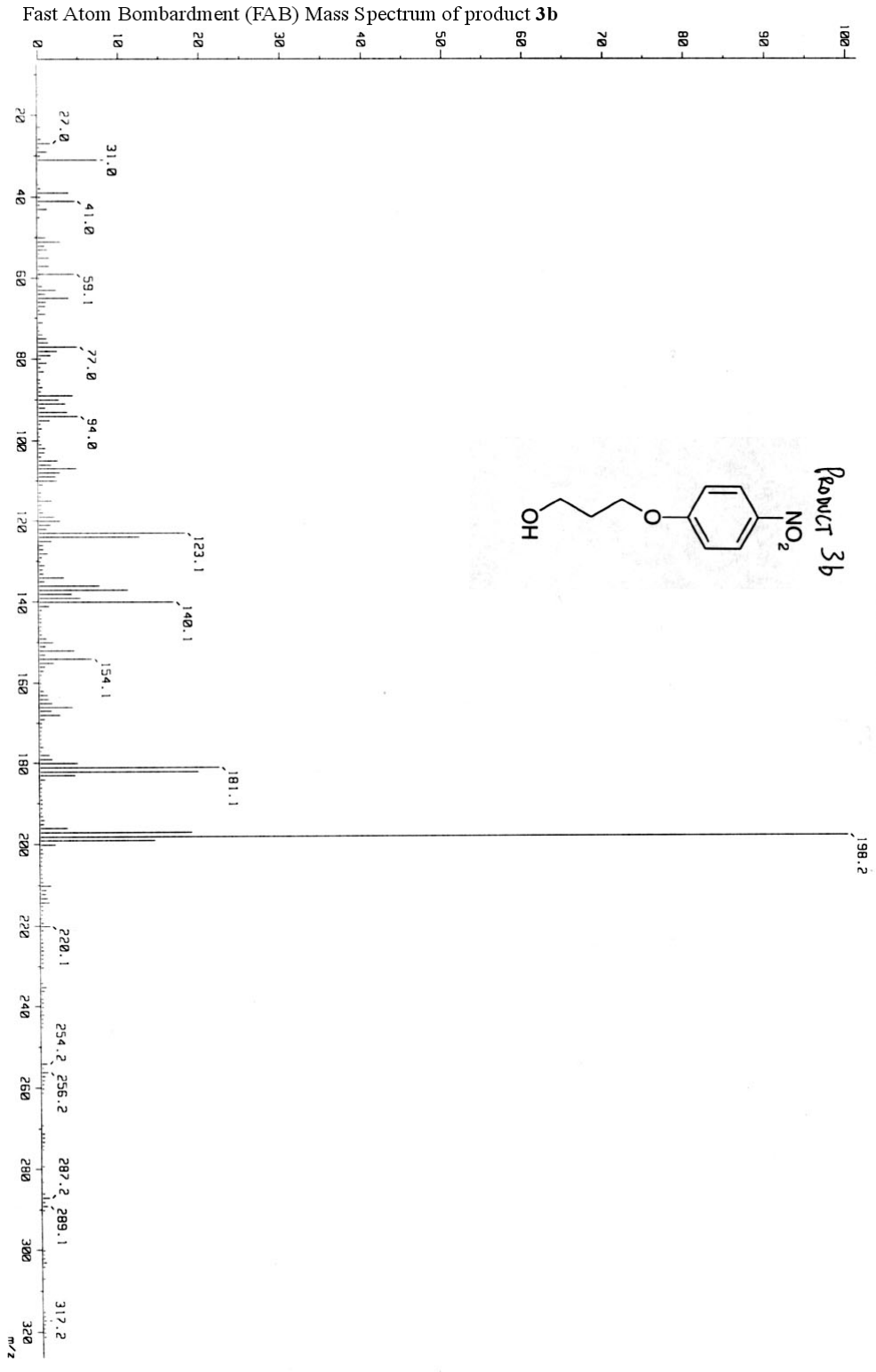

Figure A.7. Fast atom bombardment (FAB) mass spectrum of product 3b.

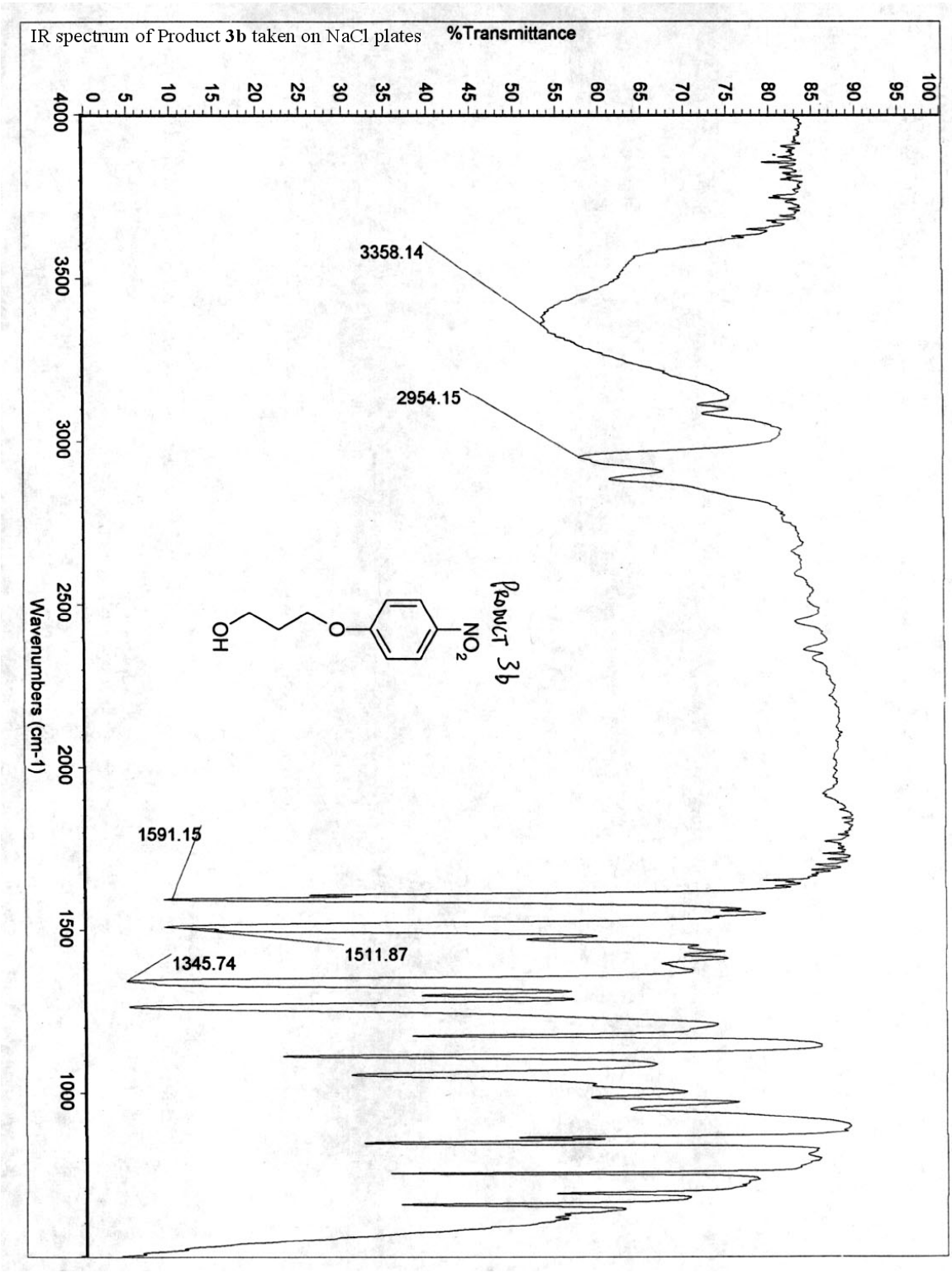

Figure A.8. IR spectrum of product 3b taken on NaCl plates.

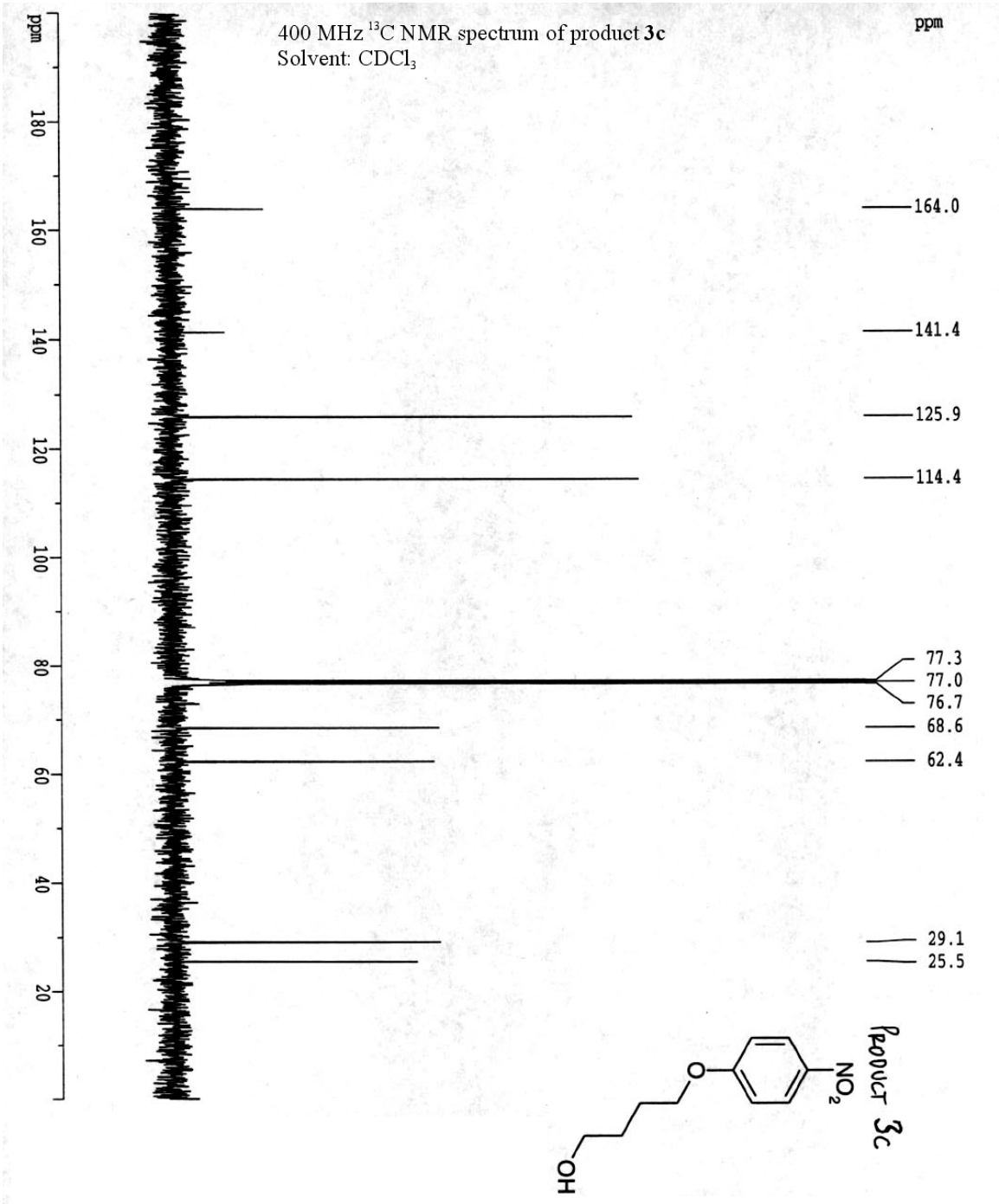

Figure A.9. ^{13}C NMR spectrum of product 3c.

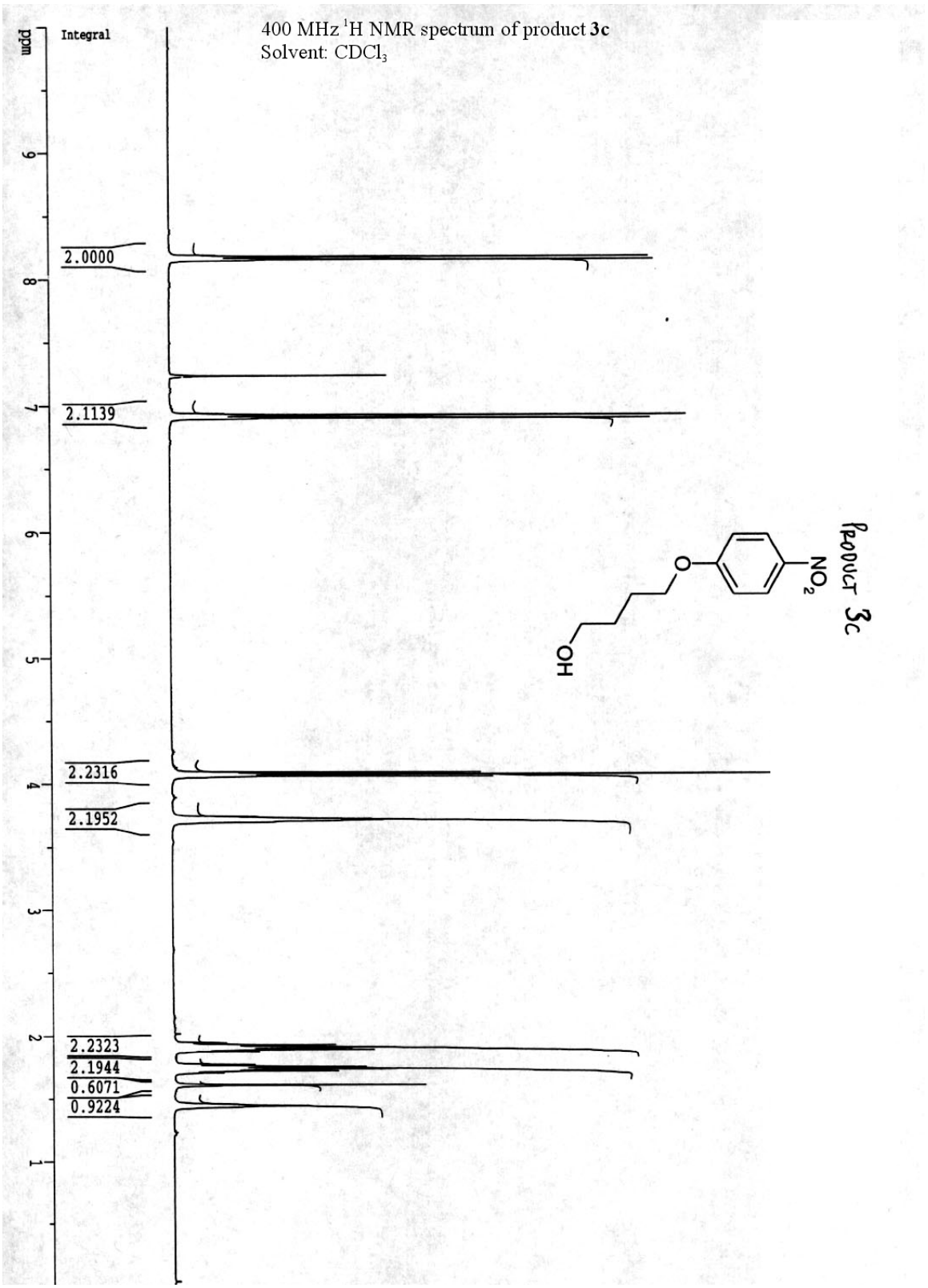

Figure A.10. ^{1}H NMR spectrum of product 3c.

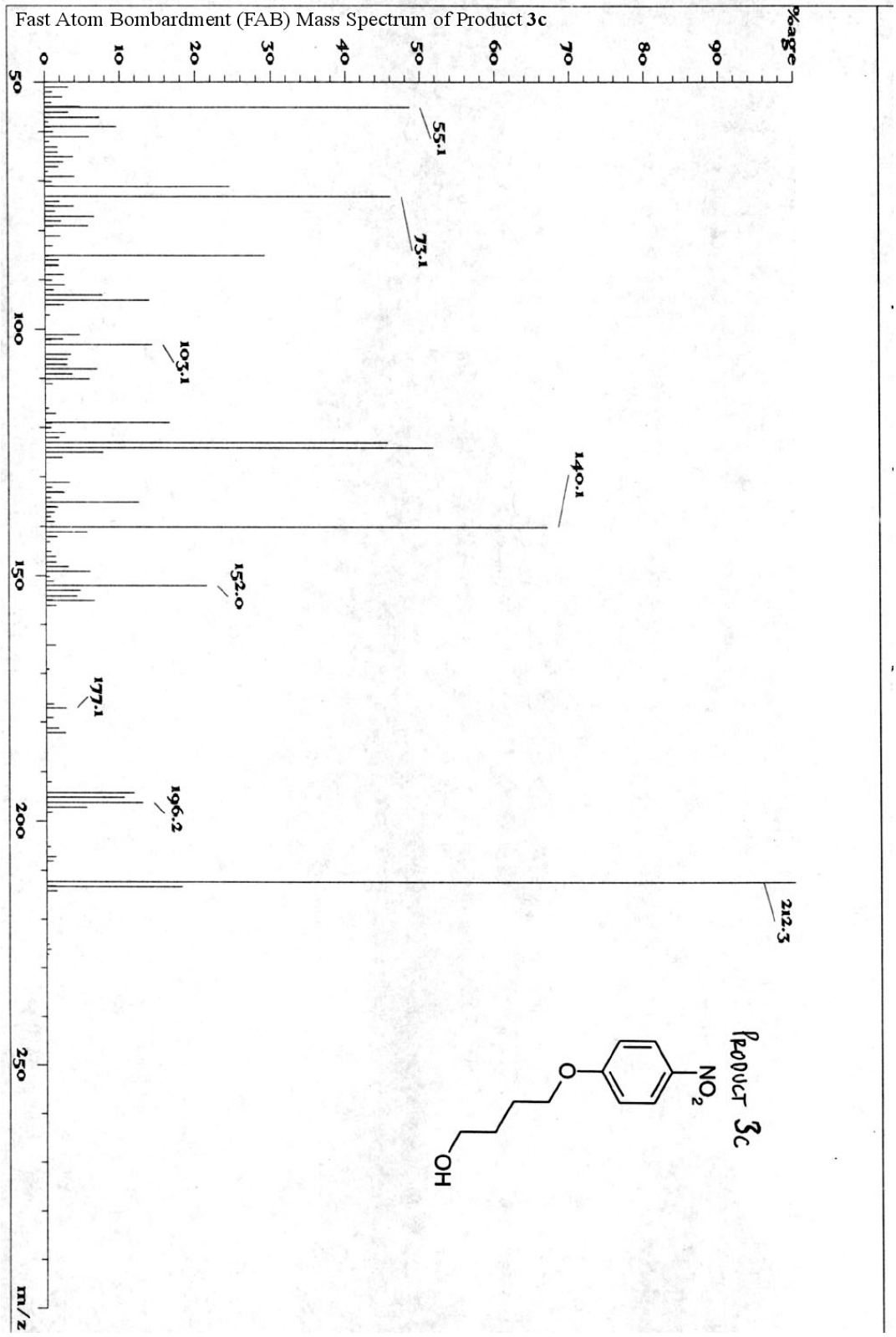

Figure A.11. Fast atom bombardment (FAB) mass spectrum of product 3c.

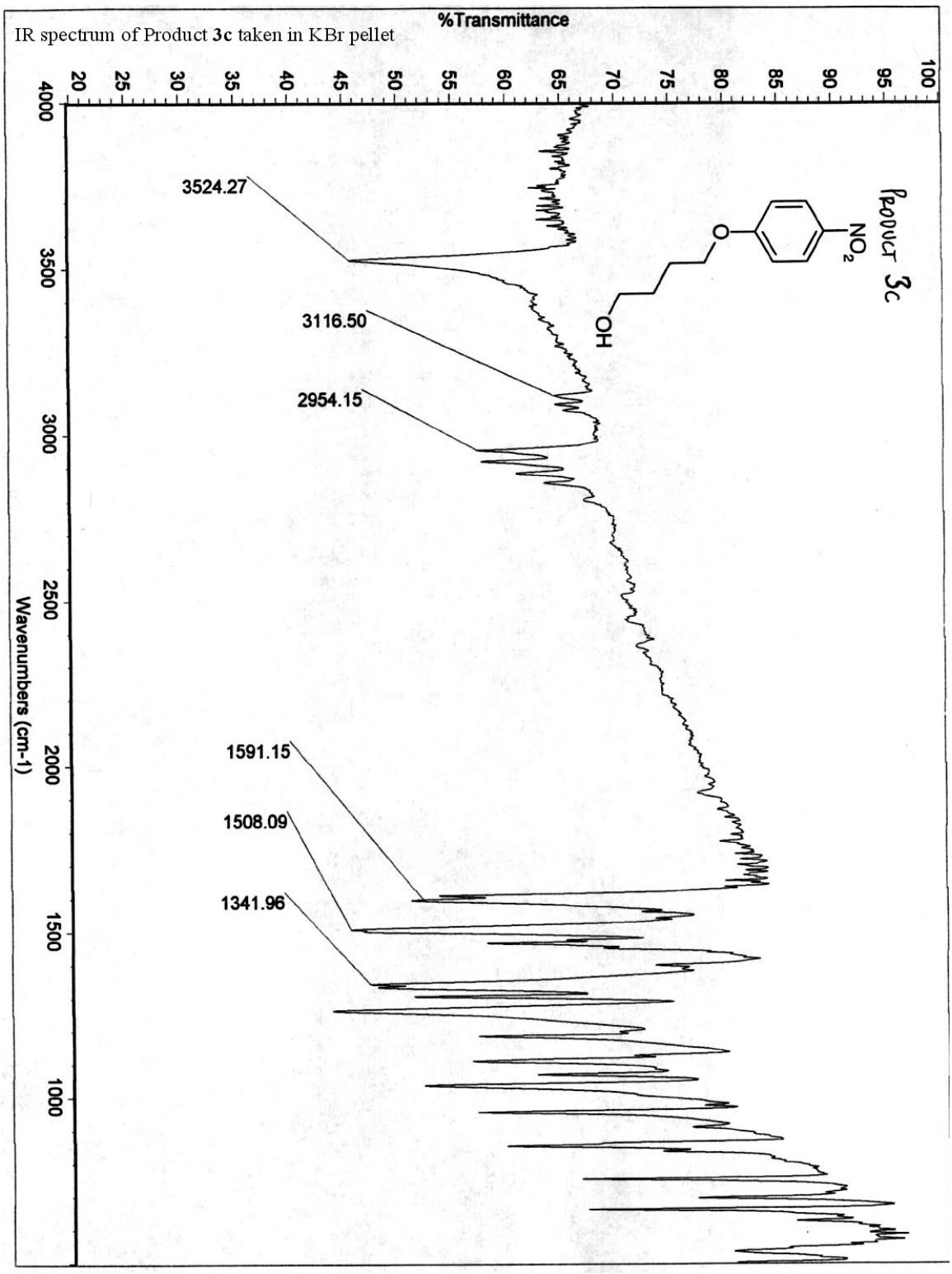

Figure A.12. IR spectrum of product 3c taken in KBr pellet.

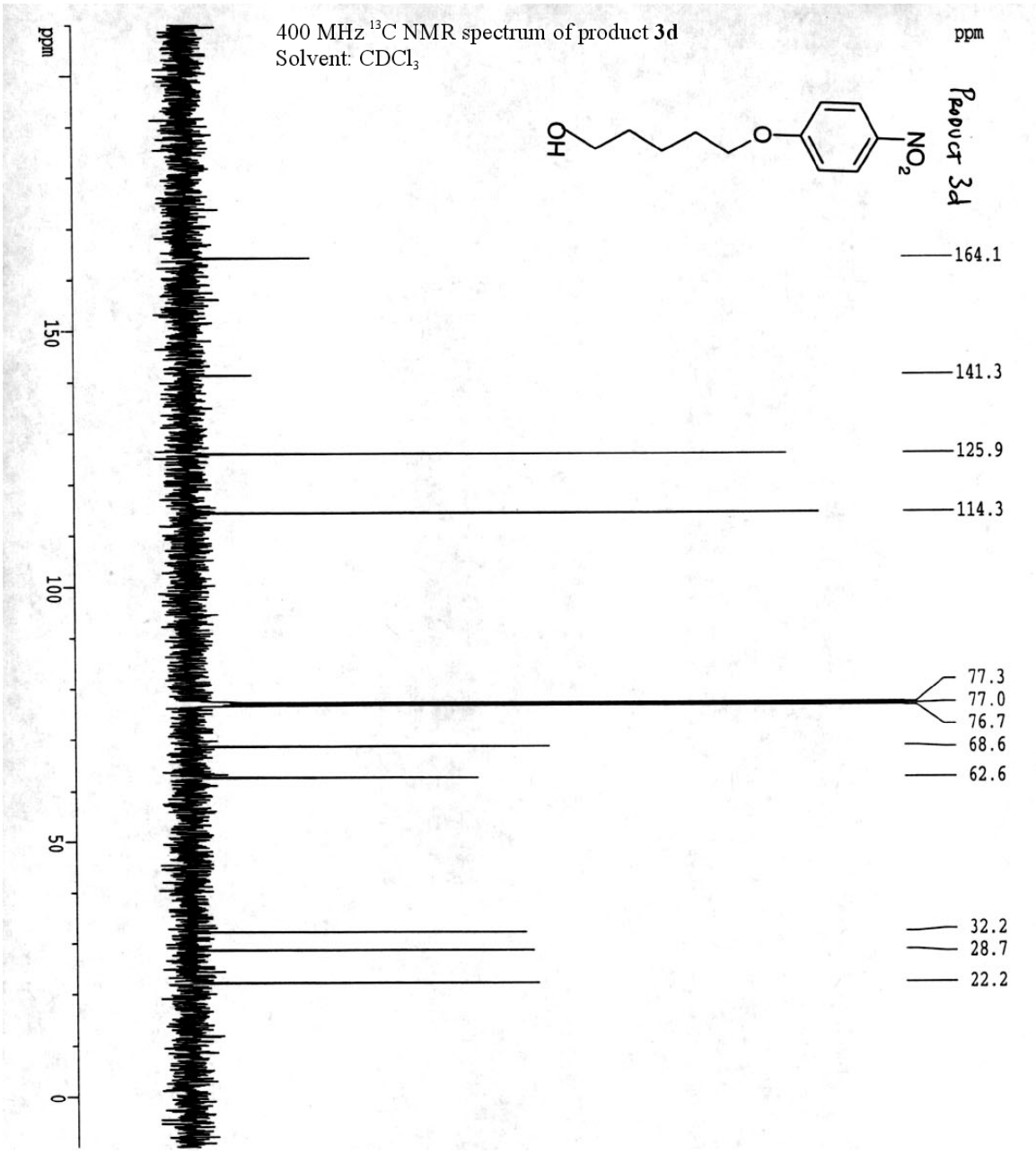

Figure A.13. ^{13}C NMR spectrum of product 3d.

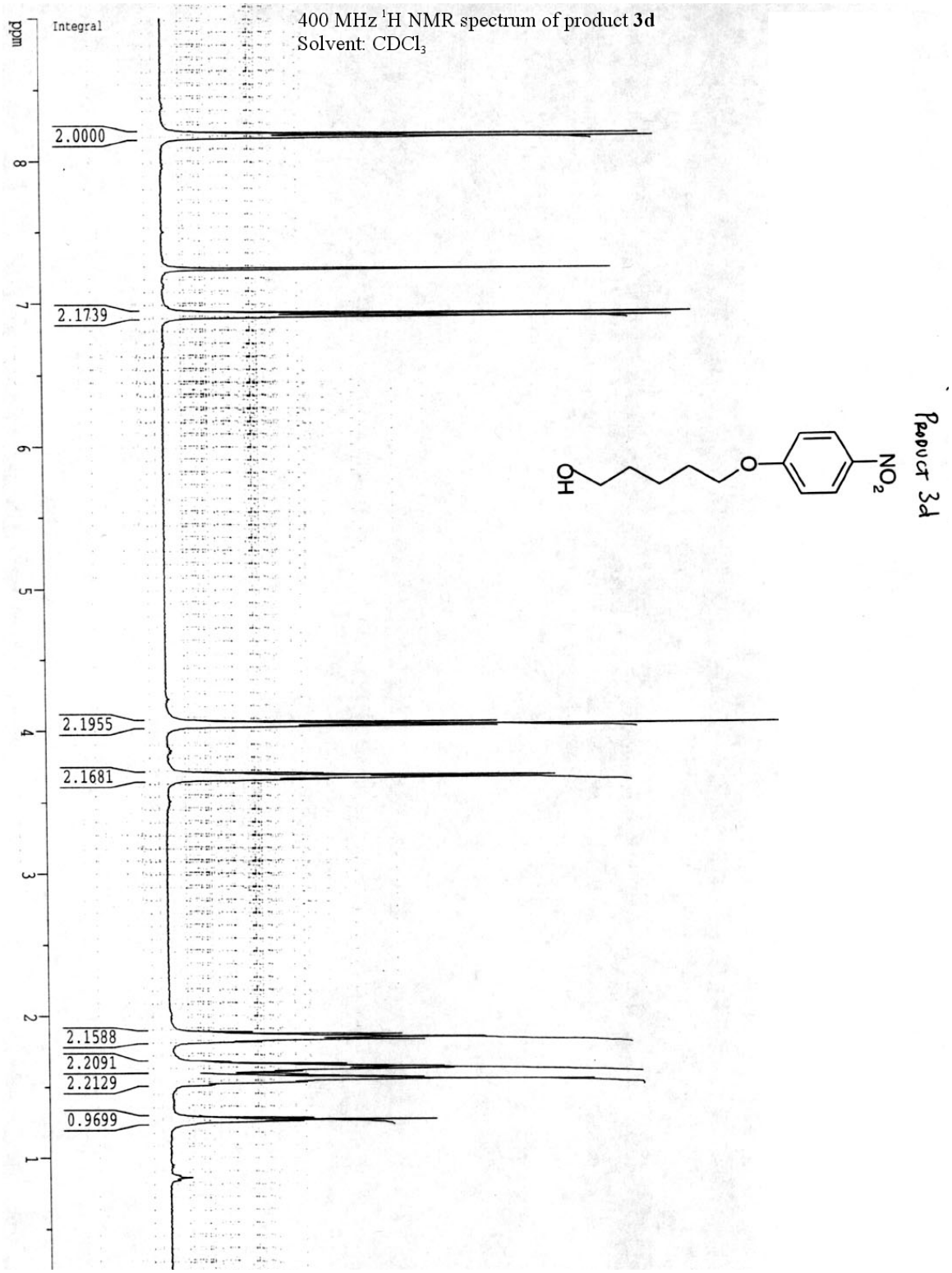

Figure A.14. ^{1}H NMR spectrum of product 3d.

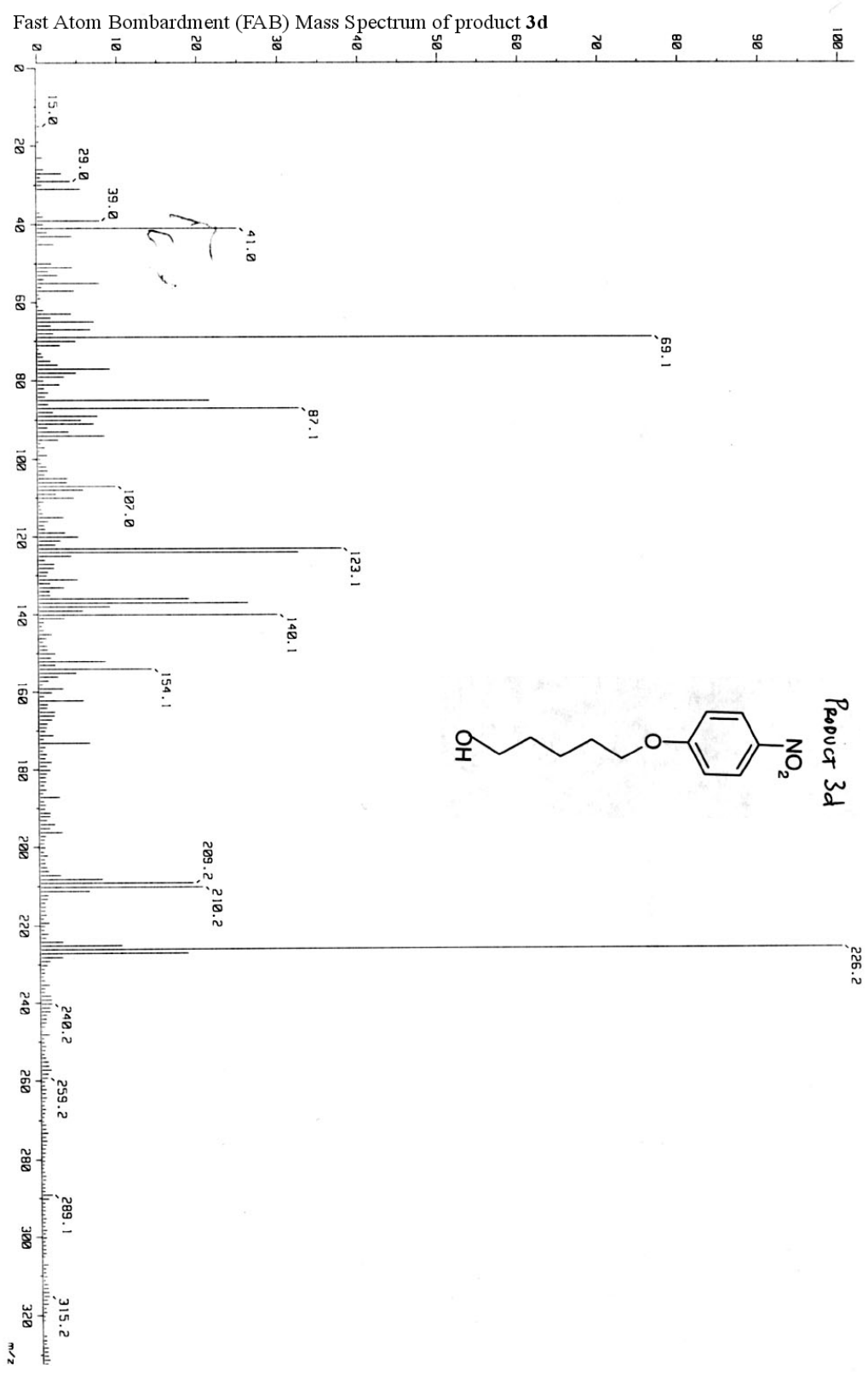

Figure A.15. Fast atom bombardment (FAB) mass spectrum of product 3d.

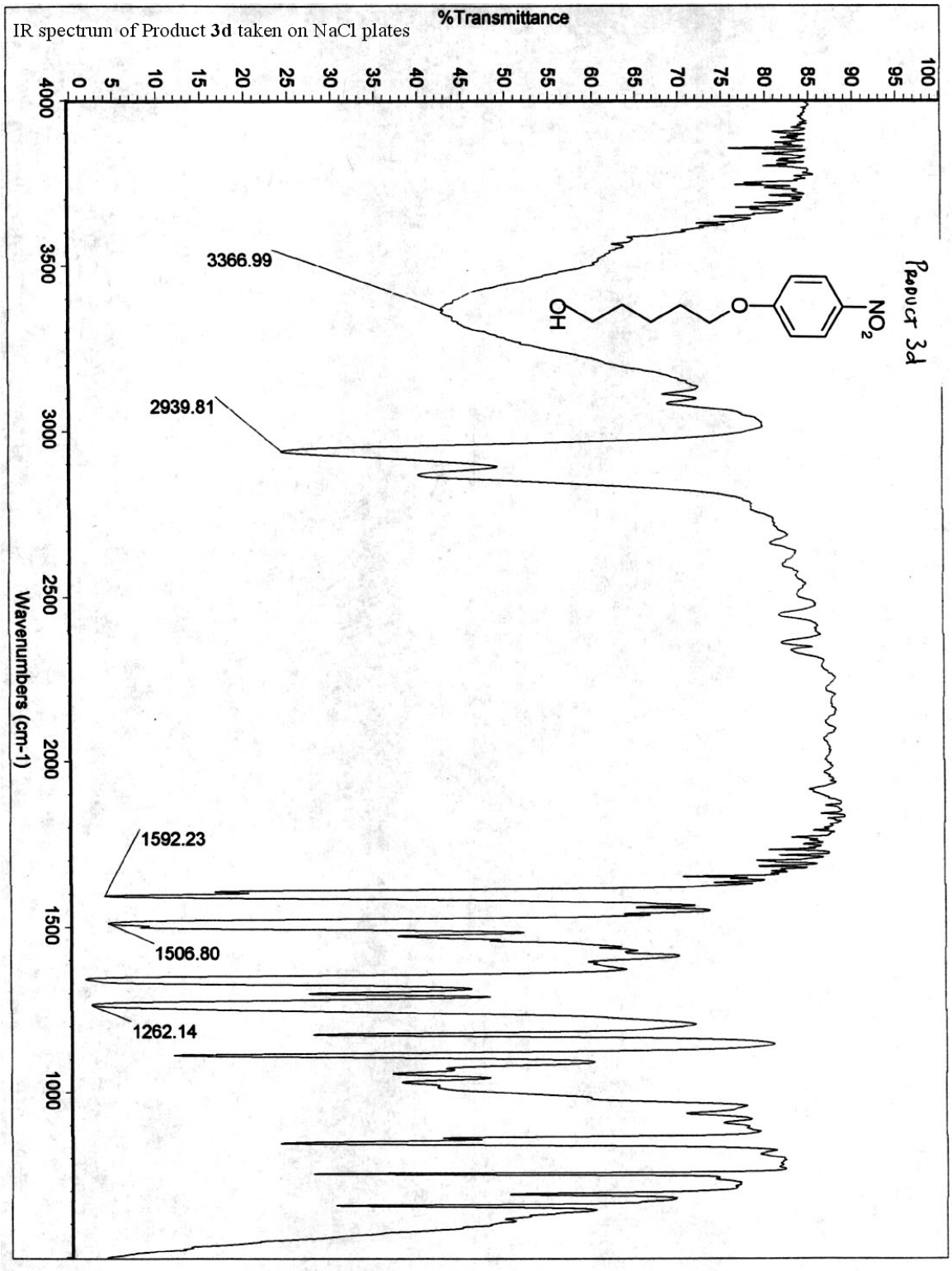

Figure A.16. IR spectrum of product 3d taken on NaCl plates.

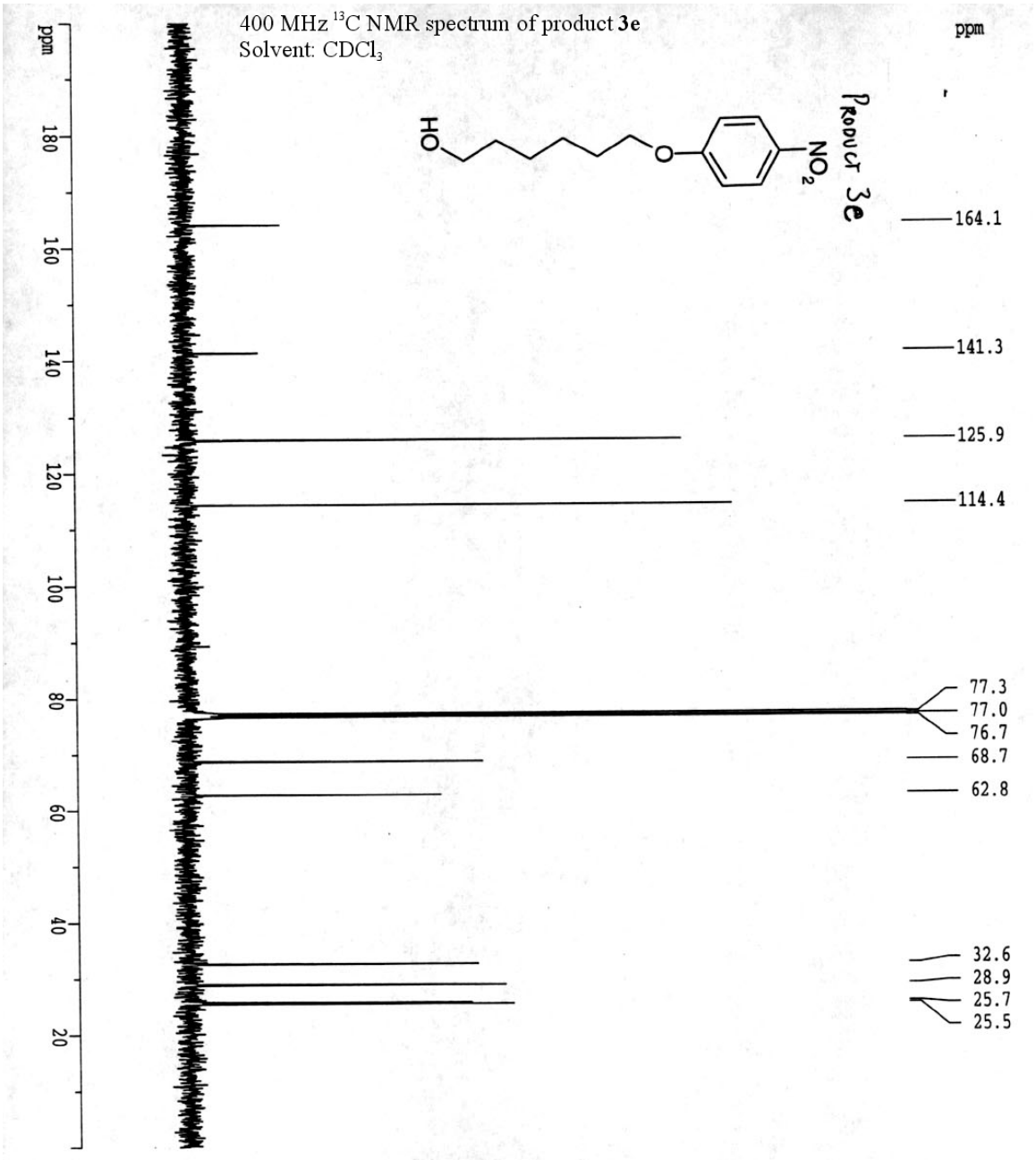

Figure A.17. ^{13}C NMR spectrum of product 3e.

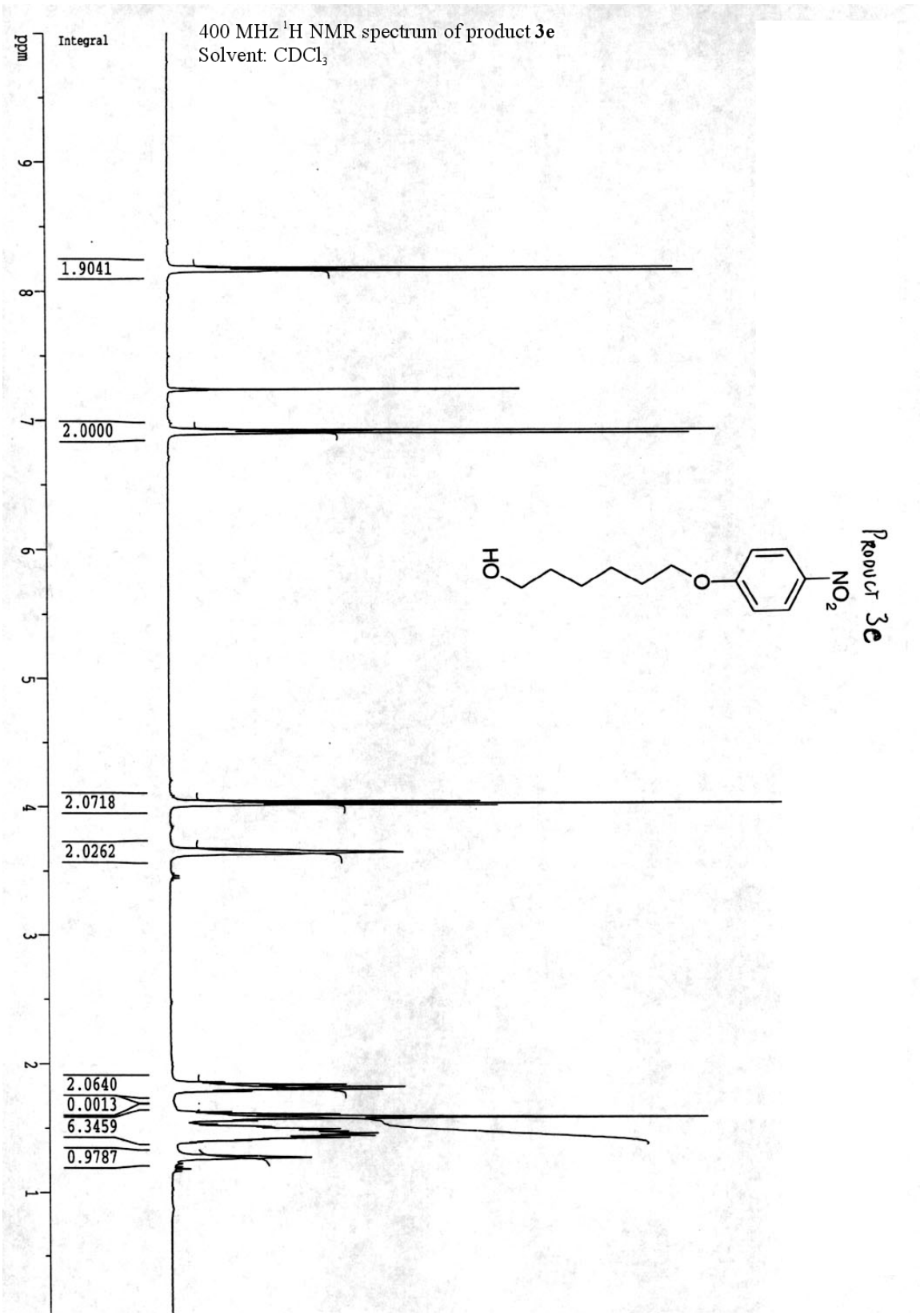

Figure A.18. ^{1}H NMR spectrum of product 3e.

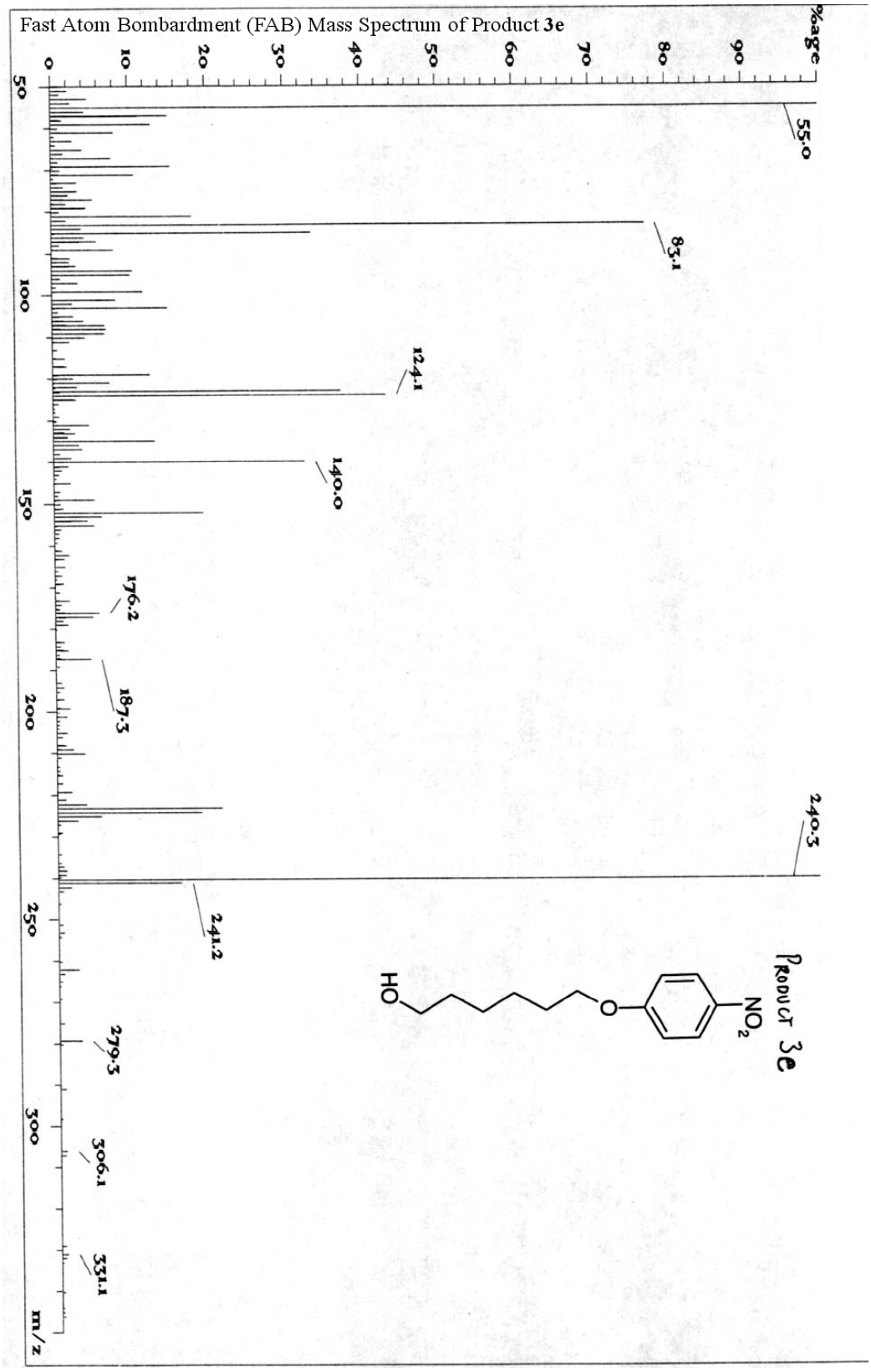

Figure A.19. Fast atom bombardment (FAB) mass spectrum of product 3e.

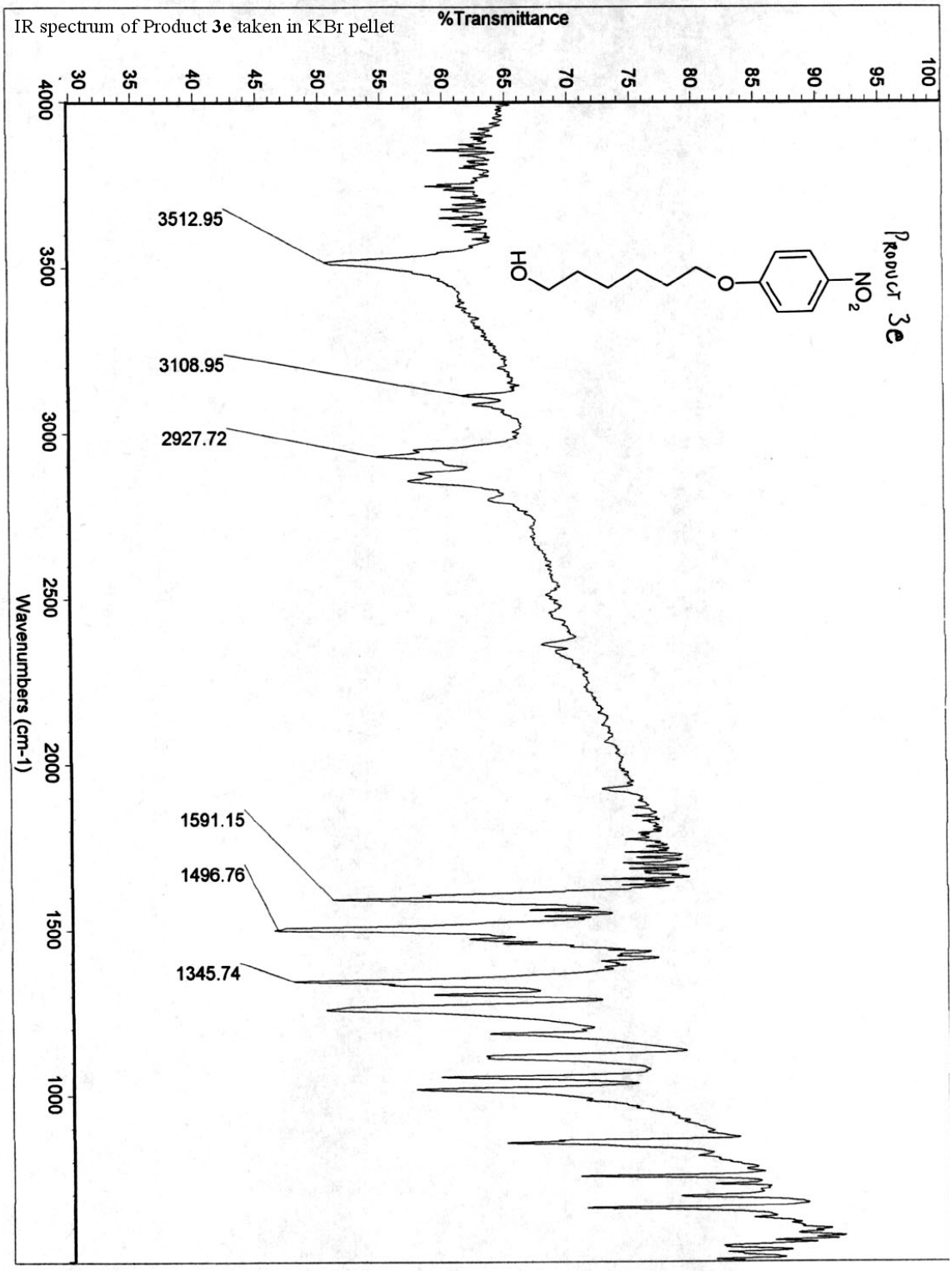

Figure A.20. IR spectrum of product 3e taken in KBr pellet.

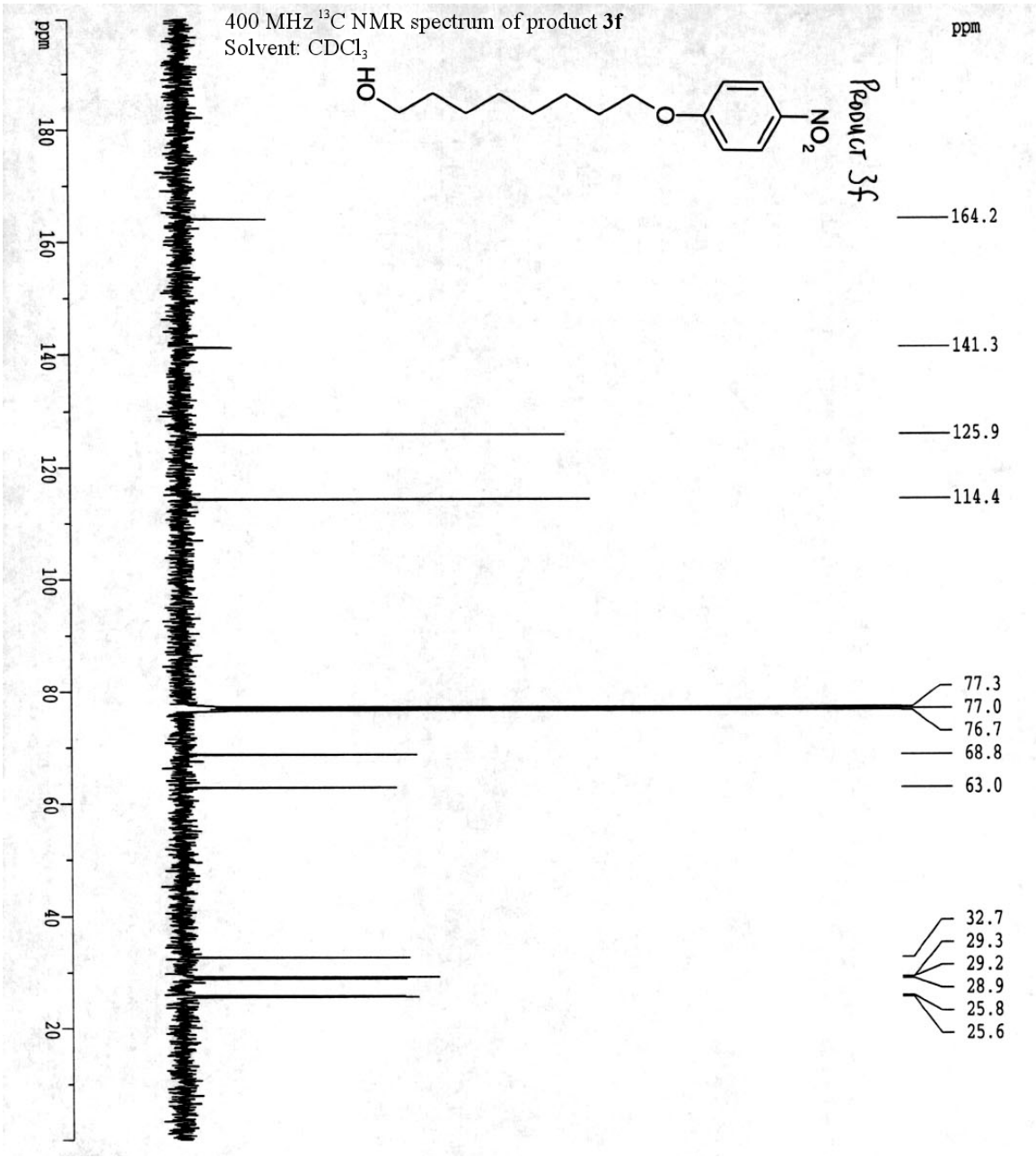

Figure A.21. ^{13}C NMR spectrum of product 3f.

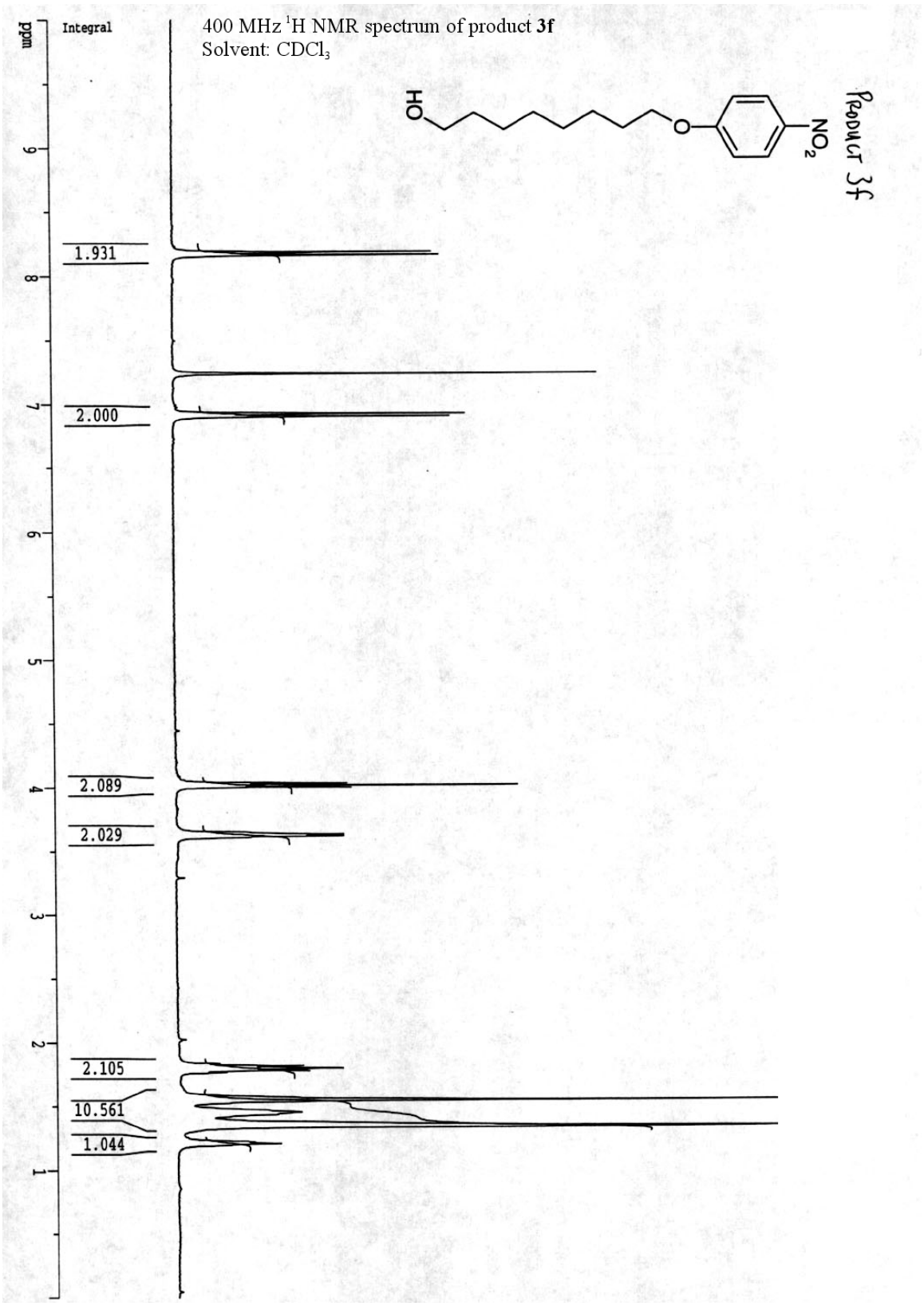

Figure A.22. ^{1}H NMR spectrum of product 3f.

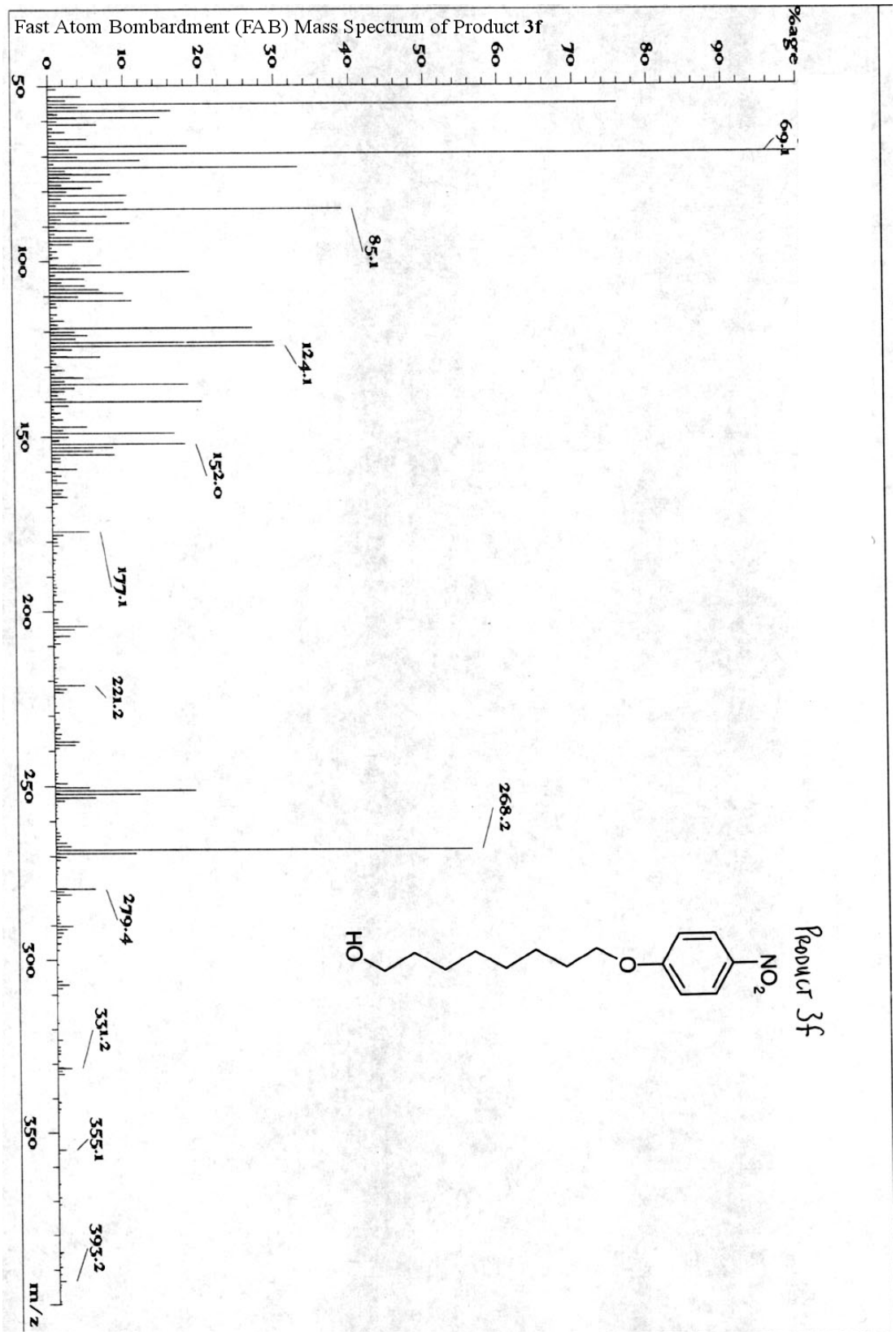

Figure A.23. Fast atom bombardment (FAB) mass spectrum of product 3f.

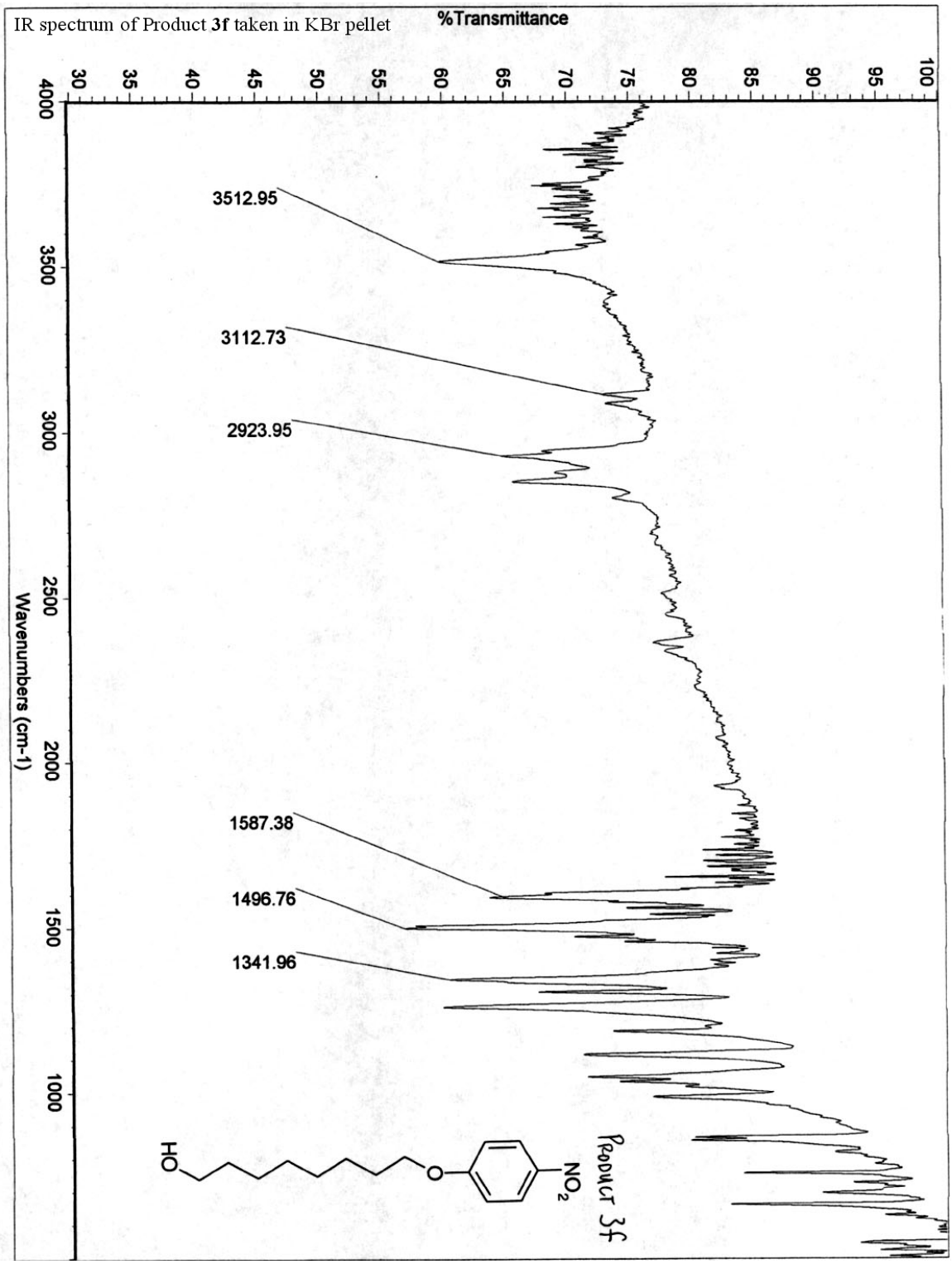

Figure A.24. IR spectrum of product 3f taken in KBr pellet.

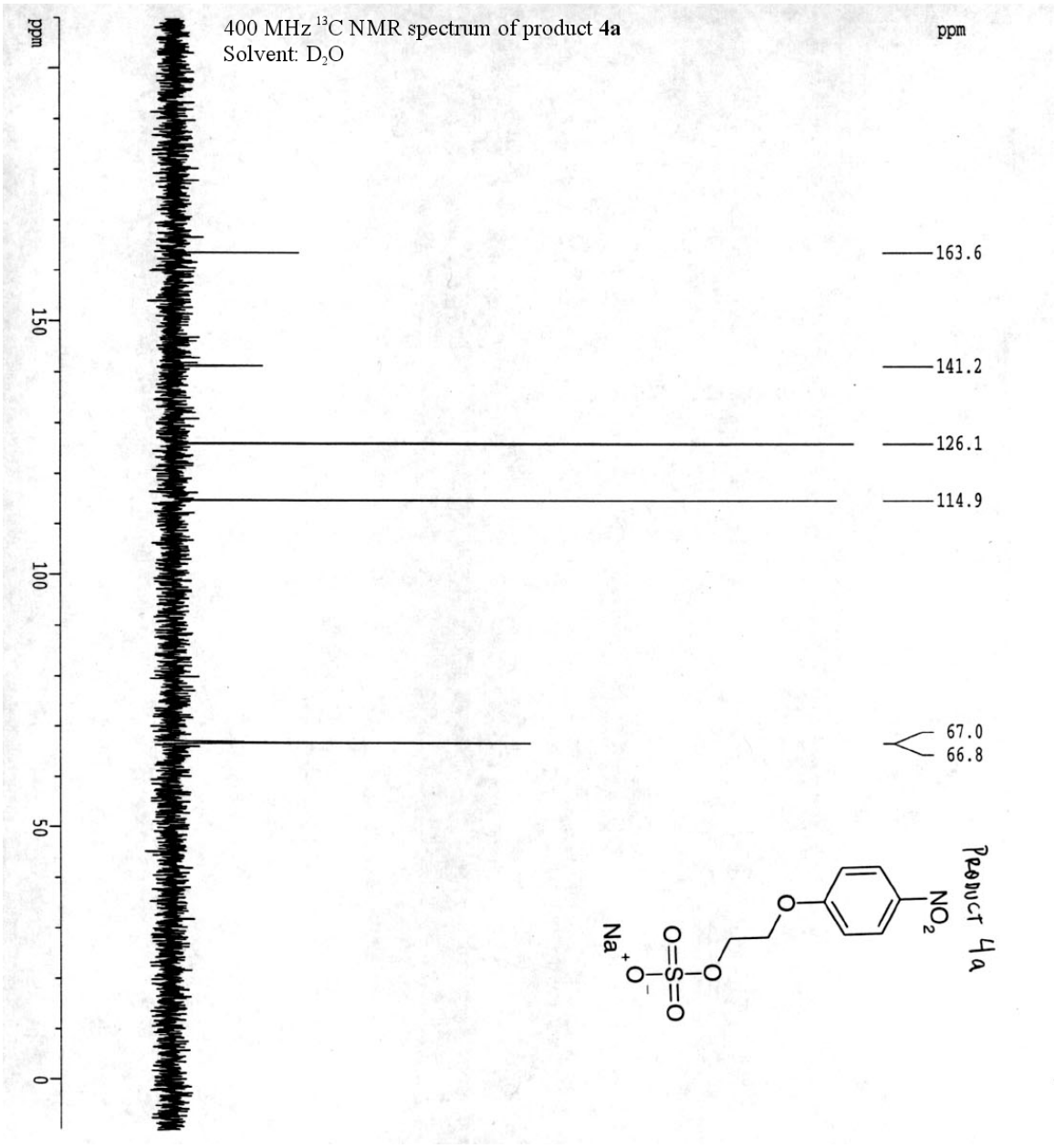

Figure A.25. ^{13}C NMR spectrum of product 4a.

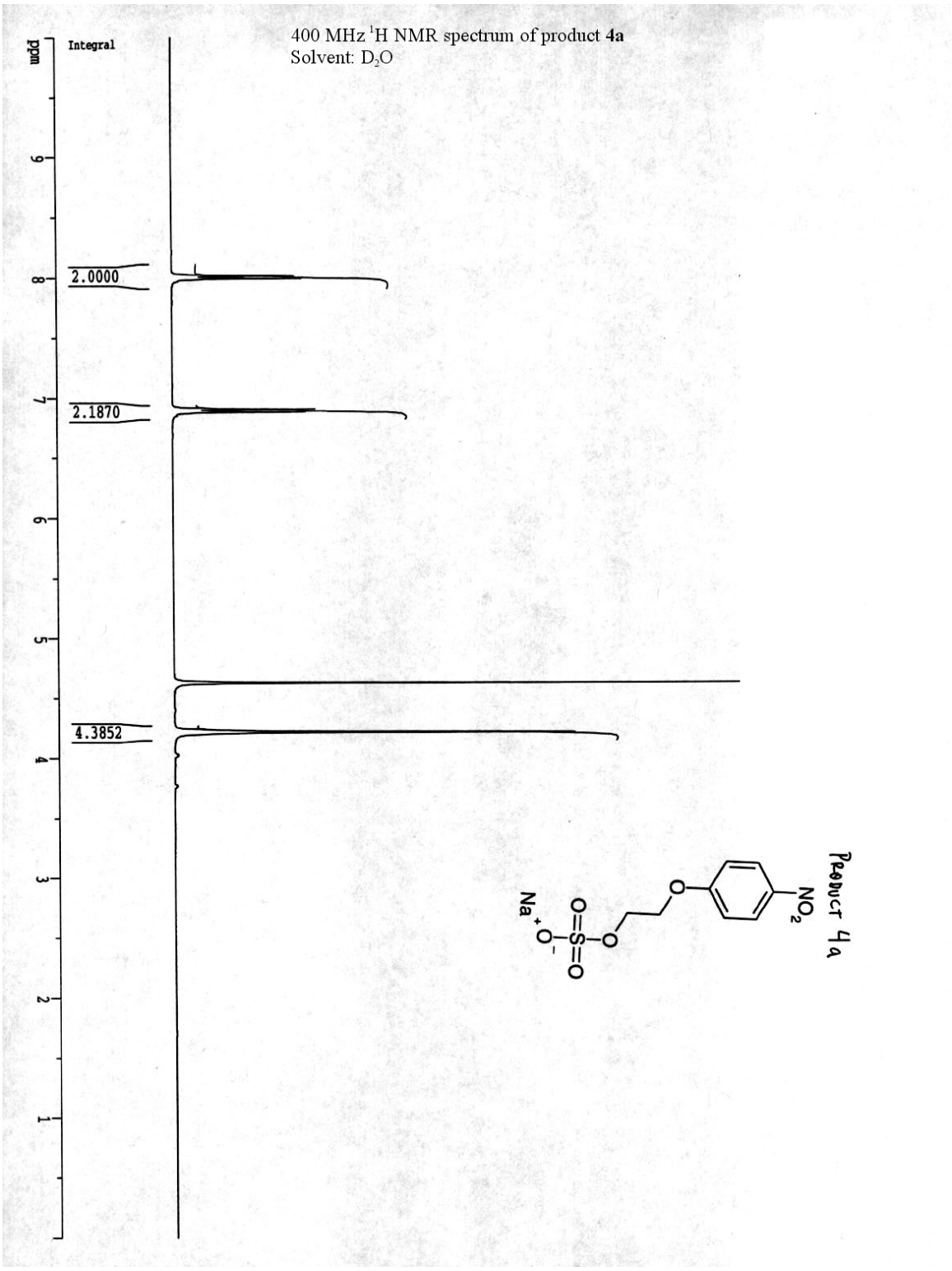

Figure A.26. ^{1}H NMR spectrum of product 4a.

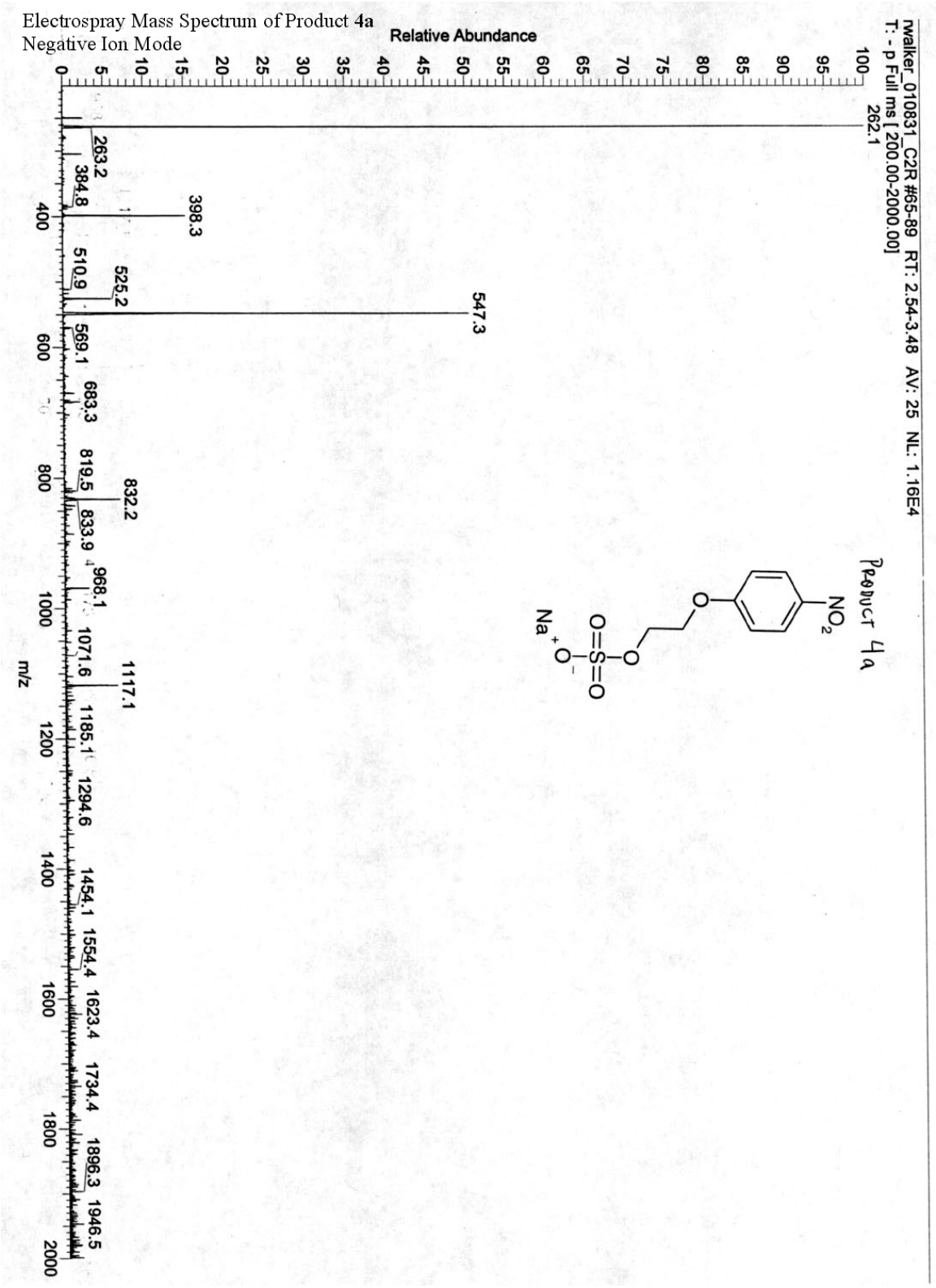

Figure A.27. Electrospray mass spectrum (negative ion mode) of product 4a.

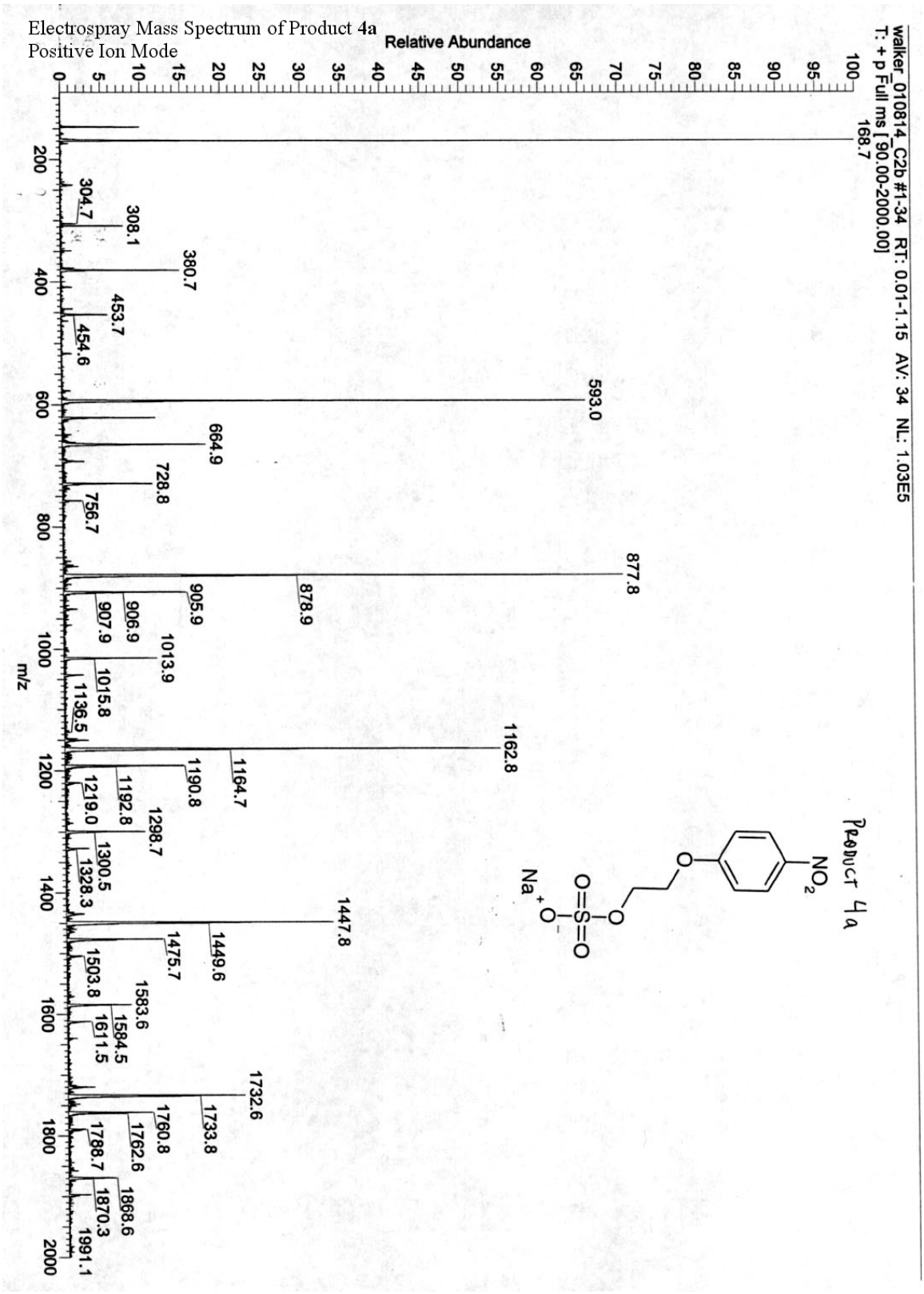

Figure A.28. Electrospray mass spectrum (positive ion mode) of product 4a.

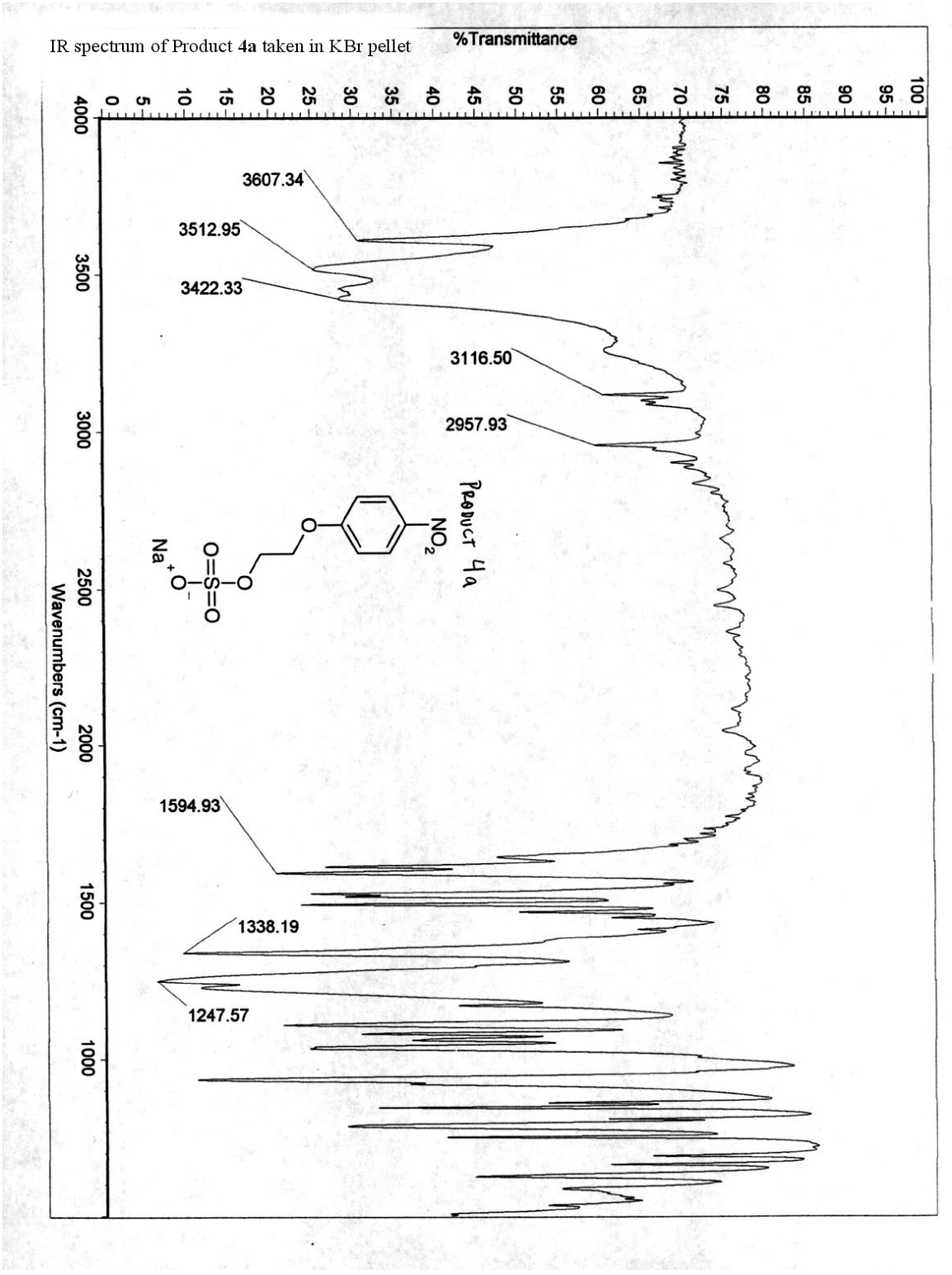

Figure A.29. IR spectrum of product 4a taken in KBr pellet.

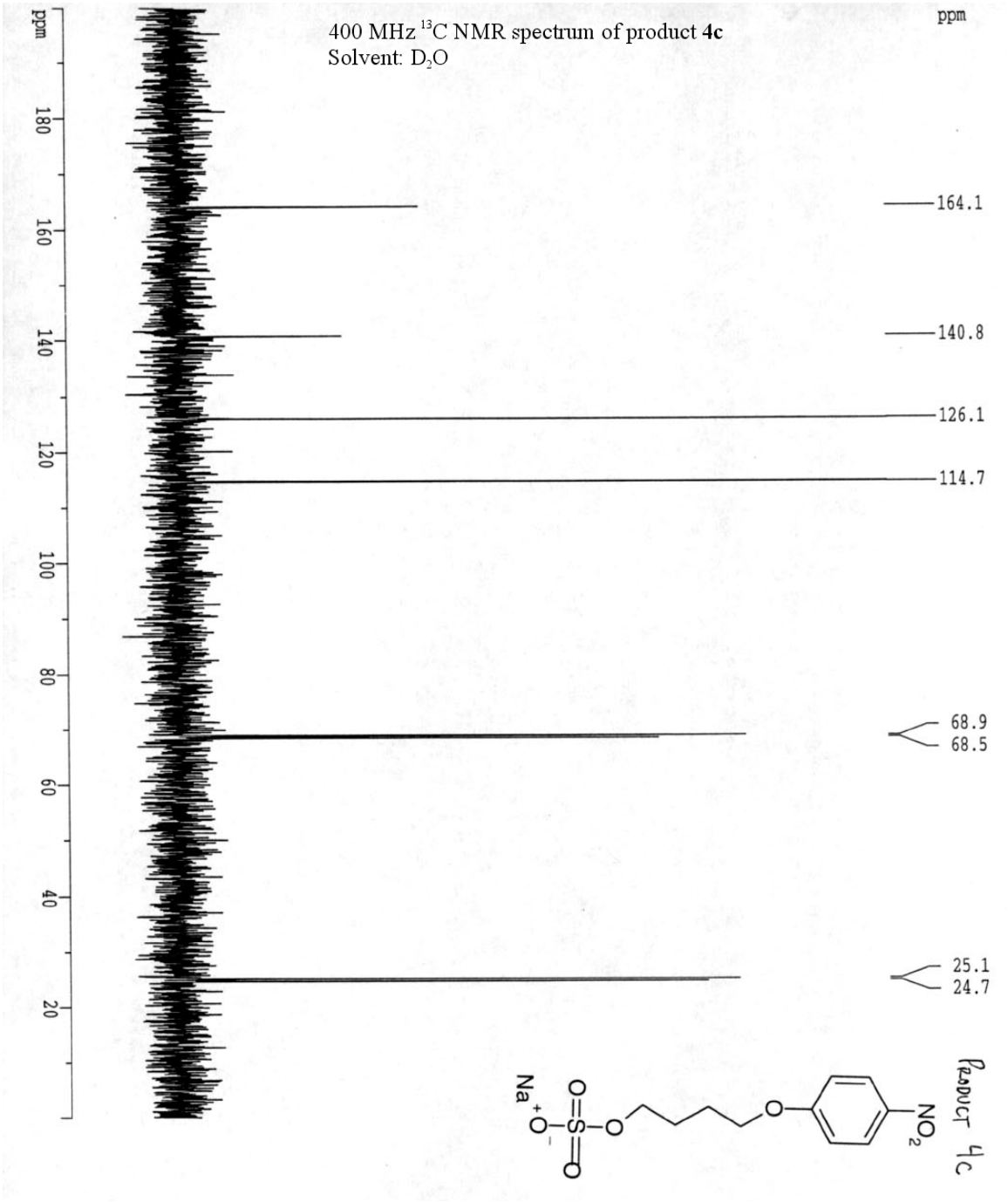

Figure A.30. ^{13}C NMR spectrum of product 4c.

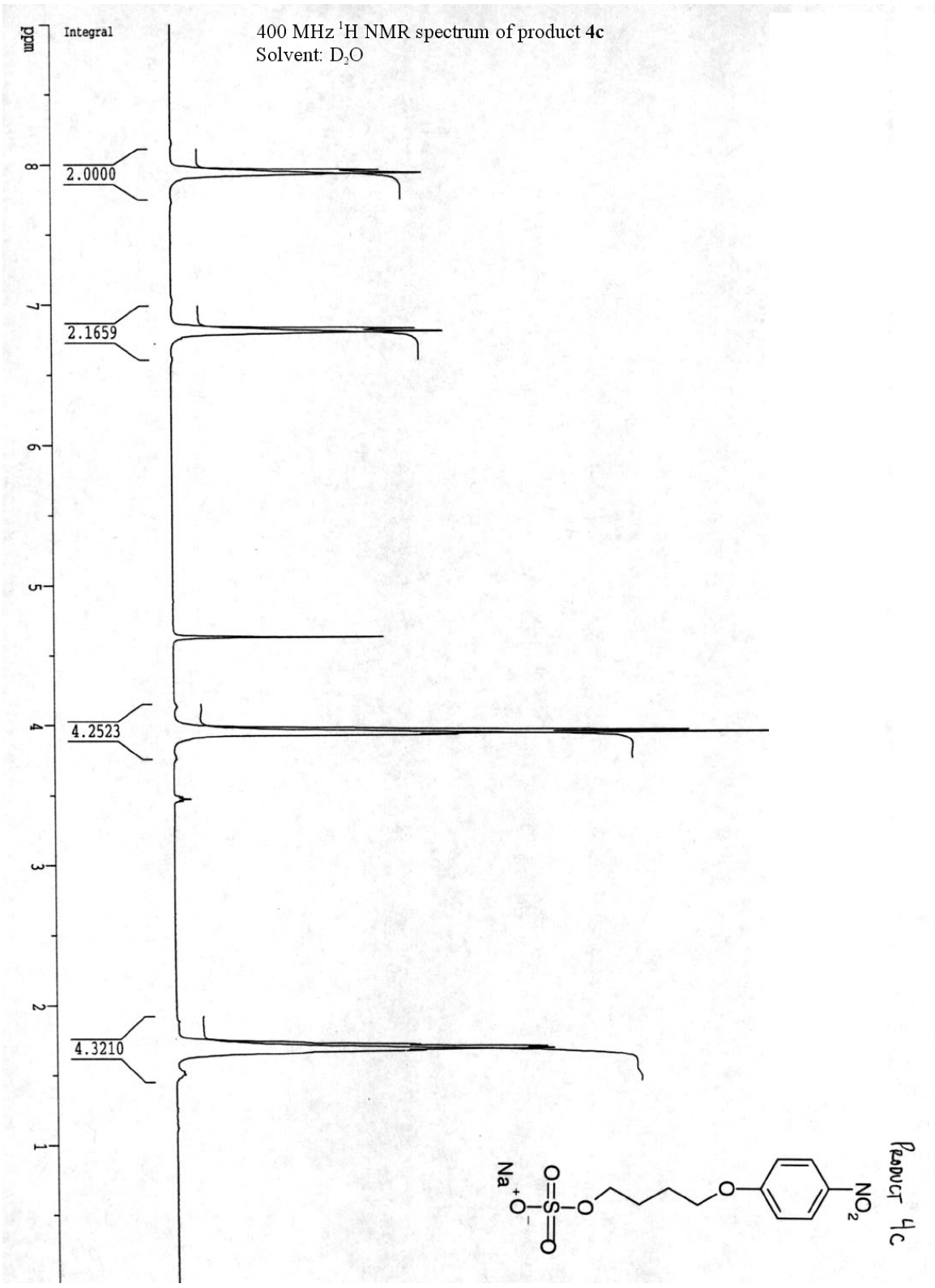

Figure A.31. ^{1}H NMR spectrum of product 4c.

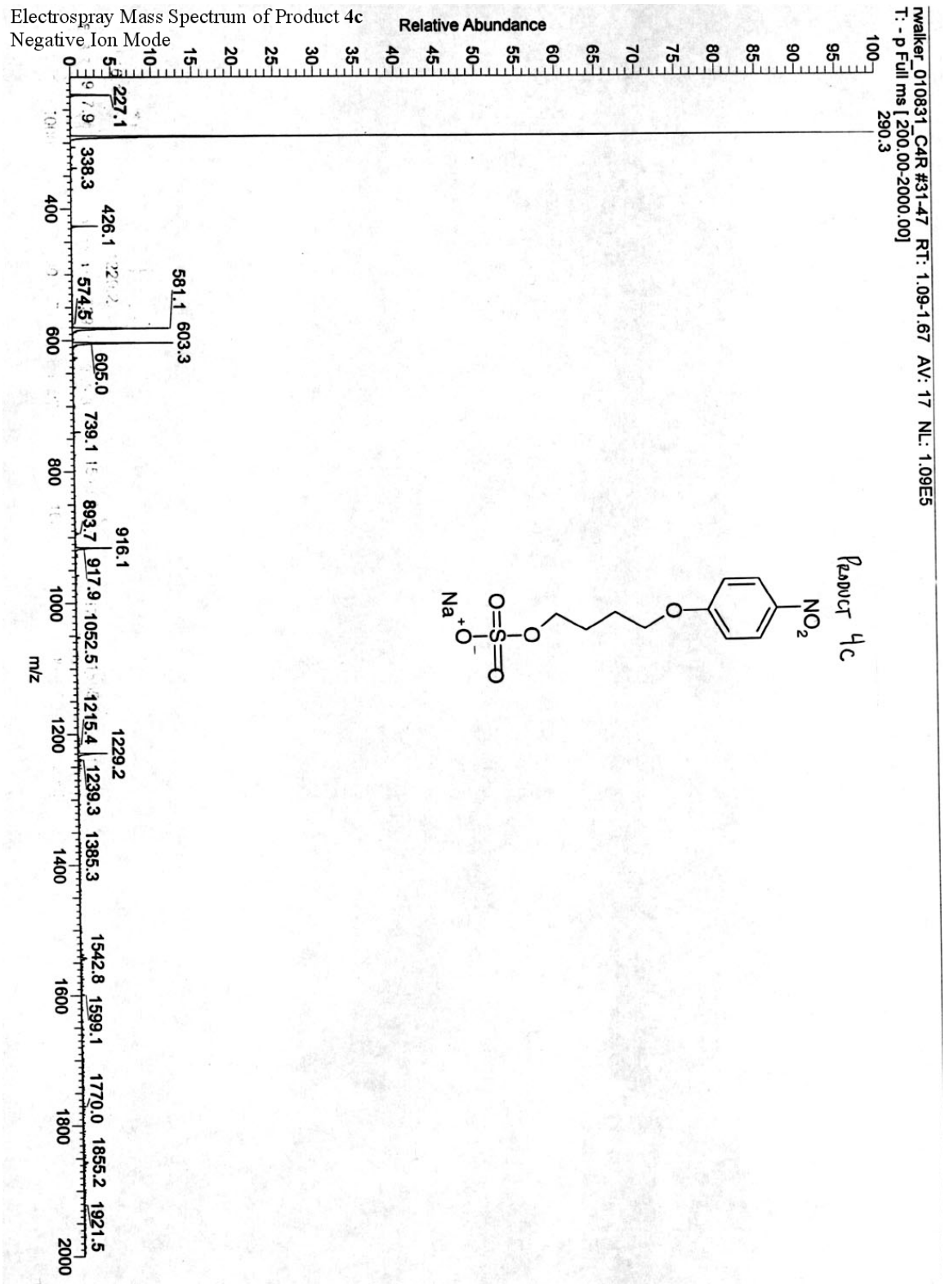

Figure A.32. Electrospray mass spectrum (negative ion mode) of product 4c.

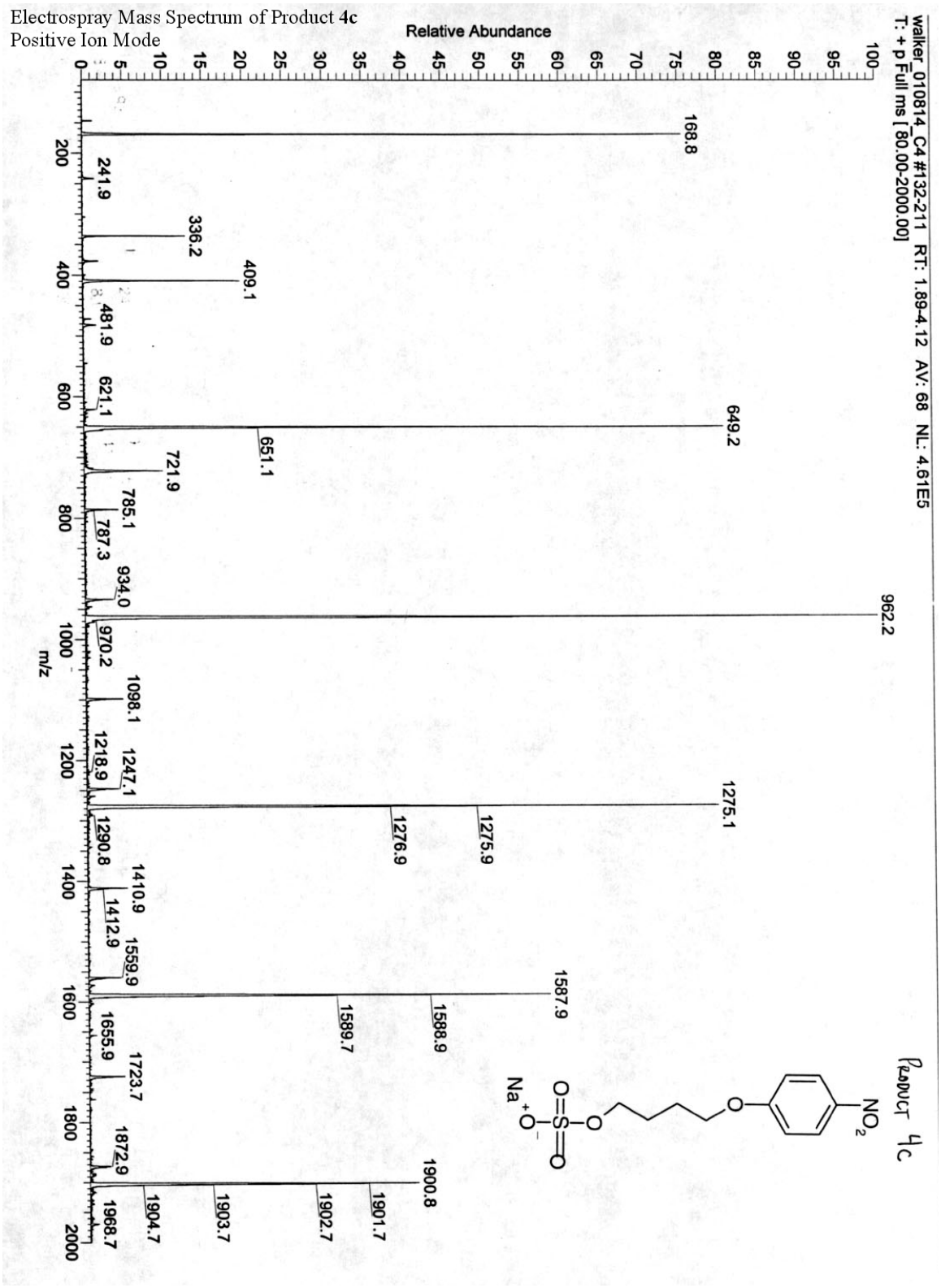

Figure A.33. Electrospray mass spectrum (positive ion mode) of product 4c.

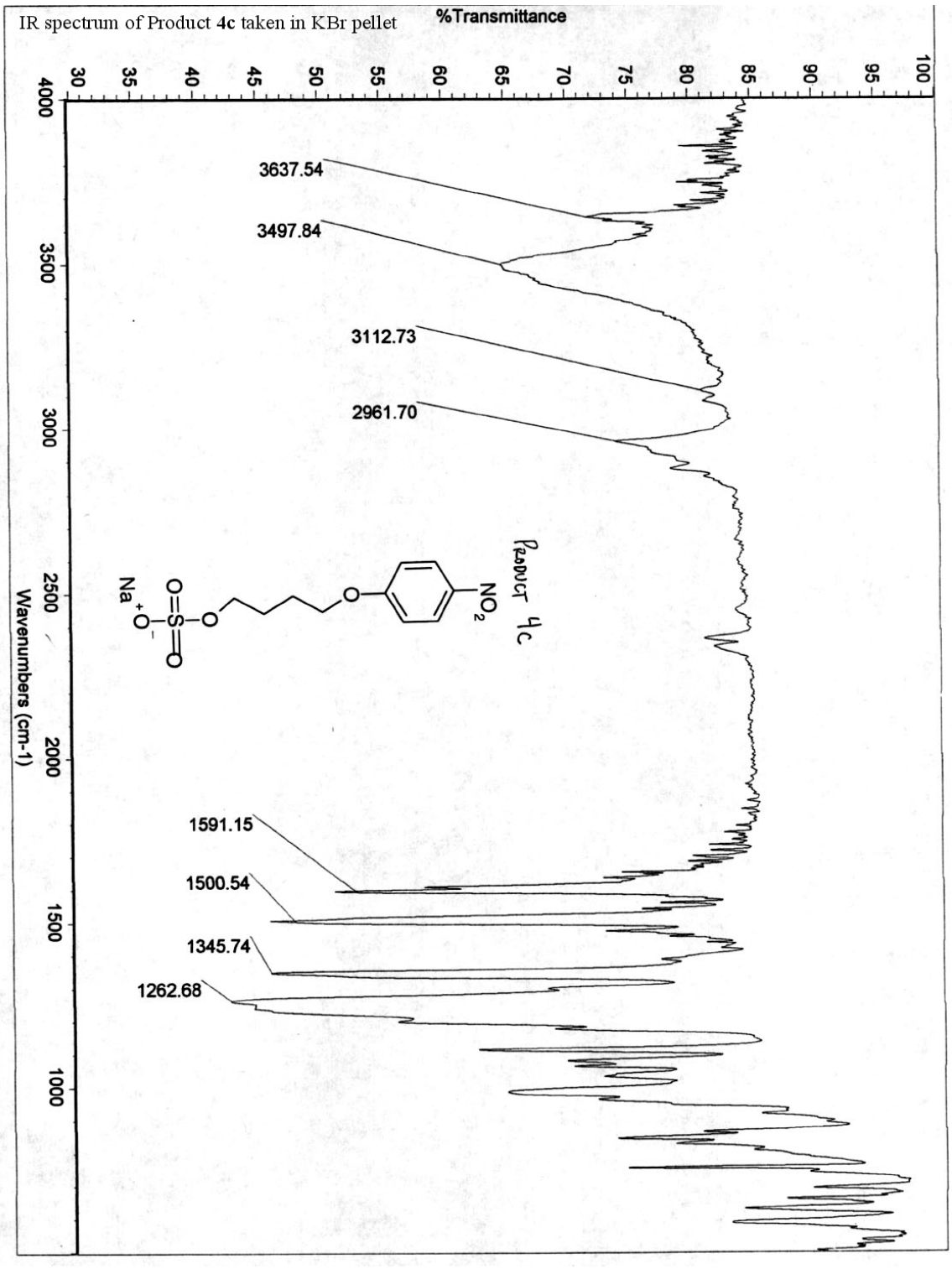

Figure A.34. IR spectrum of product 4c taken in KBr pellet.

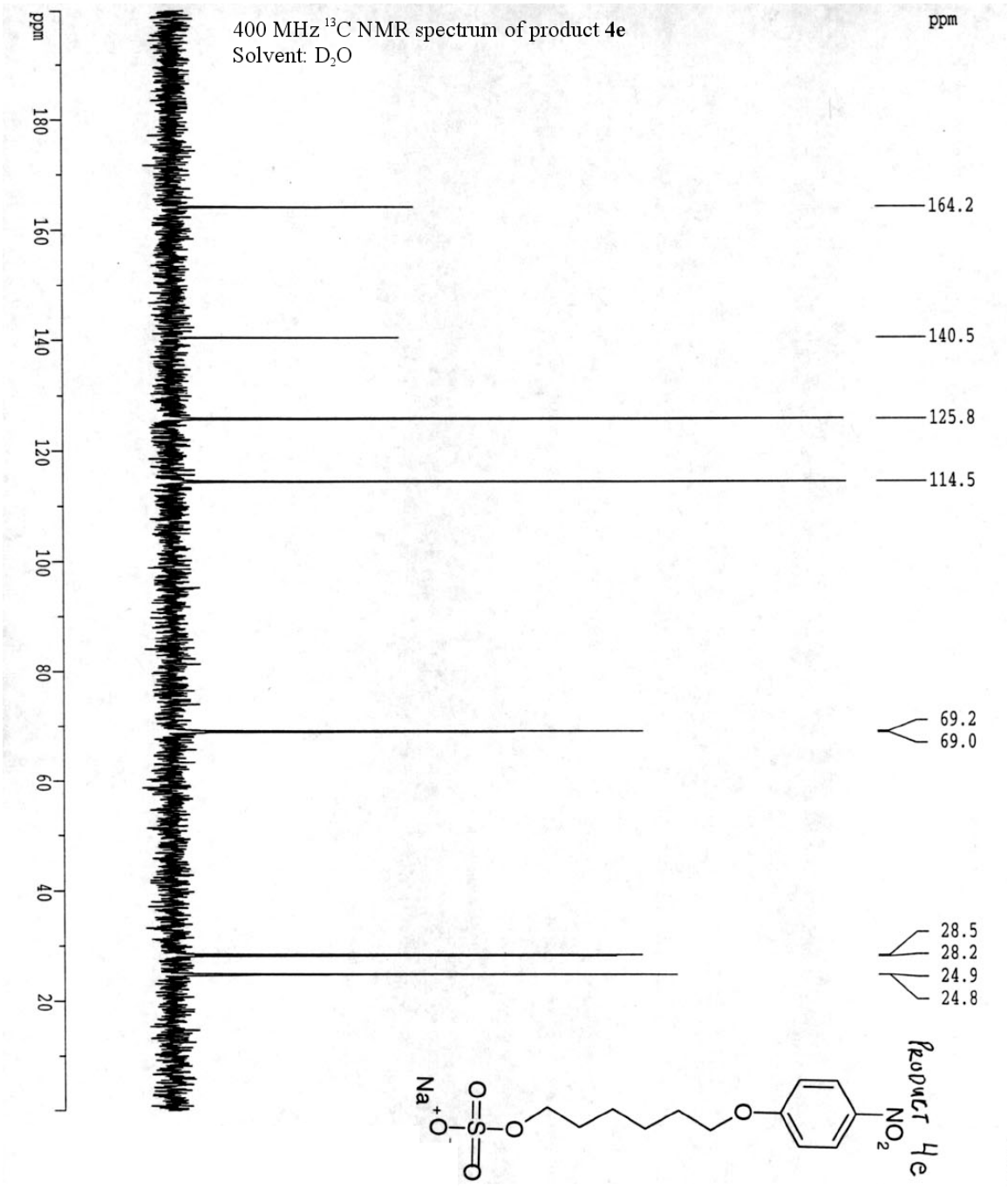

Figure A.35. ^{13}C NMR spectrum of product 4e.

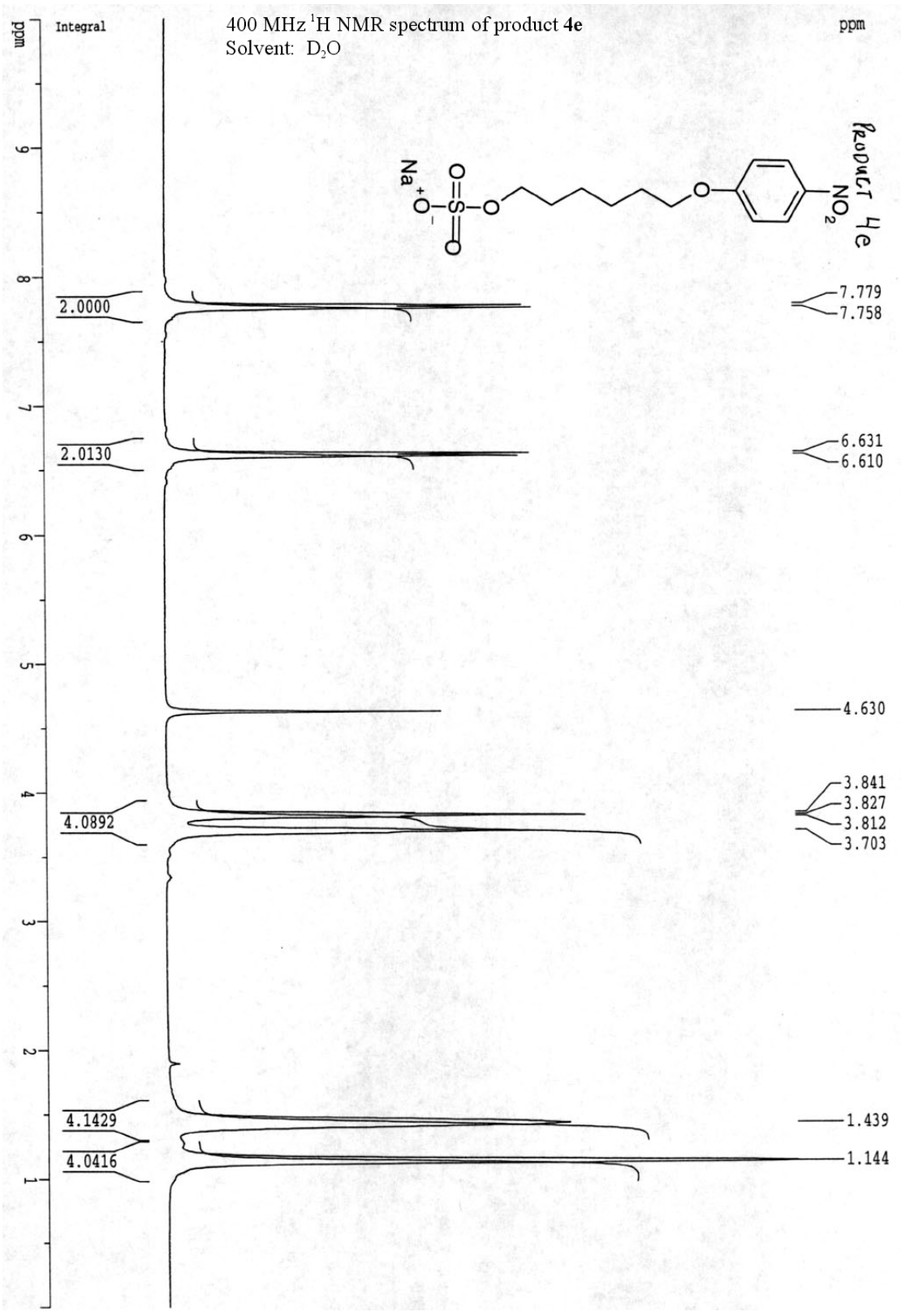

Figure A.36. ^{1}H NMR spectrum of product 4e.

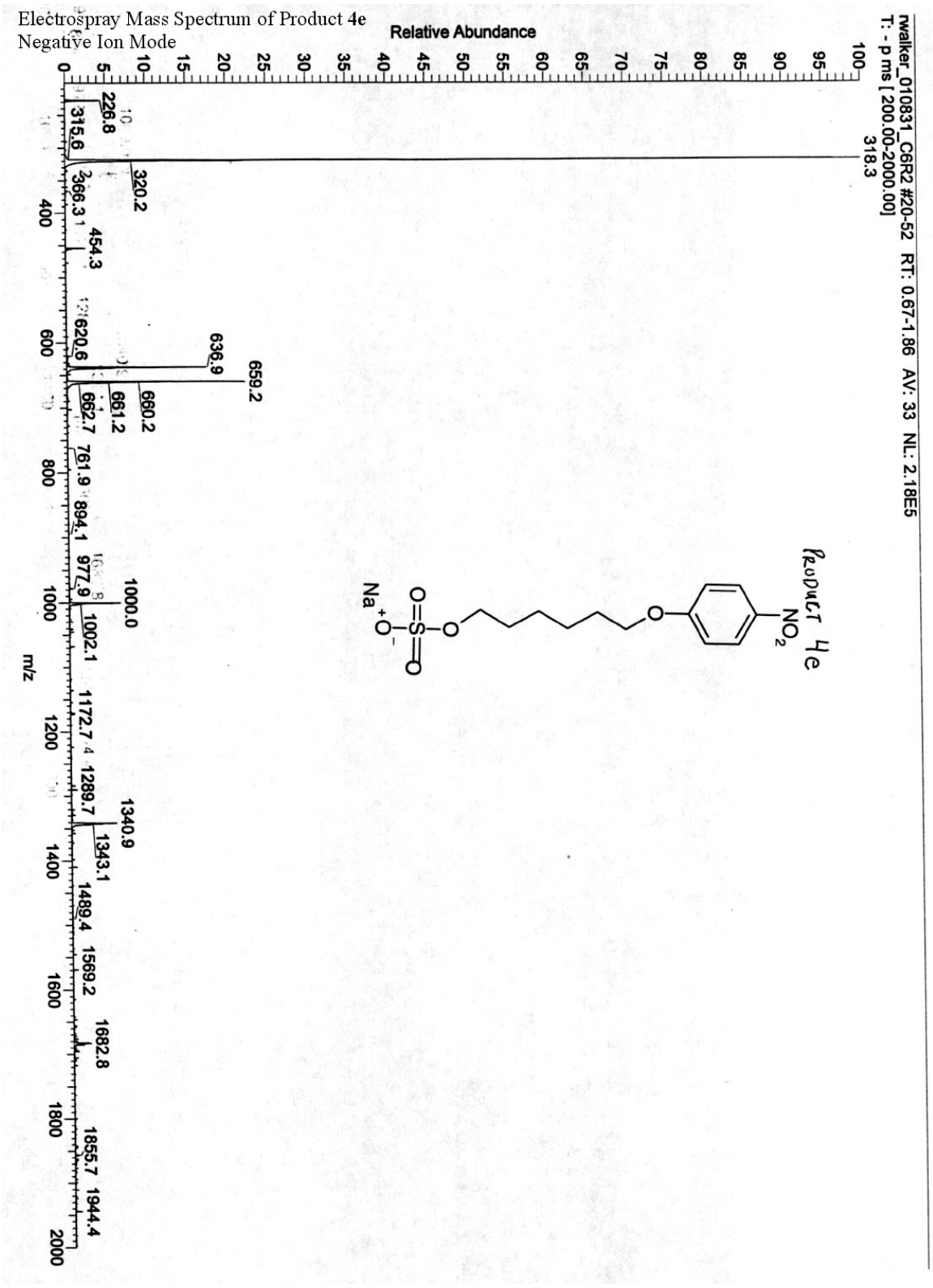

Figure A.37. Electrospray mass spectrum (negative ion mode) of product 4e.

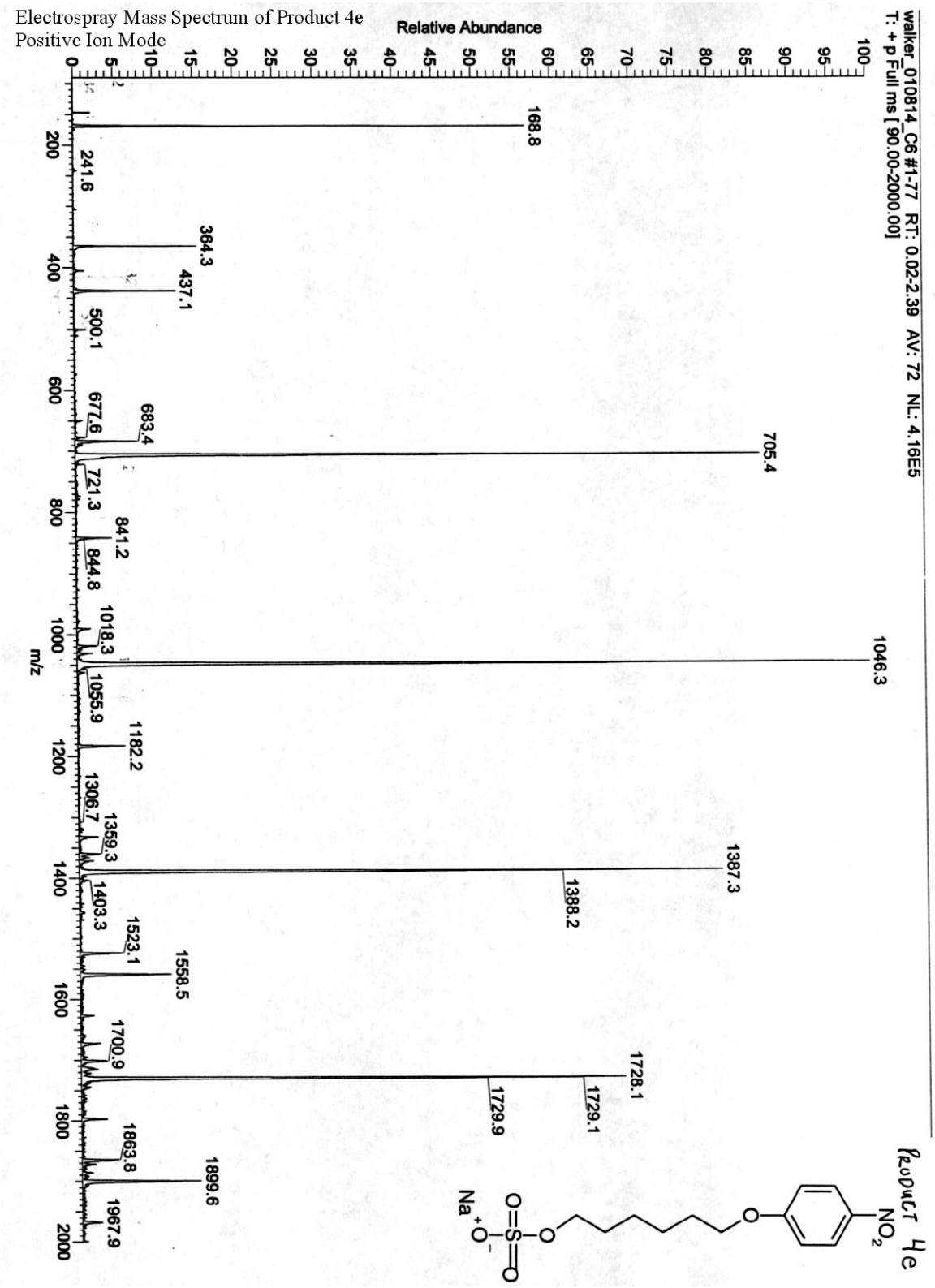

Figure A.38. Electrospray mass spectrum (positive ion mode) of product 4e.

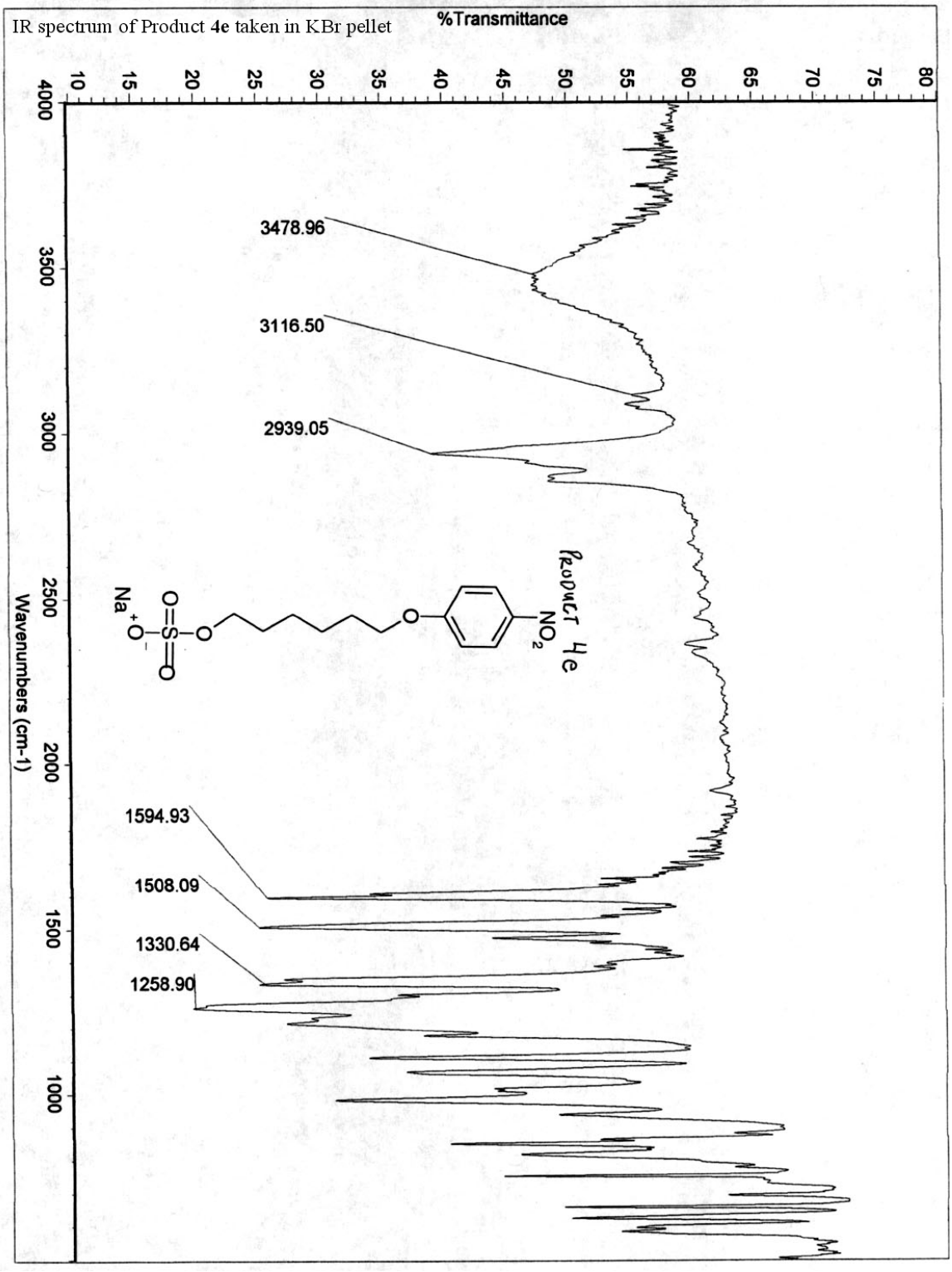

Figure A.39. IR spectrum of product 4e taken in KBr pellet.

Appendix B. Liquid/liquid Cell and Prism Designs

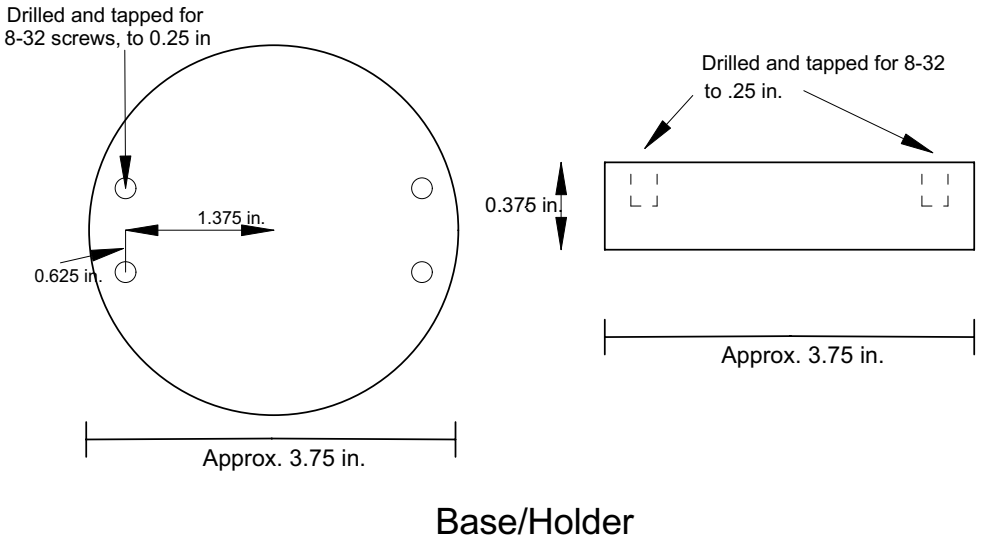

Figure B.1. Base/Holder for cell used in SHG studies described in this dissertation.

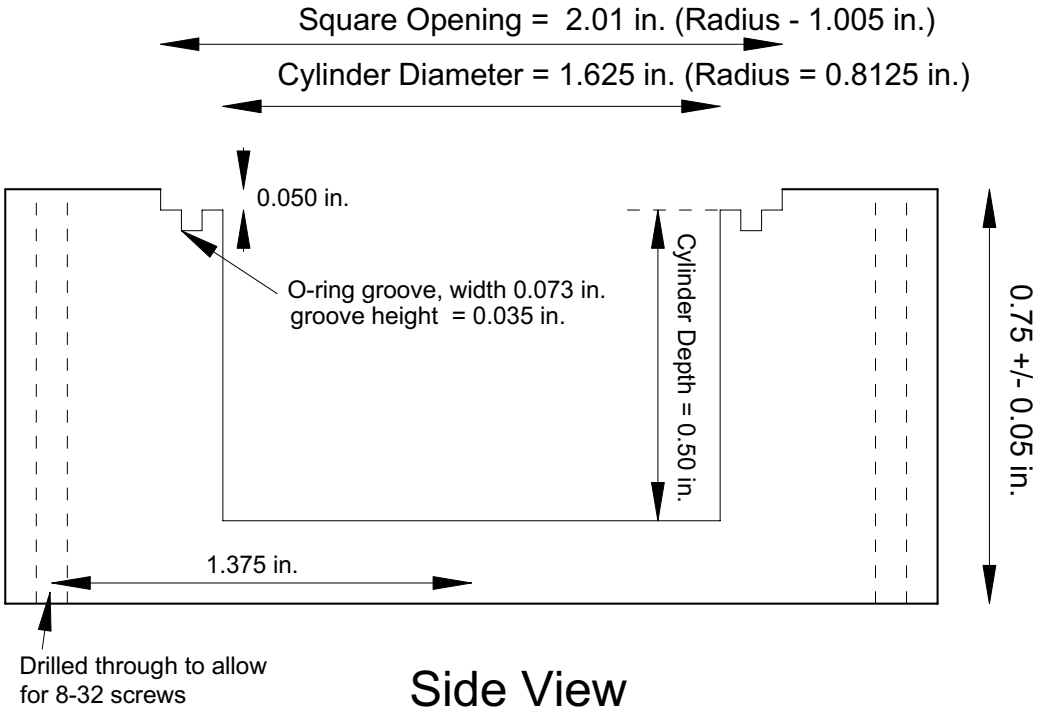

Figure B.2. Side view of cell used in SHG studies described in this dissertation.

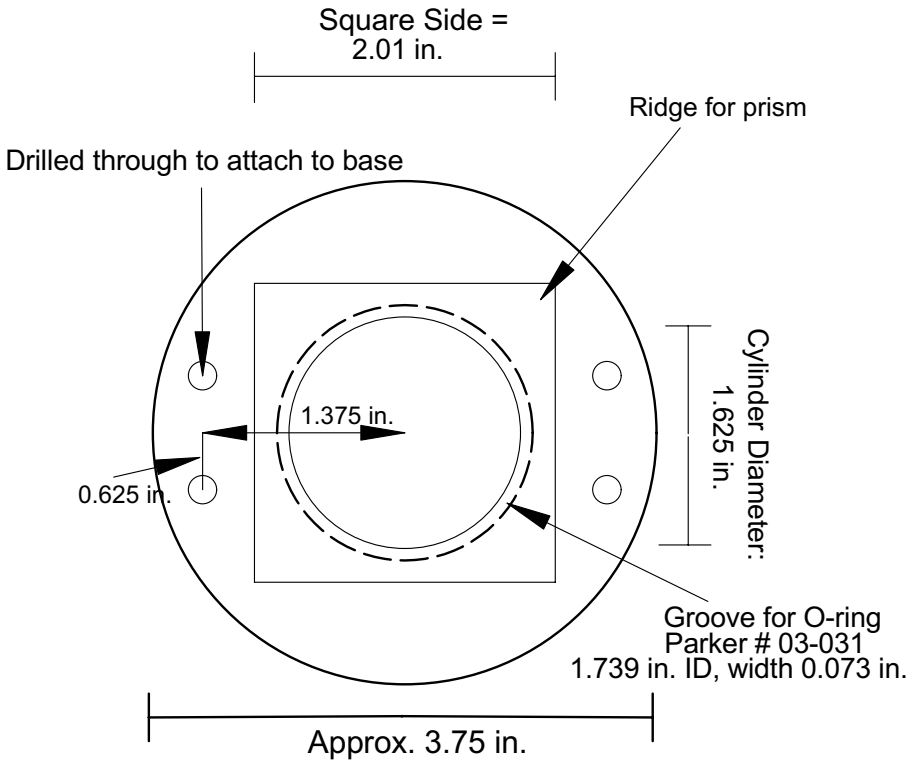

Figure B.3. Top view of cell used in SHG studies described in this dissertation.

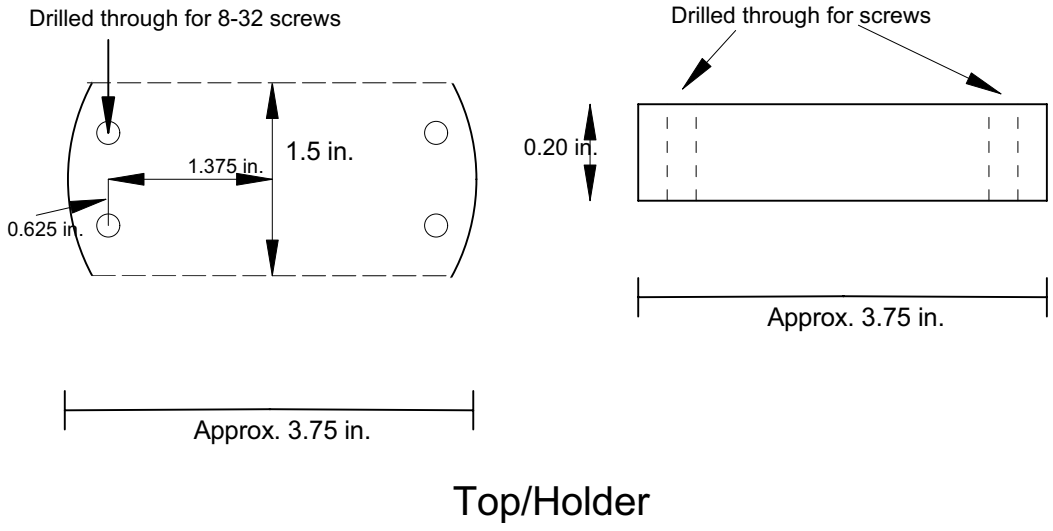

Figure B.4. Top/Holder of cell used in SHG studies described in this dissertation.

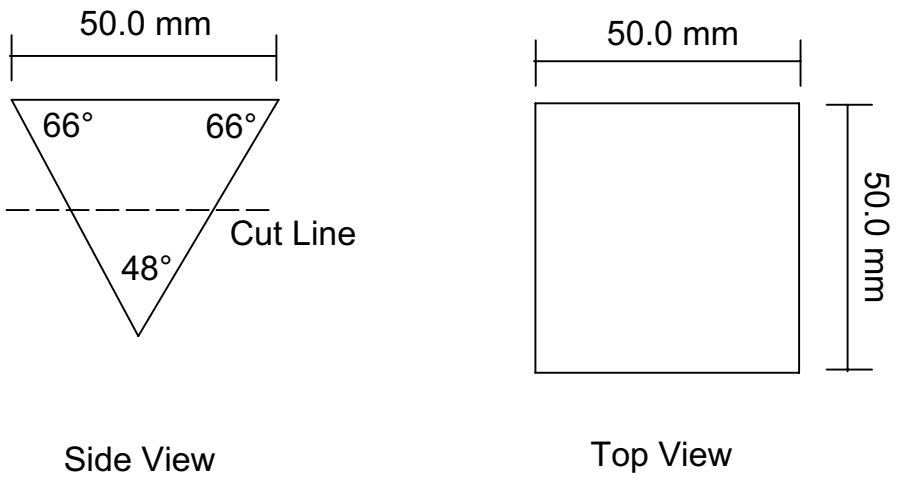

Figure B.5. Side and Top view of fused silica prism used in SHG studies described in this dissertation.

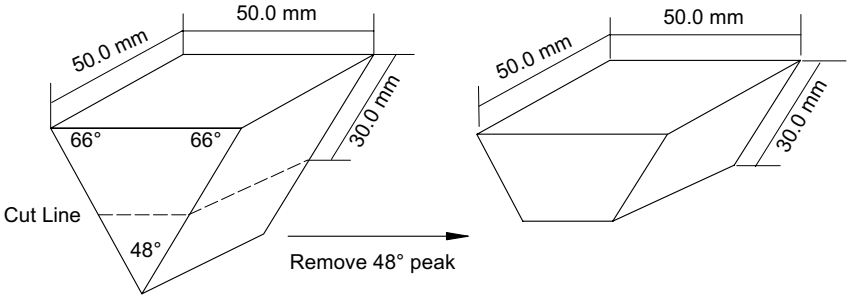

Figure B.6. Finished view of prism used in SHG studies described in this dissertation.

REFERENCES

(1) Freiser, H. *Chem. Rev.* **1988**, *88*, 611.

(2) Dorsey, J. G.; Dill, K. A. *Chem. Rev.* **1989**, *89*, 331.

(3) Piron, A.; Brevet, P. F.; Girault, H. H. *J. Electroanal. Chem.* **2000**, *483*, 29.

(4) Knock, M. M.; Bain, C. D. "Surfactant Monolayers at the Oil-Water Interface: Structure through Spectroscopy"; 223rd ACS National Meeting, 2002, Orlando, FL.

(5) Leo, A.; Hansch, C.; Elkins, D. *Chem. Rev.* **1971**, *71*, 525.

(6) Watarai, H.; Freiser, H. *J. Am. Chem. Soc.* **1983**, *105*, 191.

(7) Shioya, T.; Nishizawa, S.; Teramae, N. *Langmuir* **199**, *15*, 2575.

(8) Ueno, K.; Kitagawa, F.; Kitamura, N. *Lab on a Chip* **2002**, *2*, 231.

(9) Kile, D. E.; Chiou, C. T. *Environ. Sci. Technol.* **1989**, *23*, 832.

(10) Chhabra, V.; Free, M. L.; Kang, P. K.; Truesdail, S. E.; Shah, D. O. *Tenside, Surfactants, Detergents* **1997**, *34*, 156.

(11) Sangster, J. *Octanol-Water Partition Coefficients*; John Wiley and Sons: New York, 1997; Vol. 2.

(12) LeBlanc, R.; Konka, V. Langmuir and Langmuir-Blodgett Films of Chlorophyll a and Photosystem II Complex. In *Liquid Interfaces in Chemical, Biological and Pharmaceutical Applications*; Volkov, A. G., Ed.; Marcel Dekker, Inc.: New York, 2001; Vol. 95; pp 641.

(13) Nakano, K. DNA-Modified Electrodes. Molecular Rocognition of DNA and Biosensor Applications. In *Liquid Interfaces in Chemical, Biological and*

Pharmaceutical Applications; Volkov, A. G., Ed.; Marcel Dekker, Inc.: New York, 2001; Vol. 95; pp 515.

(14) Koester, C. J.; Simonich, S. L.; Esser, B. K. *Anal. Chem.* **2003**, *75*, 2813.

(15) Richarson, S. D. *Anal. Chem.* **2003**, *75*, 2831.

(16) Bessho, K.; Uchida, T.; Yamauchi, A.; Shioya, T.; Teramae, N. *Chem. Phys. Lett.* **1997**, *264*, 381.

(17) Perera, J. M.; Stevens, G. W.; Grieser, F. *Coll. & Surf. A* **1995**, *95*, 185.

(18) Ishizaka, S.; Kim, H.; Kitamura, N. *Anal. Chem.* **2001**, *73*, 2421.

(19) Kovaleski, J. M.; Wirth, M. J. *J. Phys. Chem.* **1995**, *99*, 4091.

(20) Tikhonov, A. M.; Mitrinovic, D. M.; Li, M.; Huang, Z.; Schlossman, M. L. *J. Phys. Chem. B* **2000**, *104*, 6336.

(21) Penfold, J.; Richardson, R. M.; Zarbakhsh, A.; Webster, J. R. P. *J. Chem. Soc. Faraday Trans.* **1997**, *93*, 3899.

(22) Cubitt, R.; Fragneto, G.; Ghosh, R. E.; Rennie, A. R. *Langmuir* **2003**, *19*, 7685.

(23) Corn, R. M.; Higgins, D. A. *Chem. Rev.* **1994**, *94*, 107.

(24) Eisenthal, K. B. *Chem. Rev.* **1996**, *96*, 1343.

(25) Suppan, P. *J. Photochem. Photobiol. A* **1990**, *50*, 293.

(26) Onsager, L. *J. Am. Chem. Soc.* **1936**, *58*, 1486.

(27) McRae, E. G. *J. Phys. Chem.* **1957**, *61*, 562.

(28) Laurence, C.; Nicolet, P.; Dalati, M. T. *J. Phys. Chem.* **1994**, *98*, 5807.

(29) Daillant, J. *Current Science* **2000**, *78*, 1496.

(30) Staples, E.; Penfold, J.; Tucker, I. *J. Phys. Chem. B* **2000**, *104*, 606.

(31) Thomas, R. K. Neutron Reflectivity at Liquid-Vapor, Liquid-Liquid, and Solid-Liquid Interfaces. In *General Review Characterization Methods of Surfactant Systems*; Marcel Dekker, Inc.: New York, 1999; Vol. 83; pp 417.

(32) Franken, P. A.; Hill, A. E.; Peters, C. W.; Weinreich, G. *Phys. Rev. Lett.* **1961**, *7*, 118.

(33) Brown, F.; Matsuoka, M. *Phys. Rev.* **1969**, *185*, 985.

(34) Lagugne-Labarthet, F.; Yu, T.; Barger, W. R.; Shenoy, D. K.; Dalcanale, E.; Shen, Y. R. *Chem. Phys. Lett.* **2003**, *381*, 322.

(35) Higgins, D. A.; Abrams, M. B.; Byerly, S. K.; Corn, R. M. *Langmuir* **1992**, *8*, 1992.

(36) Yamaguchi, A.; Kato, R.; Nishizawa, S.; Teramae, N. *Chem. Lett.* **2003**, *32*, 798.

(37) Uchida, T.; Yamaguchi, A.; Ina, T.; Teramae, N. *J. Phys. Chem. B* **2000**, *104*, 12091.

(38) Perrenoud-Rinuy, J.; Brevet, P. F.; Girault, H. H. *Phys. Chem. Chem. Phys.* **2002**, *4*, 4774.

(39) Antoine, R.; Bianchi, F.; Brevet, P. F.; Girault, H. H. *J. Chem. Soc. Faraday Trans.* **1997**, *93*, 3833.

(40) Naujok, R.; Higgins, D. A.; Hanken, D. G.; Corn, R. M. *J. Chem. Soc. Faraday Trans.* **1995**, *91*, 1411.

(41) Makov, G.; Nitzan, A. *J. Phys. Chem.* **1994**, *98*, 3459.

(42) Schweighofer, K.; Benjamin, I. *J. Phys. Chem. A* **1999**, *103*, 10274.

(43) Zhang, X.; Cunningham, M. M.; Walker, R. A. *J. Phys. Chem. B* **2003**, *107*, 3183.

(44) Zhang, X.; Steel, W. H.; Walker, R. A. *J. Phys. Chem. B* **2003**, *107*, 3829.

(45) Zhang, X.; Esenturk, O.; Walker, R. A. *J. Am. Chem. Soc.* **2001**, *123*, 10768.

(46) Zhang, X.; Walker, R. A. *Langmuir* **2001**, *17*, 4486.

(47) Wang, H.; Borguet, E.; Eisenthal, K. B. *J. Phys. Chem. B* **1998**, *102*, 4927.

(48) Ishizaka, S.; Satoshi, H.; Kim, H.; Kitamura, N. *Anal. Chem.* **1999**, *71*, 3382.

(49) Michael, D.; Benjamin, I. *J. Phys. Chem. B* **1998**, *102*, 5145.

(50) Safran, S. A. *Statistical Thermodynamics of Surfaces, Interfaces, and Membranes*; Addison-Wesley: Reading, MA, 1994.

(51) Wirth, M. J.; Burbage, J. D. *J. Phys. Chem.* **1992**, *96*, 9022.

(52) Mitrinovic, D. M.; Zhang, Z.; Williams, S. M.; Huang, Z.; Schlossman, M. L. *J. Phys. Chem. B* **1999**, *103*, 1779.

(53) Eisenthal, K. B. *J. Phys. Chem.* **1996**, *100*, 12997.

(54) Scatena, L. F.; Richmond, G. L. *J. Phys. Chem. B* **2001**, *105*, 11240.

(55) Benjamin, I. *Chem. Rev.* **1996**, *96*, 1449.

(56) Chipot, C.; Wilson, M. A.; Pohorille, A. *J. Phys. Chem. B* **1997**, *101*, 782.

(57) Dang, L. X. *J. Phys. Chem. B* **2001**, *105*, 804.

(58) Senapti, S.; Berkowitz, M. L. *Phys. Rev. Lett.* **2001**, *87*, 176101.

(59) Steel, W. H.; Walker, R. A. *J. Am. Chem. Soc.* **2003**, *125*, 1132.

(60) Reichardt, C. *Solvents and Solvent Effect in Organic Chemistry*, 3rd ed.; Wiley-VCH: Weiheim, Germany, 2003.

(61) Matyushov, D. V.; Schmid, R.; Ladanyi, B. M. *J. Phys. Chem. B* **1997**, *101*, 1035.

(62) Suppan, P.; Ghoneim, N. *Solvatochromism*; The Royal Society of Chemistry: Cambridge, UK, 1997.

(63) Wong, M. W.; Frisch, M. J.; Wiberg, K. B. *J. Am. Chem. Soc.* **1991**, *113*, 4776.

(64) Zhuang, X.; Miranda, P. B.; Kim, D.; Shen, Y. R. *Phys. Rev. B* **1999**, *59*, 12632.

(65) Dick, B.; Gierulski, A.; Marowsky, G. *Appl. Phys. B* **1985**, *38*, 107.

(66) Simpson, G. J.; Rowlen, K. L. *Acc. Chem. Res.* **2000**, *33*, 781.

(67) Stefanovich, E. V.; Troung, T. N. *J. Chem. Phys.* **1997**, *106*, 7700.

(68) Senapti, S.; Chandra, A. *Chem. Phys.* **1999**, *242*, 353.

(69) Steel, W. H.; Damkaci, F.; Nolan, R.; Walker, R. A. *J. Am. Chem. Soc.* **2002**, *124*, 4824.

(70) Richmond, G. L. *Annu. Rev. Phys. Chem.* **2001**, *52*, 357.

(71) Lee, S. H.; Rossky, P. J. *J. Phys. Chem.* **1994**, *100*, 3334.

(72) Mitrinovic, D.; Tikhonov, A. M.; Li, M.; Huang, Z.; Schlossman, M. L. *Phys. Rev. Lett.* **2000**, *85*, 582.

(73) Wang, H.; Borguet, E.; Eisenthal, K. B. *J. Phys. Chem. A* **1997**, *101*, 713.

(74) Stanners, C. D.; Du, Q.; Chin, R. P.; Cremer, P.; Somorjai, G. A.; Shen, Y.-R. *Chem. Phys. Lett.* **1995**, *232*, 407.

(75) Michael, D.; Benjamin, I. *J. Chem. Phys.* **1997**, *107*, 5684.

(76) Sola, M.; Lledos, A.; Duran, M.; Bertran, J.; Abboud, J.-L. M. *J. Am. Chem. Soc.* **1991**, *113*, 2873.

(77) Reichardt, C. *Solvent Effects in Organic Chemistry*; Verlag Chemie: New York, 1979; Vol. 3, Chapter 1.

(78) Safran, S. A. *Statistical Thermodynamics of Surfaces, Interfaces, and Membranes*; Addison-Wesley: Reading, MA, 1994; Vol. 90.

(79) Squitieri, E.; Benjamin, I. *J. Phys. Chem. B* **2001**, *105*, 6412.

(80) Michael, D.; Benjamin, I. *J. Chem. Phys.* **2001**, *114*, 2817.

(81) Pohorille, A.; Wilson, M. A. *J. Chem. Phys.* **1996**, *104*, 3760.

(82) Berkowitz, M. L.; Schweighofer, K.; Essman, U. *J. Phys. Chem. B* **1997**, *101*, 3793.

(83) Tamburello-Luca, A. A.; Hebert, P.; Brevet, P. F.; Girault, H. H. *J. Chem. Soc. Faraday Trans.* **1996**, *92*, 3079.

(84) Whitaker, C. M.; Patterson, E. V.; Kott, K. L.; McMahon, R. J. *J. Am. Chem. Soc.* **1996**, *118*, 9966.

(85) Adamson, A. W. *Physical Chemistry of Surfaces*; John Wiley & Sons: New York, 1990.

(86) Rarick, M. J.; Brewster, R. Q.; Dains, F. B. *J. Am. Chem. Soc.* **1933**, *55*, 1289.

(87) Lambrech, J. A. U.S. Patent 2573769. In *U.S. Patent 2,573,769*, 1951.

(88) Snyder, R. G.; Strauss, H. L.; Elliger, C. A. *J. Phys. Chem.* **1982**, *86*, 5145.

(89) Watry, M. R.; Richmond, G. L. *J. Am. Chem. Soc.* **2000**, *122*, 875.

(90) Habenschuss, A.; Narten, A. H. *J. Chem. Phys.* **1990**, *92*, 5692.

(91) Walker, R. A.; Gruetzmacher, J. A.; Richmond, G. L. *J. Am. Chem. Soc.* **1998**, *120*, 6991.

(92) Conboy, J. C.; Messmer, M. C.; Richmond, G. L. *Langmuir* **1998**, *14*, 6722.

(93) Oevering, H.; Paddon-Row, M. N.; Heppener, M.; Oliver, A. M.; Cotsaris, E.; Verhoeven, J. W.; Hush, N. S. *J. Am. Chem. Soc.* **1987**, *109*, 3258.

(94) Hao, C.; March, R. E. *J. Mass Spectrom.* **2001**, *36*, 509.

(95) Siuzdak, G.; Bothner, B. *Angew. Chem. Int. Ed. Engl.* **1995**, *34*, 2053.

(96) Pratt, L. R. *J. Phys. Chem.* **192**, *96*, 25.

(97) Gragson, D. E.; Richmond, G. L. *J. Am. Chem. Soc.* **1998**, *120*, 366.

(98) Xu, Z.; Dong, Y. *Surf. Sci.* **2000**, *445*, L65.

(99) Volkov, A. G.; Deamer, D. W.; Tanelian, D. L.; Markin, V. S. *Liquid Interfaces in Chemistry and Biology*; John Wiley & Sons: New York, 1998.

(100) Volkov, A. G., Ed. *Liquid Interfaces in Chemical, Biological, and Pharmaceutical Applications*; Marcel Dekker: New York, 2001; Vol. 95.

(101) Steel, W. H.; Walker, R. A. *Nature* **2003**, *424*, 296.

(102) Beildeck, C. L.; Steel, W. H.; Walker, R. A. *Langmuir* **2003**, *19*, 4933.

(103) Schlossman, M. L.; Li, M.; Mitrinovic, D. M.; Tikhonov, A. M. *High Perform. Polym.* **2000**, *12*, 551.

(104) Sassaman, J. L.; Wirth, M. J. *Coll. & Surf. A* **1994**, *93*, 49.

(105) Englin, B. A.; Plate, A. F.; Tugolukov, V. M.; Pryanishnikova, M. A. *Chem. & Tech. Fuel & oil* **1965**, *10*, 722.

(106) Weeks, J. D. *J. Chem. Phys.* **1977**, *67*, 3106.

(107) Scatena, L. F.; Brown, M. G.; Richmond, G. L. *Science* **2001**, *292*, 908.

(108) Donahue, D. J.; Bartell, F. E. *J. Phys. Chem.* **1952**, *56*, 480.

(109) Girifalco, L. A.; Good, R. J. *J. Phys. Chem.* **1957**, *61*, 904.

(110) Josserand, J.; Lagger, G.; Jensen, H.; Ferrigno, R.; Girault, H. H. *J. Electroanal. Chem.* **2003**, *546*, 1.

(111) Dang, L. X. *J. Phys. Chem. B* **1999**, *103*, 8195.

(112) Cramb, D. T.; Wallace, S. C. *J. Phys. Chem. B* **1997**, *101*, 2741.

(113) Cheng, Y.; Corn, R. M. *J. Phys. Chem. B* **1999**, *103*, 8726.

(114) Conboy, J. C.; Messmer, M. C.; Richmond, G. L. *J. Phys. Chem.* **1996**, *100*, 7617.

(115) Michael, D.; Benjamin, I. *J. Phys. Chem.* **1995**, *99*, 16810.

(116) Braun, R.; Casson, B. D.; Bain, C. D. *Chem. Phys. Lett.* **1995**, *245*, 326.

(117) Steel, W. H.; Lau, Y. Y.; Beildeck, C. L.; Walker, R. A. *submitted*.

(118) Wolfrum, K.; Laubereau, A. *Chem. Phys. Lett.* **1994**, *228*, 83.

(119) Guyot-Sionnest, P.; Hunt, J. H.; Shen, Y. R. *Phys. Rev. Lett.* **1987**, *59*, 1597.

(120) Bell, G. R.; Bain, C. D.; Ward, R. N. *J. Chem. Soc. Faraday Trans.* **1996**, *92*, 515.

(121) Chang, R. *Basic Principles of Spectroscopy*; McGraw-Hill Book Co.: New York, 1971.

(122) Esenturk, O.; Walker, R. A. *submitted*.

(123) Schweighofer, K.; Essman, U.; Berkowitz, M. L. *J. Phys. Chem. B* **1997**, *101*, 3793.

(124) Simpson, G. J.; Rowlen, K. L. *J. Am. Chem. Soc.* **1999**, *121*, 2635.